TÉCNICO LISBOA

Development of a microfluidic rolling circle amplification module for bacterial detection

Rafaela Rodrigues Rosa

Thesis to obtain the Master of Science Degree in

Biomedical Engineering

Supervisors: Prof. Dr. João Pedro Estrela Rodrigues Conde
Dr. Ricardo Jaime Pereira Rosário dos Santos

Examination committee

Chairperson: Prof.Dr. Cláudia Alexandra Martins Lobato da Silva
Supervisor: Dr. João Pedro Estrela Rodrigues Conde
Member of the committee: Dr. Verónica Cristina Baião Martins Romão

November 2021

Preface:

The work presented in this thesis was performed at INESC MN (Lisbon, Portugal), during the period February-November 2021, under the supervision of Professor João Pedro Estrela Rodrigues Conde and Dr. Ricardo Jaime Pereira Rosário dos Santos.

Declaration:

I declare that this document is an original work of my own authorship and that it fulfills all the requirements of the Code of Conduct and Good Practices of the Universidade de Lisboa.

Acknowledgments

I would like to start by thanking Prof.Dr.João Pedro Conde for the opportunity to work at INESC-MN under his involved supervision in such an exciting project. It was a pleasure to work in such a motivating and supporting environment, that allowed for many scientific discussions crucial for the development of this work. I would also like to thank Dr.Virginia Chu for all the support and advice throughout the whole project.

I would like to thank my colleagues at INESC-MN for all the support, advice and amazing environment provided throughout this semester. I would like say a special thank you to Catarina Caneira for all the support, mentorship and friendship provided through every stage of this work without which this work would not have been possible, Cristiana Domingues and Pedro Monteiro thank you for all the support, advice and encouragement that made this experience that much more special. To my colleagues Rui Meirinho, Filipa Flora, Sofia Relvas and Rodolfo Rodrigues, who were my lab partners and became friends thank you for all the amazing conversations, laughter, support and advice throughout this work, making the lab a fun and cheerful place to work.

I would like to thank my best friends that have been present at every stage of my academic journey for the past years, for all the encouragement, support and incredible friendship. Lastly, I would like to thank my parents for all the love and support throughout every stage of my life and always being present and available to help, offering comfort and advice.

Abstract

Antibiotic resistance has been a growing health concern for the past decades. The inability to kill or inhibit these resistant bacteria from proliferating has made it very challenging to treat these infections. In order to prevent these infections from spreading, it is necessary to have fast and accurate diagnostic methods.

The field of microfluidics provides an excellent platform for this type of devices, particularly for point-of-care platforms, due to its advantages such as reduced size and higher surface-to-volume ratio, as well as reduced fabrication cost. In this work a microfluidic rolling circle amplification (RCA) module for bacterial detection, using *Staphylococcus aureus* as a bacterial model was developed. This device uses a microfluidic channel packed with streptavidin beads to which a probe DNA will bind to through a streptavidin-biotin bond and hybridize with a padlock. The target DNA to be detected will then hybridize to this padlock and be amplified through RCA. Throughout this work the target DNA capture assay was optimized regarding several aspects. These included the way the molecules were introduced into the channel, flow rates, as well as blocking optimization to minimize the background signal. The target DNA capture was also performed under several saline conditions and it was verified that it was possible to capture it under all the tested conditions. The target DNA capture was quantified with capture efficiencies ranging from 27% to 77%, and through the rolling circle amplification it was possible to detect only 1% of the amplified products.

Key Words: Antibiotic resistance**,** *Staphylococcus aureus***,** rolling circle amplification, microfluidic system

Resumo

A resistência a antibióticos é um problema de saúde publica que tem piorado nas últimas décadas, e a ineficácia dos antibióticos utilizados para matar ou inibir a proliferação de bactérias resistentes, torna estas infeções bastante difíceis de tratar. De modo a prevenir a propagação destas infeções, métodos de diagnóstico rápidos e precisos são extremamente necessários.

A microfluidica proporciona uma excelente plataforma para este tipo de dispositivos, particularmente para diagnósticos em *point-of-care*, devido às vantagens que oferece, como o tamanho reduzido, uma maior razão de superfície para volume, assim como custo de fabricação reduzido. Neste trabalho foi desenvolvido um módulo microfluidico de *rolling circle amplification* (RCA) para a deteção de bactérias, utilizando *Staphylococcus aureus* como modelo. Este ensaio utiliza um canal microfluidico com *beads* de streptavidina em que uma *probe* de DNA se irá ligar às *beads* através da ligação da streptavidina e biotina e hibridiza com uma *padlock*. O DNA *target* a ser detetado irá hibridizar com a padlock e posteriormente amplificado através de RCA. Ao longo deste trabalho foram realizadas várias otimizações ao modo de captura, incluindo a forma como as moléculas eram introduzidas no canal e flow rates. Foram também realizadas várias otimizações de bloqueios de forma a minimizar o sinal não específico. A captura do DNA *target* foi efetuada em várias soluções, concluindo-se que era possível capturá-lo em todas as condições testadas. A captura do DNA *target* foi também quantificada, sendo capturado com eficiências entre 27% to 77% e através do RCA foi possível detetar apenas 1% dos produtos amplificados.

Palavras-chave: Resistência a antibióticos**,** *Staphylococcus aureus***,** *rolling circle amplification*, sistema microfluidico

Index

List of Tables

List of figures

List of Abbreviations

BSA	Bovine Serum Albumin
CDC	Center for Disease Control and Prevention
cDNA	Complementary DNA
dsDNA	Double Stranded DNA
ELISA	Enzyme-Linked Immunoabsorbent Assay
HGT	Horizontal Gene Transfer
HA-MRSA	Hospital acquired MRSA
IPA	Isopropanol
LAMP	Loop Mediated Isothermal Amplification
MALDI-TOF MS	Matrix Assisted Laser Desorption/Ionization- Time of Flight Mass Spectrometry
MRSA	Methicillin resistant *Staphylococcus Aureus*
MGE	Mobile Genetic Elements
ncDNA	Non-Complementary DNA
PA	Sodium Polyacrylate
PBP	Penicillin Binding Proteins
PBS	Phosphate Buffured Saline
PCR	Polymerase Chain Reaction
PDMS	Poly(dimethylsiloxane)
Pe	Peclet Number
PGMEA	Propylene glycol monomethyl ether acetate
PLP	Padlock
PMMA	Poly(methylmethalcrylate)
POC	Point-of-care
RCA	Rolling Circle Amplification

Re	Reynolds Number
RT-PCR	Reverse Transcriptase PCR
ssDNA	Single-stranded DNA
US	United States

1. Introduction

1.1 Motivation

Antimicrobial resistance has been a growing health concern for the past decades, almost since its discovery in the 1900's. It is currently one of the most significant global public health challenges, threatening the ability to effectively treat an ever-growing range of infections caused by bacteria, viruses or fungi. [1] [2] [3]

Antibiotics are used to treat most bacterial infections, either by killing or inhibiting bacteria proliferation. Due to the presence of resistance genes in the bacteria's genome, they are able to continue proliferating even in the presence of antibiotics, making it harder or sometimes even impossible to treat these conditions, even the ones commonly seen in an outpatient setting, such as otitis media and conjunctivitis, increasing the risk of severe illness or in some cases even death. [4] [5] [6] Additionally, antimicrobial-resistant infections disproportionally impact the most vulnerable, who often receive medical care and are at higher risk for infection, such as chronic patients. Patients with conditions like diabetes, cancer patients receiving chemotherapy, and organ transplant recipients are at a higher risk of infection. As a matter of fact, one of the main factors influencing morbidity and mortality in these patients is multidrug-resistant infections. [1] [2] [4]

According to a recent report by the Center for Disease Control and Prevention (CDC), in the United States (US), more than 2.8 million people are infected with antibiotic-resistant bacteria or fungi, and over 35,000 people die yearly as a result. [1] Similarly, in 2007 in Europe, it was estimated that approximately 400,000 multidrug-resistant infections (due to the most common multidrug-resistant bacteria) occur each year, and around 25,000 result in deaths. [2] [7] This exerts a major cost to both national economies and health systems, leading to more expensive and intensive care, and affecting the productivity of the patients and their caretakers. In the US, the yearly associated healthcare cost is estimated to be 20 billion dollars, with the cost per patient ranging from $7,000 to $29,000. In Europe, the overall economic burden was estimated to be at least 1.5 billion euros. [3] [2]

Due to the health and economic burden that antibiotic-resistant infections cause, the continued usage of antibiotics that promotes the spread of resistant bacteria, and the prolonged timescale involved in the development of new antibiotics, it is essential to develop fast, sensitive, and low-cost methods of detection, that allow for a prompt diagnosis and appropriate treatment, to prevent and stop the antimicrobial resistance problem. [8] [9]

Nowadays, the standard methods for bacterial detection are plate culturing and polymerase chain reaction (PCR). Plate culture is considered the gold standard for bacterial detection since it is a very sensitive and accurate method. However, these methods are labor intensive and often require skilled personnel, large volumes of reagents, and several days to get precise results. [8]

Given that a rapid pathogen detection would reduce the exposure to broad-spectrum antibiotics and allow for pathogen targeted therapy, point-of-care (POC) platforms, which allow for testing at or near the site of patient care, are of extreme importance in this field, especially in low resource areas, since they can improve medical decision making. These platforms should be sensitive, accurate, easy to use and interpret, portable, disposable, require small sample volumes, stable under a wide range of conditions, have a rapid turnaround time, and be cost-effective. [10][11][12]

With the emerging fields of nanotechnology and microfluidics, new horizons have opened up for POC platforms. Their intrinsic small size offers various advantages, such as portability, the higher surface to volume ratio, the faster rate of mass and heat transfer, enhancement of assay kinetics, which allows for the use of small sample and reagent volumes (ranging from nano to picolitres), all contributing to a rapid detection time. [12][13] Microfluidic devices also possess a high capability for integration, allowing sample preparation, reagent storage, and addition, mixing, washing, and the incorporation of centrifugal steps. These devices are also suitable for a wide range of detection methods. Since the detectable signal is produced by a very small area, for example, using fluorescence, microfluidic devices provide very sensitive results. [13]

1.2 Antimicrobial agents

Nowadays, infectious diseases are a significant cause of morbidity and mortality around the world, which has been made even more significant by antimicrobial resistance. Even though antibiotics were introduced in the 1900's and a large number of antimicrobial agents are available to fight these infections, in literature there is documented resistance to all. [3]

Antibiotics act by invading the organism (bacteria) rather than altering the host's physiology. Consequently, they are classified according to the mechanism through which they interact and affect

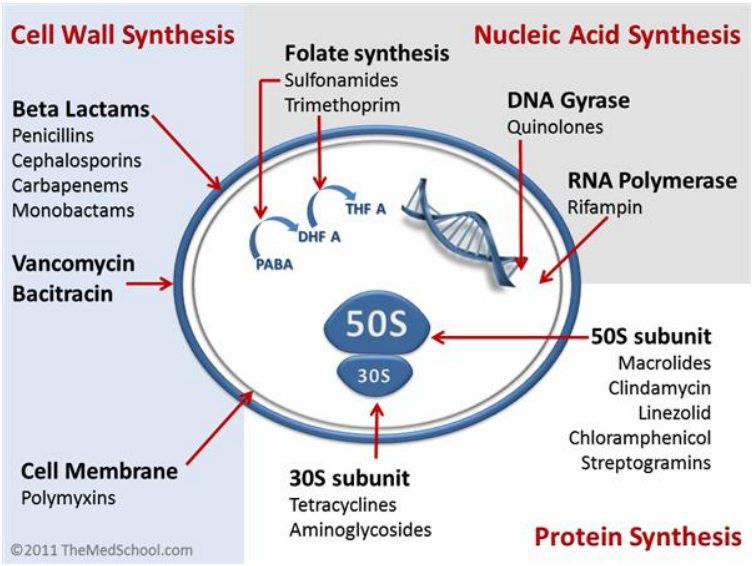

Figure 1.1: *Antibiotics mechanisms of action, and examples of several antibiotics. Antibiotics are classified according to the way they interact with the target pathogens, either by interfering with the cell wall synthesis, nucleic acid synthesis or protein synthesis. [14]*

bacteria, as represented in Figure 1.1: Affecting cell wall synthesis, nucleic acid synthesis or protein synthesis. For example, β-Lactam antibiotics are a type of antibiotics that target cell wall synthesis, interacting with penicillin-binding proteins (PBP), which are responsible for strengthening the cell wall. Due to this interaction, the PBPs become unavailable for the synthesis of a new peptidoglycan, the cell wall layer is disrupted and leads to the lysis of the bacteria. [5] [14]

1.2.1 Antimicrobial resistance

Antimicrobial resistance is a very complex issue, involving multiple factors, such as the particular microorganism, the drug being used, and the surrounding environment. Even though it was initially thought that antibiotic resistance was a problem affecting almost exclusively acute care hospitals, it has already spread from acute care settings to other inpatient settings, such as extended care facilities, and to the outpatient setting as well, with the overuse of antibiotics. [15] [5]

One of the main ways antibiotic resistance is introduced and spread is in the healthcare setting, such as in hospitals, through patients or health care workers from the outside or other institutions, from patients transferred to or from extended care facilities, or through contaminated products. [15] This is mainly due to selection pressure by antibiotic use and made worse by its inappropriate and over usage, such as inadequate dosing and excessive or improper prescription by physicians, which may happen at the time of the choice of a drug to prescribe, where low toxicity and cost must be taken into account, which antibiotics allow with a relatively low incidence of toxicity.[2][3][16] Also, physicians often prescribe broad-spectrum antibiotics that may be unnecessary or even ineffective in fighting the infection. [15] An additional issue caused by antibiotic usage is that patients who have been previously exposed to antimicrobial drugs are at risk for infections with drug-resistant organisms, and patients who are more often exposed to antimicrobials are more likely to be infected by resistant organisms. [13]

In the United States, antibiotics are the second most prescribed class of drugs, having been prescribed 258 million courses of antibiotics just in 2010. It has also been estimated that in 2011, in Europe, 35% of hospitalized patients were prescribed antibiotics, and that in the United States, one-third of patients receives antibiotics during hospitalization, and 50% of its use is unnecessary. [2][5]

Another factor driving antibiotic resistance is the usage of antibiotics in animals. There is evidence that feeding antibiotics to animals can lead to the development of antimicrobial-resistant organisms, which can then be transferred to humans through various routes, such as eating meat from those animals, ingesting feces in contaminated food or water, as well as direct contact with the animals [3]

Antibiotic resistance may be intrinsic - always expressed in the species - or induced - in which the genes are naturally occurring in the bacteria but only express antibiotic resistance after exposure. Bacteria can also acquire genetic material that grants resistance, either temporarily or permanently, from intrinsically resistant organisms present in their environment, through horizontal gene transfer

(HGT), or by spontaneous chromosomal mutations which are then transmitted vertically when the bacteria replicates. [3] [17]

HGT is a way for bacteria to acquire foreign genetic material, being a fundamental part of bacterial evolution, as well as in the propagation of antibiotic resistance.[18] Bacteria acquire genetic material through one of three the ways, represented in Figure 1.2:

- Transformation – the uptake, integration, and expression of free DNA released into the environment from closely related bacteria; [19] [20]
- Transduction – a bacteriophage mediated process, by which the bacteriophage infects a host cell, and accidentally packages its DNA into its capsid and upon infecting a new host injects it with the previously acquired DNA; [19] [20]
- Conjugation - involves cell-to-cell contact and uses mobile genetic elements (MGE), such as plasmids and transposons to transfer genetic material. [19] [20]

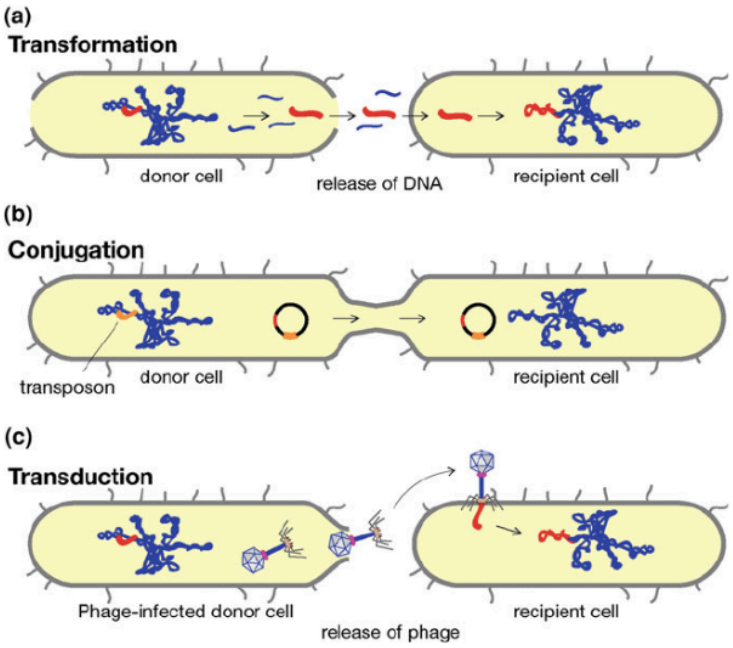

Figure 1.2: *Schematic representation of the different mechanisms of Horizontal Gene Transfer (HGT): A) Transformation- the uptake of free DNA. B) Conjugation- Transfer of genetic material mediated by mobile genetic elements (MGE), such as plasmids. C) Transduction- Transfer of genetic material mediated by bacteriophages. [21]*

1.2.1.1 Molecular Antimicrobial Resistance Mechanisms

As previously stated, bacteria can be naturally resistant to several classes of antibiotics, independently from antibiotic pressure or horizontal gene transfer, but instead due to intrinsic structural or functional characteristics. A very relevant example of intrinsic resistance is the case of several multidrug-resistant Gram-negative bacteria. [22]

One very common resistance mechanism intrinsic to Gram-negative bacteria is reduced permeability (Figure 1.4), preventing the antimicrobial molecule from reaching its target within the cell.

This is because unlike Gram-positive bacteria, which have a cytoplasmic membrane surrounding the cell wall, Gram-negative bacteria have a second lipid membrane surrounding the cell wall, called Outer Membrane (Figure 1.3). This second layer surrounding Gram-negative bacteria's cell wall provides a second layer of protection, preventing numerous substances from entering the bacteria. However, in order to allow the uptake of essential nutrients the outer membrane contains channels, called porins. Nonetheless, these channels still hinder the uptake of several antibiotics through several mechanisms, such as size exclusion, hydrophobicity and charge repulsion. This resistance can be even further enhanced in some cases due to a reduction in the number of porins or a decrease in the level of porin expression. [14] [17] [18]

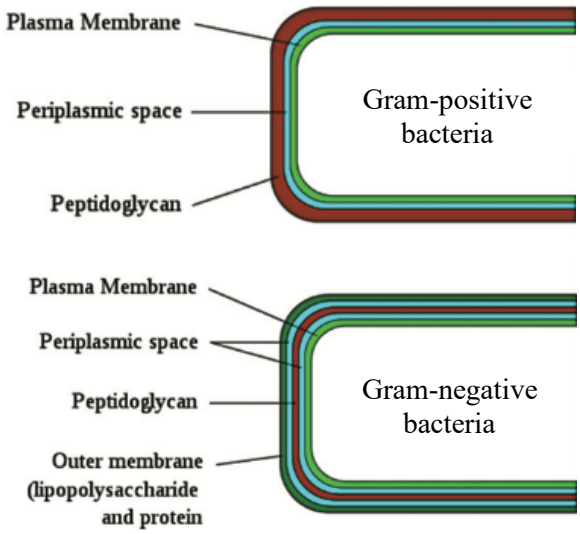

Figure 1.3: *Schematic representation of the bacterial cell envelope, highlighting the differences between Gram-positive and Gram-negative bacteria. Adapted from [14].*

Another very common resistance mechanism in Gram-negative bacteria, and more rarely present in Gram-positive bacteria, is increased efflux, that prevents the antimicrobial molecules from reaching their target through efflux pumps (Figure 1.4). These pumps actively transport molecules out of the cell and can be substrate selective or allow the transport of a wide range of substrates (usually found in multidrug-resistant bacteria), affecting several antimicrobial classes, such as Fluoroquinolones, β-lactams and Carbapenems. When overexpressed, efflux pumps confer high levels of antibiotic resistance. [18] [22]

An alternative type of resistance mechanism that has been developed by bacteria is their ability to modify or protect the antibiotic's target site (Figure 1.4). Upon altering the target site, either by point mutations in the genes, enzymatic alterations, or replacement of the original target site, there is less affinity for the antibiotic molecule leading to lower susceptibility. [18]

Lastly, bacteria can also exhibit resistance to antibiotics by having the ability of modifying the actual antimicrobial molecule (Figure 1.4). This can be through the production of enzymes capable of introducing chemical changes to the antimicrobial molecule, by adding chemical groups, such as

phosphate groups, which interfere with the antibiotics ability to bind to the target site due to steric hindrance. There are also bacteria capable of producing enzymes that destroy the antibiotic molecule, such as β-lactamases which destroy the amide bond of the β-lactam ring in β-lactam antibiotics, making them ineffective. [18] [22]

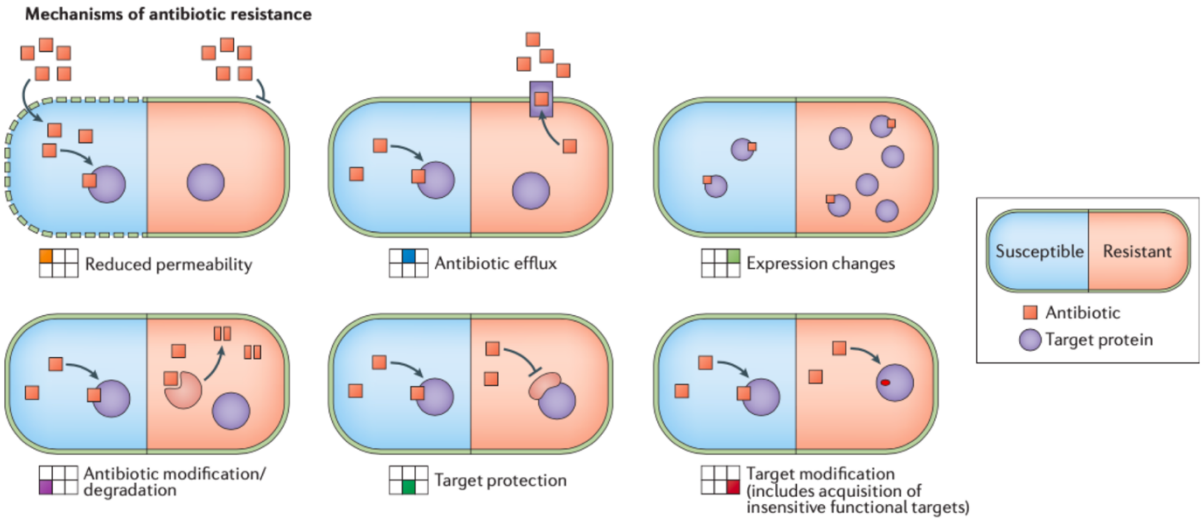

***Figure 1.4**: Molecular mechanisms of antibiotic resistance. In blue is represented the antibiotic's mechanism of action in susceptible bacteria, and in orange the way resistant bacteria react to it. Adapted from [4].*

1.2.1.2 Methicillin resistant *Staphylococcus Aureus*

Staphylococcus aureus is a Gram-positive bacteria that is commonly found in the nasal mucosa of 20 to 40% of the population. Nonetheless several other sites can be colonized, such as the axillae, groin, and gastrointestinal tract. Following colonization, if the hosts' defenses are breached, such as the cutaneous and mucosal barriers, due to wounds, chronic skin conditions, catheter insertion, or surgical intervention S*. aureus* can attach to the wounded tissues through its surface proteins which can bind to extracellular matrix proteins. The bacteria enter the bloodstream or underlying tissues and cause several types of infections, such as endocarditis, bacteraemia, pneumonia, osteoarticular infections, and skin and soft tissue infections. [2][23][24][25]

With the spread of antibiotic resistance, many previously susceptible organisms have acquired resistance (see Chapter 1- section 1.2.1.1). That is the case for *S. aureus*, as the first strains of Methicillin-resistant *Staphylococcus aureus* (MRSA) emerged in the 1960s, mostly related to elderly and immunocompromised patients, and as stated earlier, like most antibiotic-resistant bacteria, then spread to the community. Hospital Acquired MRSA (HA-MRSA) infections are usually associated with invasive medical procedures such as catheters or surgical procedures. Hence people with lengthy hospitalizations, ICU admissions or residents at nursing homes are at higher risk of HA-MRSA infections. On the other hand, community acquired MRSA infections mainly involve the skin, and primarily affect people engaged in activities that may cause skin damage or involve close contact, such as athletes and military personnel. [2][24]

The resistance to methicillin, part of the β-lactam antibiotics class, which are considered the optimal choice of treatment for *S. aureus* infections, further complicates their treatment. The action mechanism of β-lactam antibiotics affects cell-wall synthesis, as was described above. The insertion of the mecA gene in the accessory component of the *Staphylococcus aureus* genome in the staphylococcal chromosomal cassete mec is what causes resistance to β-lactams. This accessory component makes up 25% of the *S.aureus* genome and consists of MGEs, acquired by HGT and is more variable between strains and hence more strain-specific than the core genome, which is highly conserved among strains. The mecA gene encodes PBP2a, which has a low affinity for all β-lactams, rendering most of them ineffective. As this class of antibiotics is considered the optimal treatment choice, therapeutic options become limited, reeling on less effective or more expensive therapeutics, making the associated mortality rate for MRSA infections around 20-25%.[18][23][24][26][27] This, together with patient comorbidities and underlying illnesses, leads to higher morbidity and mortality than infections caused by susceptible *S. aureus* strains, and as studies have shown, patients with invasive MRSA infections have a reduced chance of long-term survival. [24] In the 2019 CDC's report of Antibiotic Resistance Threats in the United States, MRSA was declared a serious threat. It was estimated that approximately 323,700 hospitalized patients contracted a MRSA infection, and around 10,600 resulted in deaths. [1]

1.3 Current methods of bacterial detection

1.3.1 Culture and colony counting

Culture and colony counting methods are the most established for bacterial detection since they are very reliable and sensitive. There are several methods to do so, but the most common consists of performing serial dilutions of the desired bacterial culture, incubating it in the desired agar plate at 37℃, followed by enumerating the viable colonies after 2 to 4 days. In addition, when dealing with antibiotic susceptibility testing, to determine which antibiotics the bacteria are susceptible to, an additional 16 to 24 hours of culture are required. Several media types can be used depending on the target bacterial species, containing inhibitors that only the target bacteria can proliferate in, or specific substrates that only the target bacteria can degrade. One approach very often employed in clinical laboratories is the use of chromogenic media (Figure 1.5). These media contain chromogenic or fluorogenic substrates

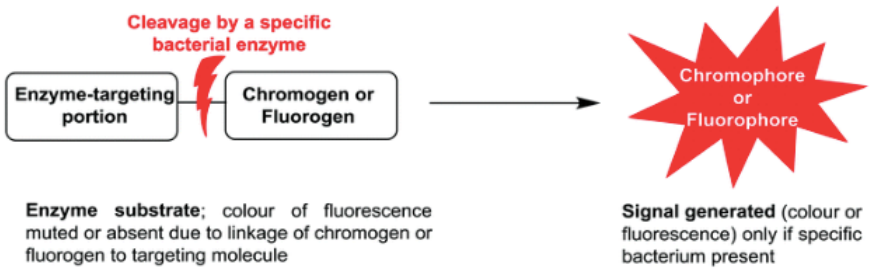

Figure 1.5: *Schematic representation of the principle behind the use of chromogenic media. Chromogenic or fluorogenic substrates in the presence of enzymes specific to the target bacteria are hydrolyzed and develop color. The color change or fluorescence emission indicates the presence of bacteria. [30]*

that in the presence of enzymes specific to the target bacteria are hydrolyzed and develop color. The color change or fluorescence emission indicates the presence of bacteria. [28] [29] [30]

Although several fast and advanced methods to calculate bacterial colonies have been developed, and the use of chromogenic media is a step further in the isolation and identification of bacteria in a single step, the process is still very time consuming, requires large amounts of equipment and trained personnel. [28] [30]

1.3.2 Immunology-based assays

Various techniques used for bacterial detection are based on immunological methods, which rely on the specific binding of an antigen to an antibody. The most established immunology-based approach is enzyme-linked immunosorbent assay (ELISA). ELISA relies on the principle of antigen-antibody binding, coupled to an enzyme. Once a specific enzymatic substrate is added produces color, providing a specific and sensitive detection method. There are several kinds of ELISA assays, such as indirect ELISA, competitive ELISA, and the sandwich ELISA, which is the most common, represented in Figure 1.6. Another immunology-based technique is immunomagnetic separation (IMS), which relies on immunomagnetic beads to separate, concentrate and can be combined with numerous strategies for pathogen detection. [29] [31] [32]

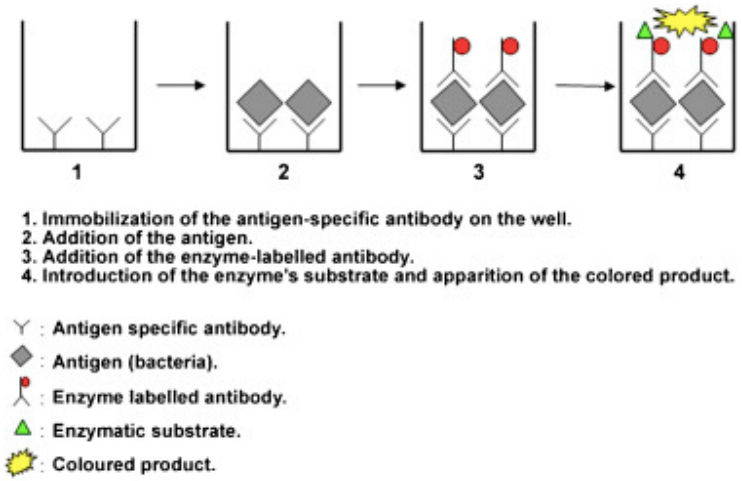

***Figure 1.6**: Schematic representation of the sandwich ELISA assay. [29]*

Although these assays are less time-consuming than culturing techniques, time is still an issue, taking several hours to obtain results. Additionally, antibody preparation makes these techniques expensive, there is the possibility of non-specific binding, and in the case of ELISA there is the possibility of misleading results due to insufficient blocking of the surface. [32]

1.3.3 Matrix assisted laser desorption/ionization-time of flight mass spectrometry (MALDI-TOF MS)

Since its introduction in 2010, MALDI-TOF MS has become a very popular method for bacterial detection. The sample is treated with a matrix, which absorbs energy from a laser, resulting in rapid

heating and the ionization of the analytes. As all ions with the same charge are given the same kinetic energy, they are then separated by the time it takes them to reach the detector. The majority of molecules observed by MALDI-TOF MS are ribosomal proteins, which have characteristic masses for a particular bacteria, resulting in a unique MS spectrum that can then be compared against a known database to identify the pathogen. However, there are some limitations to this method, such as its inability to differentiate taxonomically related bacteria, for example, *Shigella* from *E. coli*, as well as the need for extensive databases to identify the bacterial species. As MALDI-TOF MS is mainly used with culture methods to confirm the identification of the previously isolated bacteria, the time to obtain results is also lengthy. [30]

1.3.4 Molecular detection methods

Nucleic acid detection plays an important role in accurate and precise diagnostics. It carries many advantages over the previously reviewed techniques, such as:

- Nucleic acids are common to all species as their genetic material. Still their amount and distribution in the genome are unique to each species, making it possible to detect a given organism based on its unique genome.
- Nucleic acids are easy to manipulate, purify and label, making their detection easy.
- It is possible to synthesize large quantities of nucleic acid sequences *in-vitro* that can then be utilized to detect specific sequences for a reasonable cost. [33]

However, the quantity of nucleic acids that can be isolated from a given sample is very limited, and therefore, nucleic acid amplification is extremely important for diagnostics. The most commonly used amplification protocol is PCR, which is routinely used for various clinical diagnoses, for example, it is used to detect bacterial infections by identifying genes from the parasitic organism in the host. [33] It involves three types of reactions, which require three different temperatures (Figure 1.7):

- Denaturing - The temperature is raised to around 95℃ to separate the double-stranded DNA (dsDNA) into single-stranded DNA (ssDNA).
- Annealing – The temperature is lowered to approximately 56℃ so that primers, short sequences of complementary DNA (cDNA), hybridize with the denatured ssDNA.
- Extension – The temperature is again raised to 72℃ so that Taq DNA polymerase can synthesize a DNA strand complementary to the ssDNA, from the free nucleotides in solution. [33] [34]

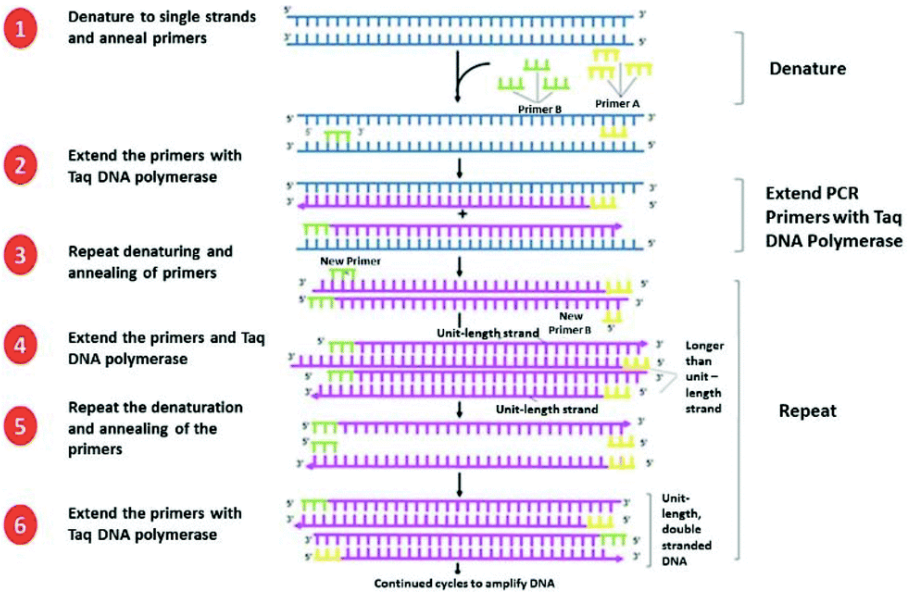

Figure 1.7: *Schematic representation of the PCR protocol. [28]*

As each new dsDNA acts as a template for a new cycle, the amplification process is exponential, and usually, 30 to 35 cycles are sufficient to generate enough DNA for diagnostic purposes. This process takes around 5 to 24 hours, depending on the variation of the PCR protocol being employed, for example, real-time PCR, multiplex PCR or reverse-transcriptase PCR (RT-PCR). In Real-time PCR the detection of the amplified DNA is done using a gene-specific probe labelled with a fluorophore, which once hybridized will be decomposed by the Taq polymerase and emit a fluorescence signal. Since the fluorescence intensity is related to the quantity of target DNA this allows for real-time quantitative results. RT-PCR allows to detect RNA and therefore to distinguish between viable and non-viable cells, by using a reverse transcriptase that generates cDNA that is then amplified through PCR. It is also possible to detect several organisms through multiplex PCR, by simultaneously using different primers. However, PCR still presents some disadvantages, such as the possibility of contamination, due to the high sensitivity intrinsic to PCR that can lead to misleading results, as well as the possibility of the primers annealing to similar DNA, that would result in incorrect nucleotides being incorporated into the newly synthesized DNA. Additionally, PCR requires highly trained personnel, expensive equipment and precise control of thermal cycling, making it difficult to perform in a POC setting. [28] [29] [33]

In order to overcome some of the limitations imposed by PCR, isothermal nucleic acid amplification techniques have gained a lot of interest, particularly for POC applications. One of the most widely studied isothermal techniques is loop-mediated isothermal amplification (LAMP) which is performed at a constant temperature of 60℃ to 65℃. [33] [35] [36]

LAMP requires 4 to 6 primers, complementary to six specific regions on the target gene and a Bst polymerase enzyme with high displacement activity. There are at least 2 sets of primers present in the reaction, the inner and outer primers. The inner primers are termed the forward (FIP) and backward

primer (BIP) and are complementary to 2 distinct parts of the target, F1c and B2c, respectively. The outer primers are termed B3 and F3 and are complementary to the outer sequences of the target B3c and F3c, respectively. The process (Figure 1.8) begins with the FIP primer hybridizing to its complementary F2c in the target DNA, with a non-hybridized over-hang (F1c), and synthesizing a complementary DNA strand. This is followed by the smaller F3 primer hybridizing with its complementary on the target sequence, F3c and displacing the previously synthesized DNA strand. The displaced strand has now 2 complementary sequences, F1 and F1c that form a loop, followed by the hybridization of the backwards primer BIP to its complementary B2c. The newly synthesized DNA strand is again displaced, now having complementary segments on both sides, originating 2 loops. This loop structure then serves as a template for a cyclic loop-mediated amplification, resulting in an exponential amplification process. Due to the different lengths of DNA fragments generated, LAMP products can be detected through agarose gel electrophoresis, as well as DNA intercalating dyes, fluorescent probes or turbidity changes. Asides from the obvious advantage over PCR of being performed under a constant

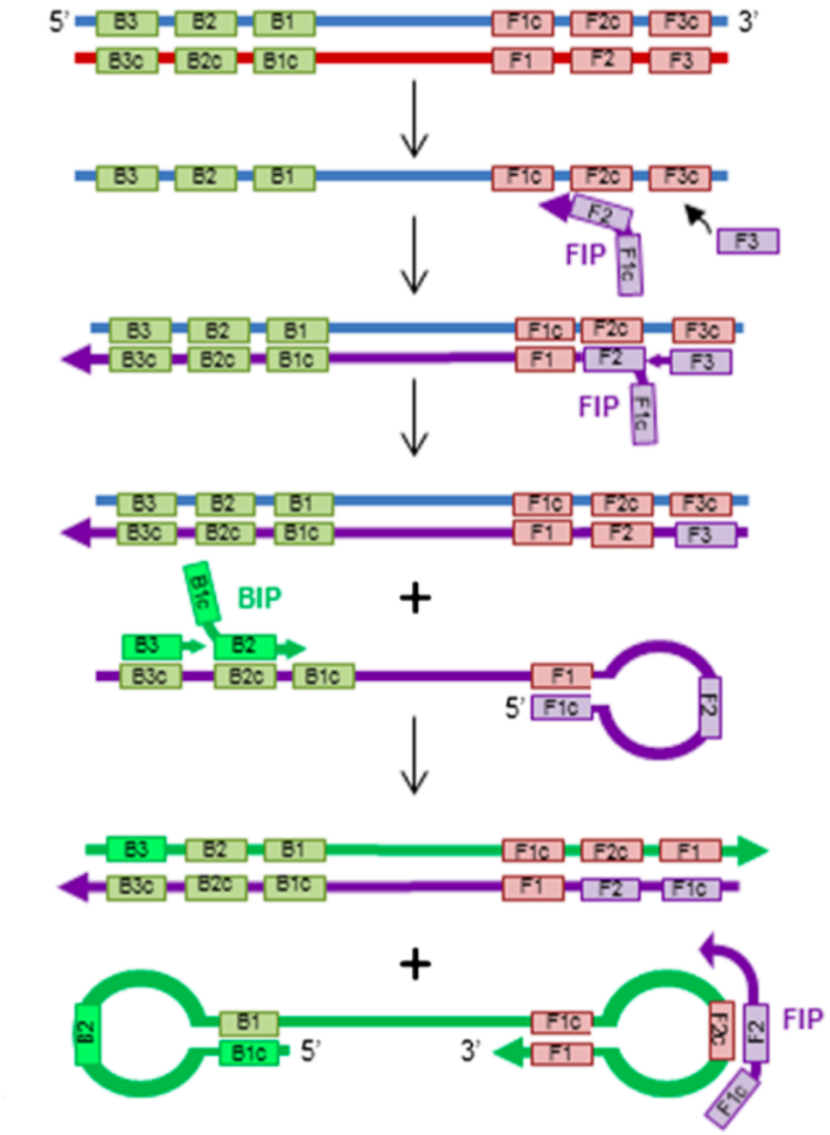

***Figure 1.8**: Schematic representation of the loop mediated isothermal amplification process. Adapted from [37]*

temperature, this technique has several advantages, such as high specificity provided by the use of 4

specific primers and an extremely high amplification efficiency. LAMP can also be used to amplify RNA simply by using a reverse transcriptase without requiring any additional time to the reaction. However, the method also carries several disadvantages, such as false positives, the complicated design of the 4 specific primers and the amplified products cannot be used for downstream experiments. [35] [36]

Another commonly used isothermal amplification technique is rolling circle amplification (RCA). The process is conducted at a constant temperature of 37℃ and it is based on the rolling circle replication mechanism present in bacteria and viruses. RCA requires a circular DNA template termed padlock (PLP), a short DNA or RNA primer/target and a DNA polymerase to start the reaction, which generates a long single-stranded molecule containing thousands of repeated copies of the circular template tethered to the original circular DNA. [33] [38] [39]

PLPs are linear oligonucleotides composed of two end-sequences and a linker sequence. The two end-sequences are complementary to a target DNA, such as the DNA of a pathogen, and upon hybridization, with the target, the PLP becomes circularized with a nick between the two linker sequences. The nick can then be closed by a DNA ligase, which demands a perfect hybridization in order to join the 5'-phosphorilated end of a DNA strand to the 3'-end of the DNA strand efficiently (Figure 1.9A) and in the presence of mismatches, ligation efficiency is significantly reduced, ensuring high specificity. T4 DNA ligase is commonly used for DNA-DNA ligation (Figure 1.9B), however another commonly used ligase, Tth ligase, offers higher specificity since it can be used at higher temperatures,

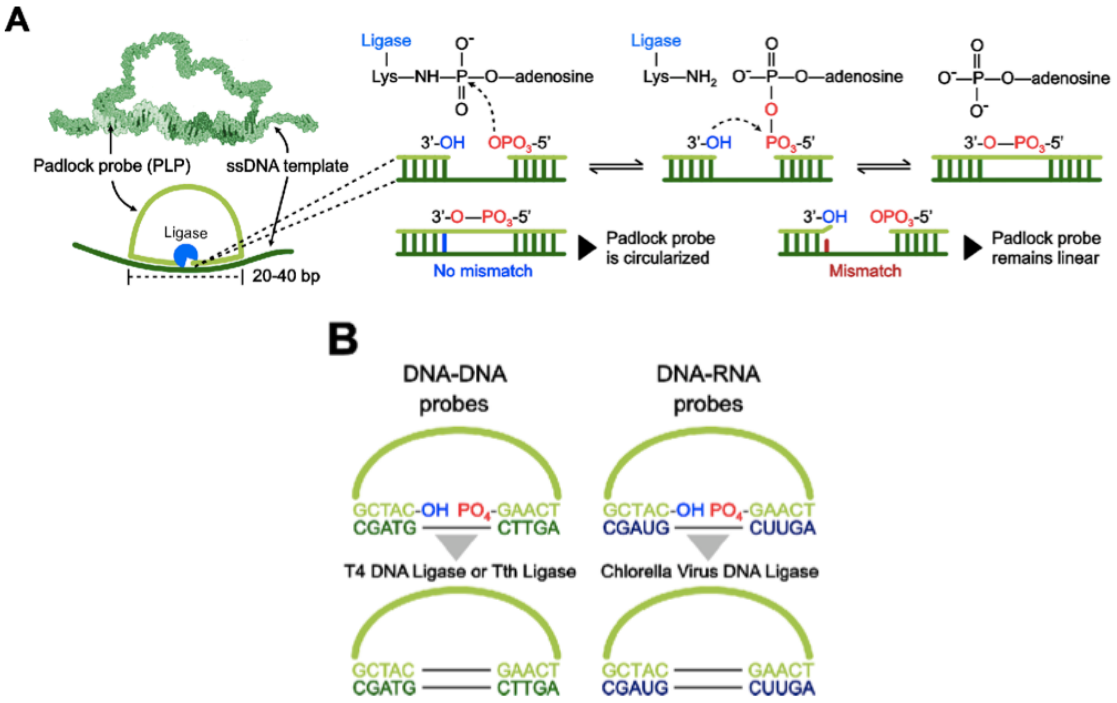

Figure 1.9: *Schematic representation of the padlock ligation. A) Ligation mechanism in the presence of no mismatches and with mismatches. B) Ligation mechanism with target DNA and RNA. Adapted from [39]*

increasing hybridization stringency conditions and mismatch discrimination. An advantage of PLP-RCA

is that it can also be used to directly detect RNA (Figure 1.9B), simplifying the process by eliminating the need for reverse transcription. [33] [39]

Upon target hybridization and padlock ligation, a DNA polymerase can synthesize a new DNA strand complementary to the padlock (Figure 1.10A). A commonly used polymerase in RCA is the Phi29 enzyme due to its high processivity and strand displacement activity, enabling the amplification of a 100bp padlock into a complementary DNA strand with approximately 1000 copies of the original template in one hour. As the new DNA strand is synthesized around the circular template it will eventually reach the initiation point. At that stage the newly formed strand will displace the previous one as polymerization continues. The generated product will be attached to the template and can then be detected by concentrating labels in a small detection area and enumerating single DNA molecules. Although this linear amplification process already provides high sensitivity, it can be even further enhanced by performing another variation of RCA that allows for an exponential amplification, such as hyperbranched RCA, multiprimed RCA or circle-to-circle RCA. Hyperbranched RCA (Figure 1.10D) uses a second set of primers targeting the amplification product that will bind along the newly formed DNA strand and initiate new primer amplification. In multiprimed RCA (Figure1.10C), several primers are hybridized to the same padlock, initiating multiple amplification events. Lastly, in circle-to-circle RCA (Figure 1.10E), restriction enzymes are used to digest the amplified product followed by circularization

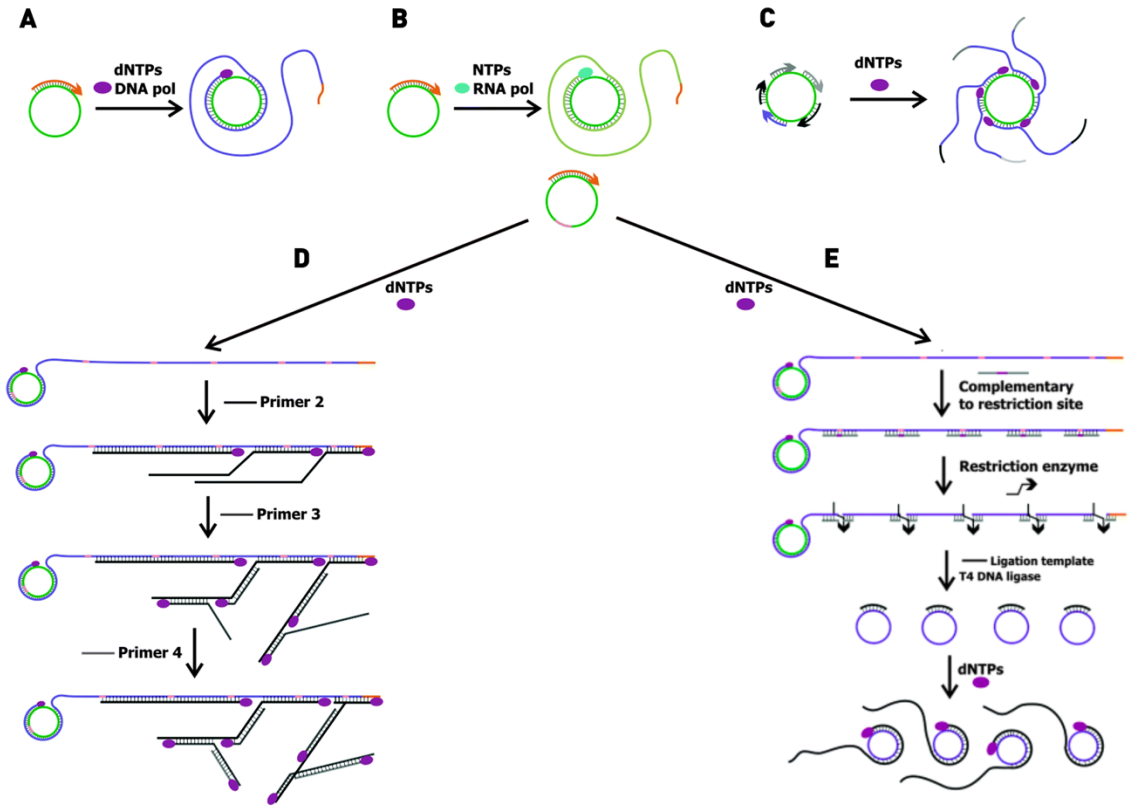

Figure 1.10: *Schematic representation of the several variations of the RCA protocol. A) Linear amplification using a target DNA. B) Linear amplification using a target RNA. C) Multiprimed RCA. D) Hyperbranched RCA. E) Circle-to-circle amplification Adapted from [38]*

and ligation. The new circular templates can then be subjected to a second round of RCA, and multiple

rounds can be performed in series. The RCA products can then be detected through several strategies, including DNA intercalating dyes, fluorescent probes and molecular beacons. [33] [35] [38] [39]

Table 1.1 summarizes the characteristics of the three methods reviewed above, and it is clear that isothermal techniques simplify the amplification assay by eliminating the need for thermal cycling, which is particularly of interest for point-of-care applications. Additionally, isothermal techniques have also been shown to perform just as well, or even better than traditional PCR assays.

Table 1.1: *Summarized list of the characteristics, as well as the advantages and disadvantages of PCR, RCA and LAMP. Adapted from [33]*

	PCR	**RCA**	**LAMP**
Template	dsDNA, RNA (RT-PCR)	Circular ssDNA	ssDNA, RNA
Amplicon type	dsDNA fragment	Concatenated DNA	Concatenated DNA
Enzyme used	Taq polymerase	Phi29 DNA polymerase	Bst polymerase
Reaction Temperature	Three cycling temperatures (95℃, 50℃-72℃ and 72℃)	Isothermal temperature 30℃-65℃	Isothermal temperature 60℃- 65℃
Sensitivity	10^1- 10^2 copies	10^1 copies	10^1 copies
Efficiency	2^{30}-fold in 2~3h	10^9- fold in 90 minutes	10^9- fold in 60 minutes
Primer required	2	1 (with padlock probe)	4-6
Detection method	Intercalating DNA dye, fluorescent probe	Intercalating DNA dye, fluorescent probe, molecular beacon	Intercalating DNA dye, fluorescente probe, turbimetric
Disadvantages	Long reaction time Lower amplification efficiency than isothermal amplification	Long padlock probe which increases the cost for nucleic acid synthesis Any unlocked padlock and unhybridized template DNA could cause high background noise	Needs specifically-designed primer pairs The amplified products cannot be used for downstream experiments, including cloning and sequencing Pseudo-positive results are easily produced
Advantages	The amplified product can be used for downstream experiments, including cloning and sequencing.	High amplification efficiency High specificity The amplified product could be used for subsequent sequencing	High amplification efficiency Shorter operating time

1.4 Microfluidics

1.4.1 Integrated Microfluidic Systems

For the past 30 years microfluidics has provided the ability to develop new devices capable of outperforming the classically used techniques in several areas of research, such as food and environmental monitoring [40] [41], biological assays, such as cell counting and cell culture [42], and health diagnostics [43].

A microfluidic device is defined as a system with a width/height scale between 100nm and 100μm. This size reduction explains many of its advantages, such as faster reaction times and enhanced assay kinetics. This can be explained by the different forces that affect fluids on the micro-scale. One crucial difference is the ratio between inertial and viscous forces, which is described by the Reynolds number (Re), where ρ is the density, υ is the velocity, L is the characteristic linear dimension of the system and μ is the dynamic velocity. [44]

$$Re = \frac{\rho \upsilon L}{\mu} \quad (1)$$

As seen from equation (1), as the dimensions decrease, so does the Reynolds number and for Re < 2000 the system is considered to be in a laminar flow regime. In the laminar regime molecular transport is carried out by diffusion, and the flow is highly predictable, which leads to highly predictable kinetics, unlike turbulent flow. Due to the small dimensions of microfluidic systems, Re is almost always bellow 2000 and therefore, the flow is laminar. Another important aspect regarding the physics of fluids in microfluidics is the relation between convective and diffusive transport, given by the Peclet number (Pe), where D is the diffusion coefficient. From equation (2) it is possible to see that with decreasing dimensions, the Pe number also decreases, and diffusive transport dominates over convective. [44][45]

$$Pe = \frac{\upsilon L}{D} \quad (2)$$

Lastly, the diffusion time can be given by equation (3), where x is the distance a molecule traveled along an axis after time t, and D is the diffusion coefficient. [44]

$$t \approx \frac{x^2}{2D} \quad (3)$$

From equation (3), it is possible to estimate (4), and it becomes evident that the reduced size of microfluidic devices leads to shorter diffusion times, allowing for faster reactions. [44] [46]

$$t \propto x^2 \quad (4)$$

Several materials have been used in microfluidic device fabrication, including silicon and glass. However, poly(dimethylsiloxane) (PDMS) is the most popular material in microfluidic device fabrication given its advantageous properties. It is non-toxic, optically transparent (between 300nm and 2200nm), it is permeable to gas, apolar organic solvents and practically impermeable to water. PMDS is also cheaper than silicon or glass and can be easily replicated and bonded. The fabrication process of PDMS microfluidic devices is also straightforward and does not require cleanroom facilities, unlike other materials. The process is termed soft lithography (Figure 1.11) and in addition to having low manufacturing costs, it also provides high replicating accuracy. The procedure consists of using a master mold where the microchannel design is defined, onto which a mixture of PDMS base and curing agent are cast over. The process of cross-linking and polymerization is then accelerated by heat (65℃ to 90℃ for 2 to 4 hours), and once it is complete the elastomer can be peeled off the master mold, creating a negative replica. [46] [47]

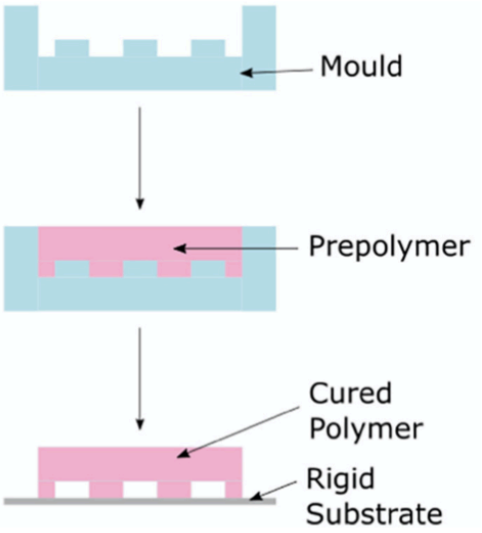

Figure 1.11: *Schematic representation of the soft lithography process. A mixture of PDMS base and curing agent are cast over a master mold where the microchannel design is defined, cross-linking and polymerization is then accelerated by heat (65℃ to 90℃ for 2 to 4 hours). The elastomer can then be peeled off the master mold. [44]*

Another advantage of using PMDS is that it can be easily bonded to various substrates through multiple processes, creating an irreversible, high-pressure seal. One method to do so is through plasma treatment. PDMS is inherently hydrophobic due to the methyl groups present on its surface, but upon exposure to oxygen it becomes hydrophilic and allows irreversible Si-O-Si bonds to form upon contact with another oxidized PDMS surface. [44] [47]

1.4.2 Microfluidic DNA amplification assays

The intrinsic characteristics of microfluidics make it an attractive platform for nucleic acid amplification assays. Given that DNA-based detection is a powerful tool for diagnostics moving it from centralized laboratories to POC platforms would allow for faster and more cost-effective diagnostic tools. Several nucleic acid amplification and microfluidic detection devices have been developed, taking

advantage of the reduced size allowing for faster reaction times, less reagent and sample consumption, as well as a more precise temperature control due to rapid heat conduction. [33] [34]

As PCR is the standard method for molecular diagnostics, several microfluidic platforms have been developed on the basis of the rapid heat transfer provided by the reduction in size, allowing for faster heating and cooling necessary for PCR reactions. These PCR chips can be divided into two categories: flow-through PCR chips, in which the sample is flown through 3 different temperature areas, or stationary PCR chips, where the sample remains stationary, and the temperature is cycled between the 3 reaction temperatures. [33] For example, a microfluidic chip with an integrated thermal cycler with a thin-film microheater and fan for rapid heating and cooling has been developed. The PDMS microfluidic device translated into a low-cost fabrication and allowed for a real-time optical detection of a fluorescence signal. [48]

However, for POC applications, the need for a thermal cycler complicates the device fabrication. Due to this an increasing amount of these platforms focus on isothermal amplification techniques, such as RCA and LAMP. Several microfluidic devices integrating LAMP for DNA or RNA detection have been developed, for example, a PDMS microchip for the detection of prostate-specific antigen gene. The device allowed for the detection of as little as 23fg/μL of the target DNA by performing LAMP at 65℃ with integrated detection using microchip electrophoresis or by the naked eye with a DNA intercalating dye. [49] There have also been several devices that integrate beads to capture of the target DNA or the amplified products, which allow for higher sensitivity due to the increased surface-to-volume ratio provided by the beads. A microfluidic system to detect MRSA that used specific probe conjugated magnetic beads for target DNA capture, followed by amplification through LAMP provided a limit of detection of 10fg/ μL, using a spectrophotometer to detect the LAMP amplicons. [50] Another example is a centrifugal microfluidic platform designed to detect Sars-Cov-2 viral RNA, which used dried n-benzyl-n-methylethanolamine modified agarose beads for signal amplification allowing fluorescence detection with a smartphone camera. This device allowed the detection of 100 to 1000 RNA copies in a 10μL reaction volume. [43]

Several other devices take advantage of the RCA technique, which can be performed at even lower temperatures. An example of such device is a platform developed for the detection of *V.cholerae*, which used RCA, circle-to-circle amplification and microchip electrophoretic detection, resulting in the detection of as little as 25ng of genomic DNA in less than 65min. [51] Another device, similar to the one developed in this work, used beads to capture and amplify the target *Salmonella* DNA through RCA, with a limit of detection of 10copies/μL. [52]

As hybridization in solution is generally more efficient than on a solid surface due to several factors, including molecule diffusion, another approach that has been developed involves performing RCA or circle-to-circle amplification in solution, and capture the amplification products in beads. The isothermal amplification of Zika Virus cDNA, performing circle-to-circle amplification combined with a

microfluidic affinity chromatography enrichment platform, allowed the detection of less than 17 viral RNA copies per reaction mixture. [53] Another device that incorporated circle-to-circle amplification used digital microfluidic droplets as reaction chambers to capture the target DNA, perform its amplification, and use magnetic particles to move the molecules between droplets. The amplification products were detected using fluorescently labeled oligonucleotides, allowing the detection of 1aM of synthetic *Pseudomonas aeruginosa* DNA. [54]

All these devices provide low detection limits, ideal for clinical diagnosis with reduced costs and analysis time compared to benchtop methods. Integrated and automatic microfluidic devices also help reduce contamination and human error, which together with all the other advantages provided by microfluidics makes them attractive platforms for POC diagnostics.

1.5 Objectives

The aim of this work was to develop a microfluidic rolling circle amplification module for bacterial detection. The system was optimized regarding several aspects, including the way of capturing the target DNA, the flow rates used, the influence of the saline conditions on the target DNA capture, as well as the on the rolling circle amplification assay. Quantification of the target DNA captured using this system was also done, with capture efficiencies ranging from 27% to 77% for concentrations of 250nM and 50nM, respectively. Upon an attempt at integration with a microfluidic cell lysis module several problems arose, leading to blocking optimization, that culminated in changing the detection oligonucleotides used to detect the amplified product. Lastly, the optimized rolling circle amplification module was tested for several concentrations of target DNA in order to access the system's amplification and detection rate. The final goal would be to capture and amplify DNA from a real sample of *Staphylococcus Aureus.*

2. Materials and Methods

2.1 Microfluidic structure fabrication

2.1.1 Hard mask fabrication

The fabrication process of the hard mask was performed under cleanroom conditions (INESC MN, 100/10), and all equipment and material used throughout the process are summarized in Table 2.1. The process started by cutting a 5x5*cm* piece of corning glass and cleaning it for 30min in an Alcanox solution with ultrasounds. The glass substrate was then rinsed with deionized water and blow-dried. Next, a 2000Å layer of aluminum was deposited by magnetron sputtering (Figure 2.1A), followed by a coating of a 1.5μm layer of photoresist using an SVG track.

***Table 2.1**-Summarized list of equipment, materials and reagents used for the hard mask fabrication.*

Equipment and Materials	AutoCAD software (Autodesk Inc., Mill Valley, CA/USA)
	Kerry ultrasonic cleaning bath, Guyson (Skipton, North Yorkshire, UK)
	Nordiko 7000 magnetron sputtering system, Nordiko Technical Services Ltd (Havant, Hampshire, UK)
	SVG resist coater and developer track, Silicon Valley Group Inc. (San Jose, CA/USA)
	DWL lithograph, Hiderberg Instruments (Heidelberg, DE)
	Glass substrate, Corning Inc (Corning, NY/USA)
Reagents	Alcanox solution, Alcanox Inc. (White Plains, NY/USA)
	Deionized water
	Photoresist PFR 7790, JSR (Sunnyvale CA/USA)
	Aluminum etchant TechniEtch Al 80, Microchemicals (Ulm,DE)
	Acetone (99,6%), LabChem Inc. (Zelienople, PA/USA)

The substrate is then baked for 1min at 85℃, followed by the transfer of the mask design, previously created in AutoCAD, to the photoresist by Direct Writing Lithography (DWL) (405nm,blue) (Figure 2.1B).

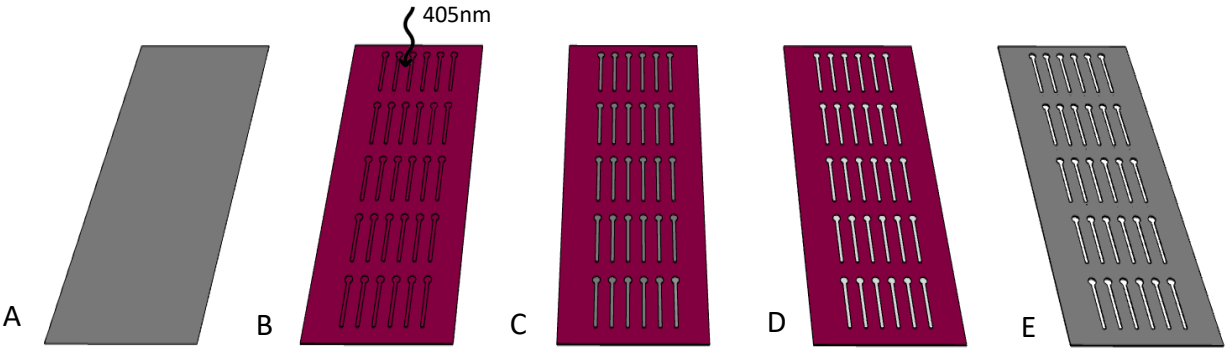

***Figure 2.1**: Schematic representation of the aluminum hard mask fabrication. A) Aluminum deposition B) Photoresist coating and DWL lithography. C) Photoresist development. D) Aluminum wet etching E) Final aluminum hard mask.*

The substrate is again baked for 1min at 110℃, and subsequently the photoresist is developed, leaving the selected parts of the aluminum exposed (Figure 2.1 C). Lastly, the exposed aluminum is etched by wet etching (Figure 2.1D) for 5min, and the remaining photoresist is removed with acetone.

The microfluidic structures used throughout this work have columns with two different heights. As such the fabrication of the final mold required the usage of two aluminum hard masks, that were fabricated following the process described above, one for the height of 100μm and one for the height of 20μm (Figure 2.2).

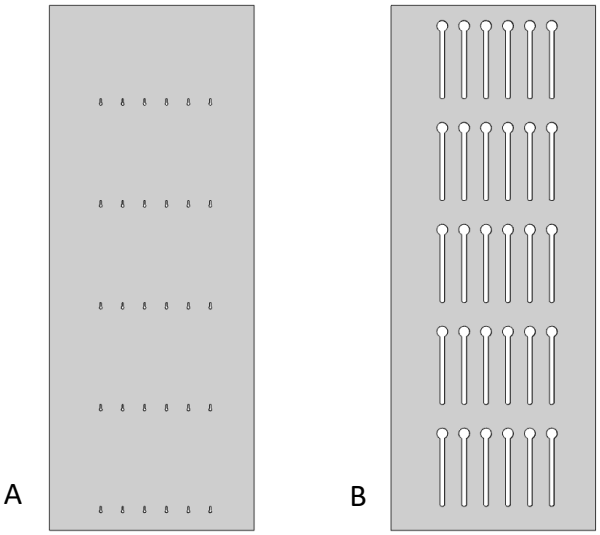

***Figure 2.2**: Schematic representations of the aluminum hard masks. (A) Hard mask for the 20 μm channel portion. (B) Hard mask for the 100 μm channel portion.*

2.1.2 Master mold fabrication

The two previously fabricated hard masks were used to fabricate the SU-8 master mold, for which the equipment and materials used are summarized in Table 2.2. Firstly, a silicon substrate was cleaned using acetone to remove any residues present on the surface and submerged in Alcanox for 20min in a hot water bath at 65℃. Afterwards, the substrate was washed with deionized water and isopropanol (IPA) and blow-dried to remove any remaining liquids.

The next step was the fabrication of the 20μm layer. An SU-8 layer was spin-coated on top of the silicon substrate in a two-step process. The first step was performed at 500rpm with an acceleration of 100rpm/min for 10sec followed by a second step performed at 2176rpm with an acceleration of 300rpm/min for 30sec. Afterwards, the substrate was placed onto a hotplate at 95℃ for 4min for a pre-exposure bake. After cooling down for 1min, the 20μm hard mask was placed with the aluminum surface facing down over the SU-8, then both the hard mask and silicon substrate were exposed to UV-light for 14sec (Figure 2.3 A). Following the UV-light exposure, the substrate was again placed onto a hotplate at 95℃ for 5min for a post-exposure bake. After cooling down for 2min, the substrate was submerged in a propylene glycol monomethyl ether acetate (PGMEA) 99% solution in order to develop the non-exposed photoresist. Lastly, the substrate was rinsed with IPA and blow-dried (Figure 2.3 B).

***Table 2.2**- Summarized list of equipment, materials and reagents for the SU-8 master mold fabrication.*

Equipment and Materials	Vertical laminar airflow cabinet, FASTER-BSC-EN (Cornaredo, IT)
	Spinner, Laurel Corp. (North Wales, PA/USA)
	Hotplate, Stuart (Staffordshire, UK)
	UV light, UV-KUB 2 Kloé SA (Montpellier, France)
	Stereo microscope, AmScope (Irvine, CA/USA)
	Silicon wafer, university Wafer (South Boston, MA/USA)
Reagents	Acetone (99,6%), LabChem Inc. (Zelienople, PA/USA)
	Deionized water
	IPA (99,9%), LabChem Inc. (Zelienople, PA/USA)
	PGMEA (99,5%), Sigma-Aldrich (St.Luis, MO/USA)
	Alcanox solution, Alcanox Inc. (White Plains, NY/USA)
	SU-8 2015 photoresist, Microchem Corp. (Newton, MA/USA)

Following the 20μm layer, the 100μm layer was fabricated. As for the 20μm layer, the process begins with the spin coating of SU-8 in a two-step process. The first step was performed at 500rpm with an acceleration of 100rpm/min for 10sec, followed by a second step performed at 1030rpm with an acceleration of 300rpm/min for 30sec. The substrate is then placed onto a hotplate at 65℃ for 10min followed by another 30min at 95℃ for a pre-exposure bake. After cooling down for 1min, the 100μm hard mask is placed on top of the SU-8 with the aluminum surface facing down and aligned with the previous structure, using a AMSCOPE microscope. Afterwards, both the substrate and the hard mask were exposed to UV-light for 60sec, followed by a post-exposure bake at 65℃ for 1min and 95℃ for

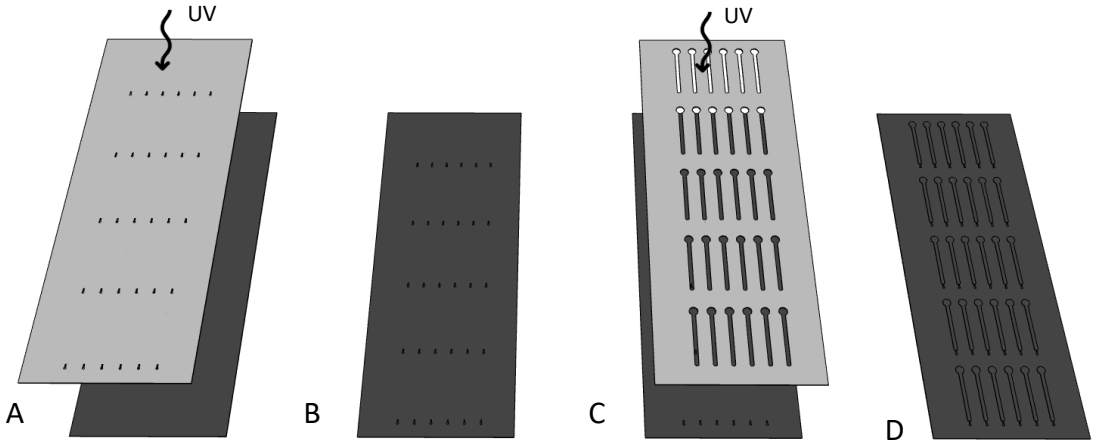

***Figure 2.3**: Schematic representation of the SU-8 master mold fabrication. (A) 20μm layer exposure to UV-light. (B) 20μm layer photoresist development. (C) 100μm layer mask alignment and exposure to UV-light. (D) 100μm layer photoresist development.*

another 10min (Figure 2.3 C). Subsequently, the substrate was submerged in a PGMEA solution in order to develop the non-exposed photoresist for 10min (Figure 2.3 D). Lastly, the substrate was rinsed with isopropanol, blow-dried and went under a final hard bake for 15min at 150℃.

2.1.3 PDMS structure fabrication

The PDMS microfluidic structures were fabricated using a soft lithography technique, for which all the equipment and materials are summarized in Table 2.3. Firstly, a mixture of curing agent and PDMS was prepared in a weight ratio of 1:10. The mixture was then placed in a vacuum for at least 40min in order to degasify. Subsequently, the elastomer was poured on top of the previously fabricated SU-8 master mold, fixed on a poly(methyl methacrylate) (PMMA) frame and placed in the oven at 70℃ for 90min to cure (Figure 2.4 A). After removing the cured PDMS from the oven, the structure was removed from the frame, and holes were punched in the inlets and outlets of the columns (Figure 2.3 B), using 18- and 20-Gauge needles, respectively.

***Table 2.3**-Summarized list of equipment, materials and reagents used for the PDMS microfluidic structure fabrication.*

Equipment and Materials	Analytical scale d=0.0001g, Scientech (Bradford, MA/USA)
	Vacuum desiccator, Bel-Art Products (South Wayre, NJ/USA)
	Oven loading model 100-800, Memmert (Schwabach,DE)
	Spin coater, Laurel Corp. (North Wales, PA/USA)
	Expanded oxygen plasma cleaner PDC-002-CE, Harrick Plasma (Ithaca, NY/USA)
	Silicon wafer, university Wafer (South Boston, MA/USA)
	Rounded syringe tips (20 and 18 Guage), Instech Laboratories, Inc. (Plymouth Meeting,PA/USA)
Reagents	Sylgard 184 PDMS and curing agent kit, Dow Corning (Midland, MI/USA)

In order to seal the microfluidic structures, a PDMS membrane was also fabricated. The PDMS and curing agent mixture was prepared and left in the vacuum to degasify, as mentioned previously. After degasifying, the mixture was poured on top of a silicon wafer, and placed in a spinner, spinning at 250rpm, with an acceleration of 100rpm/min for 25sec, in order to obtain a thickness of 500μm. Afterwards, the membrane was placed in the oven at 70℃ for 90min to cure and was then cut into pieces, slighter bigger than the microfluidic structure (Figure 2.3 C).

To perform the sealing, both the structure and the cut membrane were placed in a plasma cleaner for 60sec at medium intensity. The oxygen plasma treatment oxidizes the surfaces, allowing Si-O-Si bonds to be formed, and when placed in contact with each other, after the treatment, the creation of a strong seal, between the two surfaces.

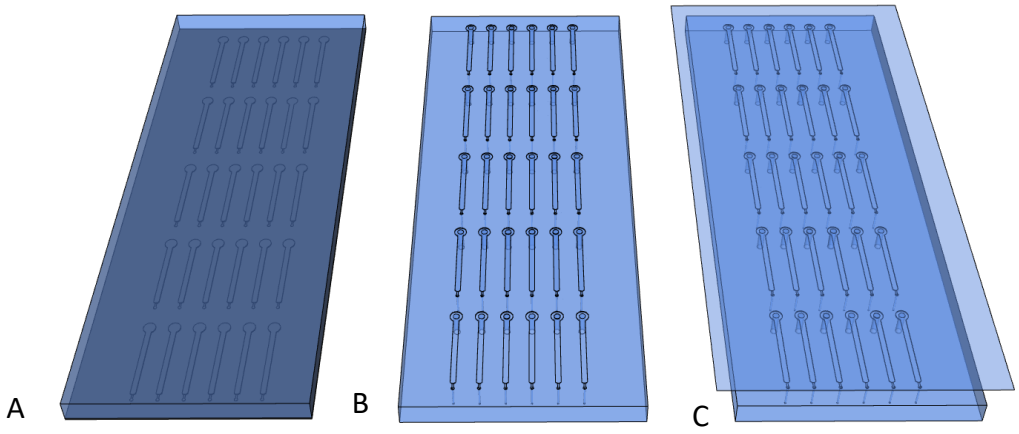

***Figure 2.4**: Schematic representation of the PDMS microfluidic structure fabrication. (A) Pouring and curing of the curing agent and PDMS mixture onto the SU-8 mold. (B) Punching the holes in the inlets and outlets of the PDMS structure. (C) Sealing of the microfluidic structure.*

2.2 Biological Assays

2.2.3 Solutions

In all assays that were performed throughout this work several solutions had to be prepared. All reagents used for the solutions are summarized on Table 2.4.

***Table 2.4**- Summarized list of the reagents used in the preparation of solutions.*

Reagents	**General usage**		PBS 10x, Thermo Fischer (USA)
	Saline Conditions and specificity assays		GenoLyse ® KIT for Extraction of Bacterial DNA, Hain Lifescience (Nehren, Germany)
			B-PER™ Bacterial Protein Extraction Reagent 78243, Thermo Fischer Scientific (USA)
	Blocking assays		Polyacrylate (PAA) 45% (w/w) 416029, Sigma- Aldrich (USA)
	Rolling Circle Amplification assays	**All solutions**	Bovine Serum Albumin 98% (BSA) A7906, Sigma-Aldrich (USA)
			MiliQ Water
		Ligation Solution	T4 DNA Ligase, SciLifeLab (Sweden)
			T4 DNA Ligase 10x Reaction Buffer, SciLifeLab (Sweden)
			ATP, Thermo Fischer Scientific (USA)
		Amplification Solution	dNTPs, SciLifeLab (Sweden)
			Phi29 Polymerase, SciLifeLab (Sweden)
			Phi29 Polymerase Reaction Buffer, SciLifeLab (Sweden)
		Detection Oligonucleotides Solution	Hybridization Buffer (1.4 M NaCl, 0.01% TWEEN® 20, 20 mM of Tris-HCl, pH 8 and EDTA)

Phosphate Buffered Saline (PBS) was used in all assays in the preparation of several solutions and was prepared by diluting a 10x PBS solution down to 1x in MiliQ Water. A BSA solution was used as blocking for the channel walls in the rolling circle amplification assays, as well as in the preparation of several solutions, and was prepared from a stock solution diluted to a 4% (w/v) with PBS.

During the blocking optimization experiments, several blocking strategies were tested, one of these strategies was Sodium Polyacrylate (PA) 8000 (average molecular weight), which was diluted with PBS to a 5% (w/w) working solution.

2.2.2 Column packing

Along this work two types of beads, Q-Sepharose and streptavidin agarose beads, were used to immobilize DNA (Figure 2.5). The Q-Sepharose beads are strong ion exchangers, with 6% agarose and quaternary ammonium (Q) ion exchange groups. Their positively charged surface allows for the electrostatic immobilization of the DNA. The streptavidin agarose beads, which are cross-linked agarose beads covalently coupled with streptavidin, on the other hand, allow the immobilization of biotinylated DNA trough streptavidin-biotin bond.

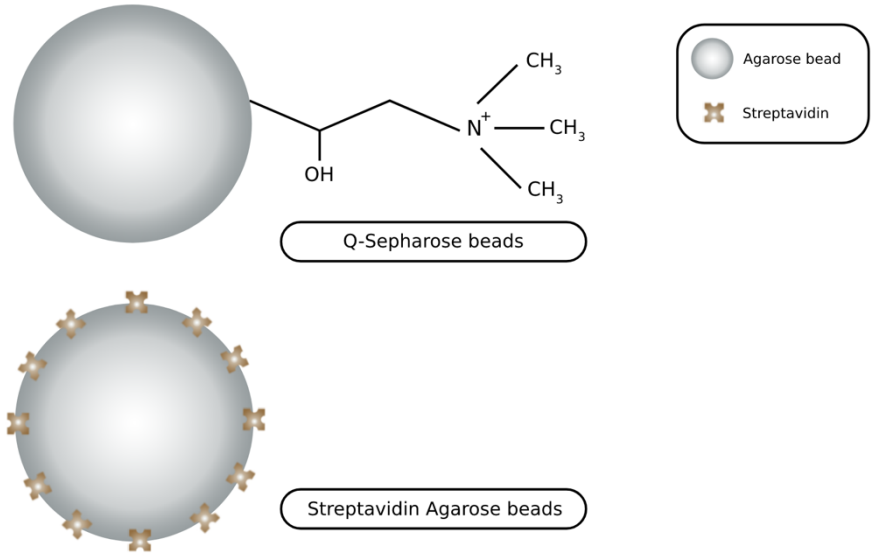

***Figure 2.5**: Schematic representation of the beads surface functionalization.*

All the equipment and materials used to pack the columns with the desired beads are summarized in Table 2.5. In order to pack the columns, a pumping system, comprised of a syringe pump

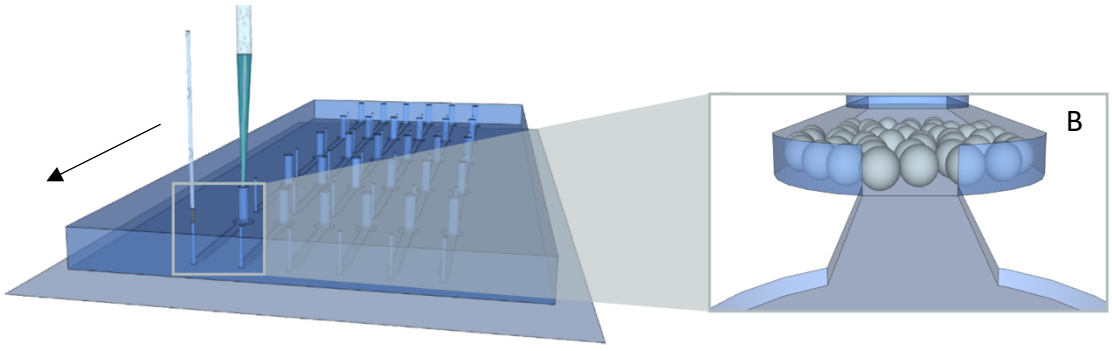

***Figure 2.6:** Schematic representation of the column packing procedure. (B) The trapping of the beads in the column.*

was used. The syringes were connected to the microfluidic structures through tubing and metal adaptors at the outlets, and the bead solutions were flown through the channel by placing a pippete tip with the desired bead solution at the inlet and pulling the solution from the outlet, using a flow rate of 5μL/min, creating negative pressure inside the column (Figure 2.6).

***Table 2.5**- Summarized list of equipment and materials used for column packing.*

Equipment and Materials	Syringe pump NE-1002X, New Era Pump Systems, Inc. (Farmingdale, NY/USA**)**
	Insulin syringe 1*mL* U-100 Luer-Lock, Codan (Lensahn, DE)
	Polyethylene tubing (BTPE-90), Instech Laboratories, Inc. (Plymouth Meeting, PA/USA)
	Rounded syringes tips (20 and 18 Gauge), Instech Laboratories, Inc. (Plymouth Meeting, PA/USA)
	Tubing adapters SC20/15, Instech Laboratories, Inc. (Plymouth Meeting, PA/USA)
	Q-Sepharose ™ Fast Flow beads, GE Healthcare Bio-Sciences AB (Uppsala, Sweden)
	Streptavidin Agarose beads, EMD Milipore Corp USA, Merck kGaA (Darmstadt, Germany)

As represented in Figure 2.6B, the beads are trapped inside the column using a step strategy. The column has a height of 100μm followed by a smaller channel with a height of 20μm, and since both the Q-Sepharose and Streptavidin Agarose beads have a diameter larger than 20μm (90 and 40-165 μm, respectively) they become trapped in the column.

2.2.3 Fluid handling

Throughout this work the fluid handling was done using a pumping system comprised of a syringe pump which was able to push the liquids inside the syringes, creating a positive pressure inside the column, making the solutions flow through the columns.

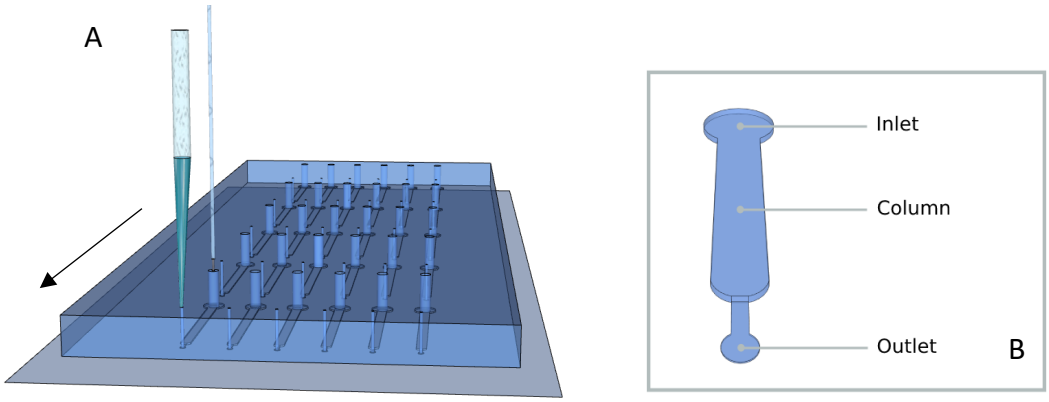

***Figure 2.7:** Schematic representation of fluid handling in the microfluidic device. (A) Metal adaptors are used to connect the tubing from the syringe operated by a syringe pump to the PDMS punched holes, and a pipette tip is used to collect the solution after flowing through the column. B) Representation of the microfluidic channel.*

The syringes were connected to tubing and metal adaptors and filled with PBS, followed by an air gap, before the desired solution was pulled into the tubing, and placed in the punched holes in the inlet, (Figure 2.5A) allowing the desired solutions to flow through the columns, which were then collected at the outlet, by a pippete tip. The equipment and materials used are summarized in Table 2.4.

***Table 2.6**- Summarized list of equipment and materials used for fluid handling.*

Equipment and Materials	Syringe pump NE-1002X, New Era Pump Systems, Inc. (Farmingdale, NY/USA**)**
	Insulin syringe 1 *mL* U-100 Luer-Lock, Codan (Lensahn, DE)
	Polyethylene tubing (BTPE-90), Instech Laboratories, Inc. (Plymouth Meeting, PA/USA)
	Rounded syringes tips (20 and 18 Gauge), Instech Laboratories, Inc. (Plymouth Meeting, PA/USA)
	Tubing adapters SC20/15, Instech Laboratories, Inc. (Plymouth Meeting, PA/USA)

2.2.4 DNA Oligonucleotides

In all assays performed along this work, several synthetically modified oligonucleotide sequences were used, and are summarized in Tables 2.7 and 2.8.

***Table 2.7**- Summarized list of the source and storage conditions of all oligonucleotides.*

Oligonucleotides	Purchased from	Storage conditions
Padlock probe	Integrated DNA Technologies (Leuven, Belgium)	-20℃ in aliquots of 100μM
Padlock	Integrated DNA Technologies (Leuven, Belgium)	
Complementary target ssDNA	Integrated DNA Technologies (Leuven, Belgium)	
Biotinylated Detection Oligonucleotides	SciLifeLab (Sweden)	
Non-complementary target ssDNA	Stabvida Genomics Lab (Caparica, Portugal)	
Non-complementary target ssDNA	Stabvida Genomics Lab (Caparica, Portugal)	
Complementary target ssDNA labeled with Atto-430LS	Integrated DNA Technologies (Leuven, Belgium)	
Detection Oligonucleotides (complementary to padlock probe)	SciLifeLab (Sweden)	-20℃ at 100μM in TE buffer
Detection Oligonucleotides (non-complementary to padlock probe)	Eurogentec (Seraing,Belgium)	
Detection Oligonucleotides (non-complementary to padlock probe)	Eurogentec (Seraing,Belgium)	
Amplirun *S.aureus* DNA control $mecA^-$ (genomic DNA)	Vircell (Granada, Spain)	-20℃ in aliquot of 14,000 copies/mL

All oligonucleotide sequences were kept in the conditions described above and were then serially diluted with PBS to the concentrations used in the assays, with the exception of the detection

oligonucleotides, which were diluted in Hybridization Buffer. The padlock probe modification at the 5'end with a biotin molecule was to allow the biding of the synthetic oligonucleotide sequence to the Streptavidin Agarose beads. Several oligonucleotides were modified at the 5'end with a fluorophore, either Cy3 or Atto-430LS, both for the optimization, capture quantification and rolling circle amplification assays. The Cy3 fluorophore has an excitation peak at 555nm and emission peak at 569nm, and the Atto-430LS has an excitation peak at 433nm and an emission peak at 545nm.

***Table 2.8**- Summarized list of the oligonucleotides sequences used in this work, as well as their modifications (mod) and usage.*

Oligonucleotides	**Sequence (5'-3')**	**5' mod**	**3' mod**	**Used for**	
Padlock probe (31bp)	TTTTTTTTTTGTAAGACAC TATTACTGAGGA	Biotin	none	Immobilization on the beads	**All assays**
Padlock (90bp)	TGCTTTGTTTCAGGTGTAG TGTATGCAGCTCCTCAGT AATAGTGTCTTACGGCAT CACTGGTTACGTCTGTCT CTACACCTTTTTTAGGA	PO4-phosphorilation	none	Hybridization with padlock probe and target DNA capture	
Complementary target ssDNA (90bp)	TTAAATTAATGTACAAAGG TCAACCAATGACATTCAGA CTATTATTGGTTGATACAC CTGAAACAAAGCATCCTA AAAAAGGTGTAGAGA	Atto-430LS	none	Target molecule	**Optimization assays (flow rate and saline conditions) and capture quantification assays**
Biotinylated Detection Oligonucleotides (31bp)	AAAAAAAAAACATTCTGTG ATAATGACTCCT	Biotin	none	Blocking of non-specific signal	**Blocking assays**
Non-complementary target ssDNA (22bp)	CGTGTCGTTCACATCTGT CCGT	Atto-430LS	none	Negative control	**Specificity assays**
Non-complementary target ssDNA (29bp)	TCGCGACATTCATTATGC CCAATTTTTAA	Atto-430LS	none	Negative control	
Complementary target ssDNA (90bp)	TTAAATTAATGTACAAAGG TCAACCAATGACATTCAGA CTATTATTGGTTGATACAC CTGAAACAAAGCATCCTA AAAAAGGTGTAGAGA	none	none	Target molecule	**Rolling circle amplification assays**
Detection Oligonucleotides (complementary to padlock probe) (31bp)	AAAAAAAAAACATTCTGTG ATAATGACTCCT	Cy3	none	Molecule used for detection of amplified product	
Detection Oligonucleotides (24bp)	GGCATCACTGGTTACGTC TGTTTT	Cy3	none	Molecule used for detection of amplified product	
Detection Oligonucleotides (24bp)	GGCATCACTGGTTACGTC TGTTTT	Atto-430LS	none	Molecule used for detection of amplified product	

2.3 Analysis Methodology

2.3.1 Fluorescence measurements

In order to obtain the fluorescence measurements necessary for this work, a Leica DMLM fluorescence microscope coupled to a DFC300FX camera was used. All images throughout the work were acquired under the same conditions, using a 10x magnification, gain of 1x, gamma of 1x and exposure time of 1sec. In this work two different fluorophores were used as labels, with different excitation and emission wavelengths, Cy3 and Atto-430LS. For the experiments using Atto-430 LS as a label, a blue excitation filter was used, with a band-pass excitation of 450-490nm and a long-pass emission of 510nm, and for the experiments using Cy3 as a label, a green excitation filter was used, with a band-pass excitation of 560/40nm and a long-pass emission of 595nm.

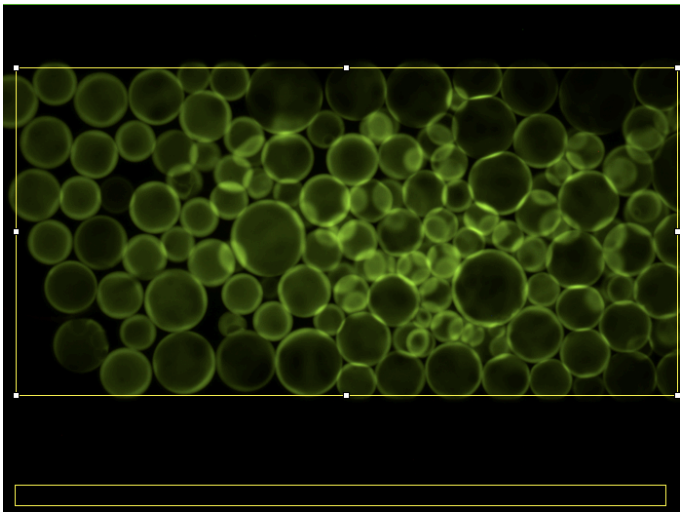

***Figure 2.8**: Fluorescence analysis methodology using ImageJ software.*

To analyze the images obtained from the microscope, the ImageJ software was used. The software separates the images into 3 channels: green, blue and red, and the channel chosen to analyze a given image is based on the observed fluorophore's emission. In order to retrieve the desired fluorescence measurements, a rectangular area inside the column, packed with beads, was selected in order to obtain an average fluorescence over the entire area, as well as a smaller rectangular area outside the column in order to obtain the average background fluorescence (Figure 2.8). The measurements from the background are then subtracted to the fluorescence from the beads to attain the absolute fluorescence.

3. Results and discussion

3.1 Rolling circle amplification using a padlock probe as a target sample

In previous work, a microfluidic module for a rolling circle amplification assay was developed (Figure 3.1). In the beginning of this work, this assay was used in order to understand the working principles of the rolling circle amplification process, its optimization, as well as the need for a different system.

As the RCA is an isothermal amplification technique, the entire assay is performed at 37℃ since it is the optimal reaction temperature for both the enzymes that were used. Firstly, the microfluidic channel was packed with streptavidin beads and blocked by flowing 4% BSA at 2.5μL/min. The biotinylated target DNA (10nM) and padlock (100nM) were then flown into the channel at 0.5μL /min for 40min, binding to the streptavidin beads, hybridizing and circularizing, respectively. In solution is also present the T4 DNA ligase enzyme (0.2U/μL), ATP (0.5mM), BSA (0.04%) as well as the T4 DNA ligase reaction buffer (1X), diluted with MiliQ water. Next, the amplification solution is flowed through the channel at 0.25μL/min for 60min with the Phi29 polymerase enzyme (0.5U/μL), dNTPs (0.4mM), Phi29 reaction buffer (1X) and BSA (0.053%) diluted in MiliQ water. The amplification products are then detected by flowing, at 2.5μL/min, a solution with a sequence of biotinylated detection oligonucleotides complementary to the amplified product bound to Quantum Dots through the streptavidin-biotin interaction. Afterwards, a wash is performed, in order to remove any unbound detection nucleotides, with hybridization buffer at 2.5μL/min for 2min.

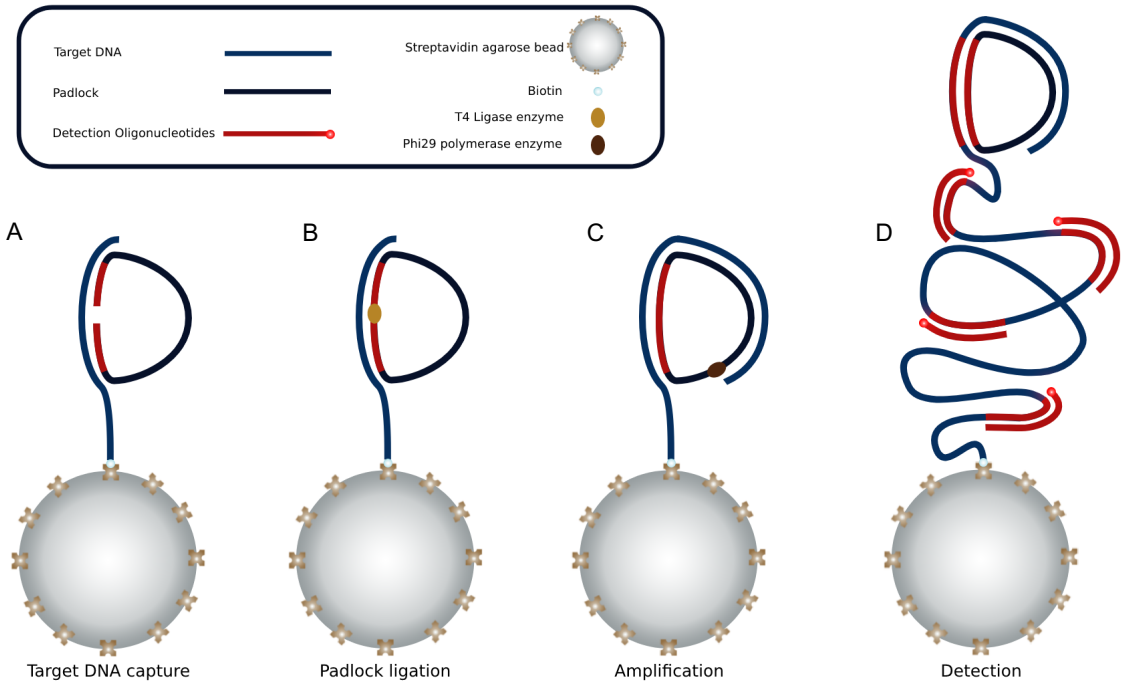

Figure 3.1: *Schematic representation of the RCA assay. A) Capture of the biotinylated target DNA on the streptavidin beads, and hybridization with the padlock. B) Ligation of the padlock with T4 DNA ligase. C) Amplification of the complementary padlock sequence using the Phi29 DNA polymerase. D) Detection of the amplified product by hybridizing a Quantum Dot labelled detection oligonucleotide sequence with highlighted section of the amplified sequence.*

All conditions for the amplification process were optimized using this assay, including the flow rates used, enzyme, ATP and dNTPs concentrations. For this work only one experiment following this protocol was performed, with a fluorescence signal of 52873.322 A.U, using a UV filter, an exposure time of 510ms, a gain of 1x and magnification of 10x. From this it is possible to conclude that the amplification products can be detected with a very strong fluorescent signal, since the detection oligonucleotides bound to the Quantum Dots are complementary to the highlighted section of the padlock (Figure 3.1), and if no amplification occurs the detection oligonucleotides will have no complementary DNA strand to hybridize to. The same principle applies if there is no biotinylated target DNA present, as the padlocks won't be able to circularize for the amplification to occur or bind to the beads and therefore no fluorescence signal will be obtained.

The T4 ligase catalyzed reaction ensures a high specificity for the target DNA hybridization, as even a single mismatched base pair at the site of ligation strongly inhibits the reaction. The T4 ligase joins the two DNA strands through the formation of a phosphodiester bond which requires ATP, and so one optimization that was performed was the addition of ATP to the ligation solution, in order to have a higher reaction yield. Another factor that contributes to a higher yield was the prior blocking of the channel walls with BSA, as well as its addition to both the ligation and amplification solutions, as it acts as a sacrificial protein, reducing interactions between the enzymes and inhibitory molecules, as well as preventing adsorption of the enzymes to the channel walls. [55] [56]

Despite the robustness of this method, it cannot be used with a real sample of target DNA since it has to be biotinylated in order to bind to the beads, allowing for the amplification process to occur in the microfluidic channel. This led to the need of developing a different method for the capture of the target DNA, which was the focus of this work.

3.2 Rolling circle amplification using a *Staphylococcus Aureus* DNA strand as a target sample

3.2.1 Target DNA capture optimization

In order to overcome the shortcoming of the previous method of capturing the target DNA to amplify it, this method was developed. The biotinylated padlock probe is bound to the beads through the biotin-streptavidin bond and hybridized to the back of the padlock, leaving the end strands free to which the target DNA will hybridize to, as represented in Figure 3.2

To prove that the concept worked two different experiments were performed, in order to understand which would be the best strategy to capture the target DNA. For both strategies, the channel is packed with streptavidin beads, followed by a wash with PBS with a flow rate of 5μL/min for 1min. In the first strategy, which will be referred to as the target DNA capture with no incubation, the padlock probe (100nM) is first flown through the channel at 1μL/min for 20min followed by simultaneously flowing the padlock (250nM) and target DNA labelled with Atto-430LS (250nM) at a flow rate of 1μL/min for

20min. In the second strategy, which will be referred to as the target DNA capture with incubation, the padlock probe (100nM) and padlock (250nM) were simultaneously flown through the channel at a flow rate of 1μL/min for 20min followed then by the flow of the target DNA labelled with Atto-430LS (250nM) using a flow rate of 1μL/min for 20min. In both strategies, after flowing all the solutions, a wash with PBS is again performed to remove any unbound molecules at 5μL/min for 1min. The controls for both experiments were performed following the protocols above, but with no padlock probe present.

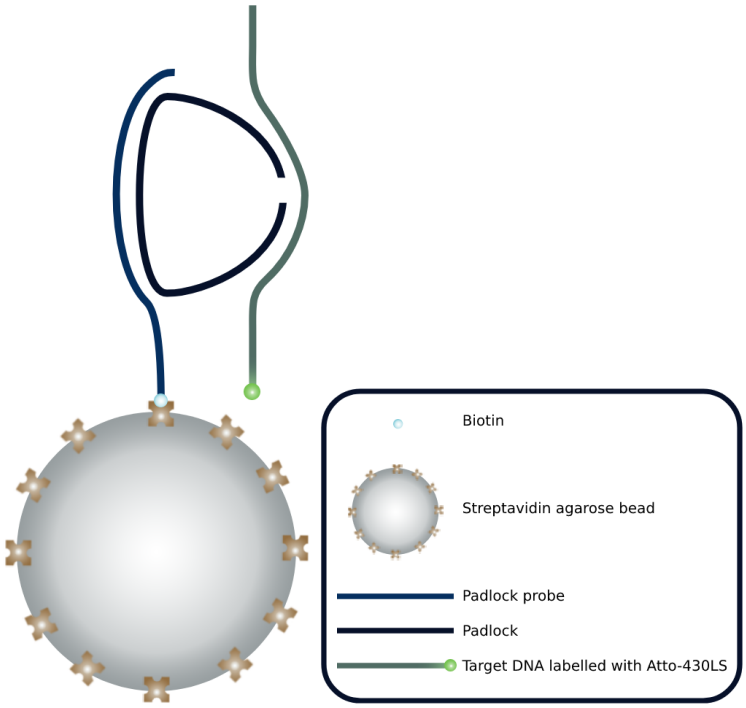

Figure 3.2: *Schematic representation of the target DNA capture. The padlock probe is bound to the streptavidin bead through the biotin-streptavidin bond and hybridized to the padlock, which in turn is hybridized to the target DNA.*

The two strategies were tried for different reasons, the target DNA capture without incubation was performed in that way due to the similarity of the capture method used in the RCA assay described in the previous section. The reasoning behind the target DNA capture with incubation is the fact that the end-goal of this work will be to have an integrated device in which the target DNA will come from a sample collected at the time the assay is performed, and the padlock probe and padlock will already be present in the device.

The results are presented in Figure 3.3, and it is possible to see that the capture of the target DNA with incubation presented a slightly higher fluorescence signal than without incubation. Although, when taking into account the variability, the difference between the two strategies is very small, it may be due to the fact that in the microchannel the molecules are moving mainly through diffusion. The DNA diffusion coefficient is very low, and when capturing the target DNA without incubation, flowing the padlock and target DNA simultaneously implicates that the padlock hybridizes to the padlock probe and the target DNA hybridizes to the padlock, and the likelihood of both events taking place is smaller than just the target DNA hybridizing with the padlock already immobilized on the surface, as is the case for

the capture with incubation. [57] Hence, for all the following experiments the target DNA capture with incubation was the chosen method.

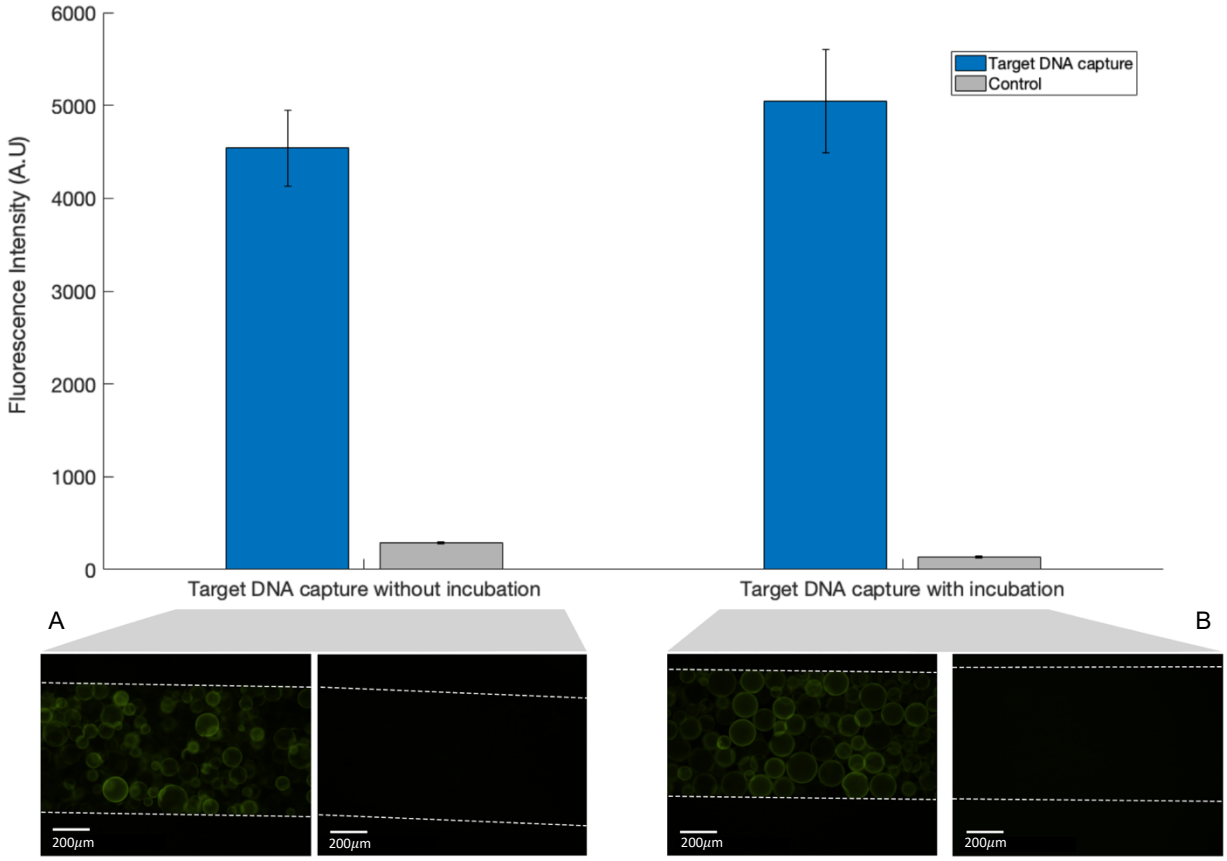

Figure 3.3: *Target DNA capture with and without incubation. The error bars in the graphic are the standard deviation of the measured signal of two experiments. A) Experimental images for the positive and control of the target DNA capture without incubation. B) Experimental images for the positive and control of the target DNA capture with incubation. (Leica DMLM microscope, Exposure time: 1s, Gain: 1X, Magnification: 10X)*

Both controls showed a very low signal, highlighting the fact that without the padlock probe it is not possible to capture the padlock, and consequently the target DNA. This also points out that even though the agarose beads are porous, the DNA strands don't become trapped in these pores and specifically bind to the beads through the streptavidin-biotin bond.

3.2.1.1 Flow Rate Optimization

In order to enhance the capture of the target DNA, several flow rates were tested. In these experiments, all concentrations, volumes, and washes were the same ones as described above and maintained constant. The only parameter that changed was the flow rate used for both the padlock probe and padlock solution, as well as the target DNA solution. Four different flow rates were tested, 0.25μL/min, 0.5μL/min, 1μL/min and 1.5μL/min, and the results are presented in Figure 3.4. It is noticeable that there is a large difference between the two higher flow rates (1.5μL/min and 1μL/min) and the two lower ones (0.25μL/min and 0.5μL/min), but that the difference between either the two

higher flows and the two lower ones is very small, particularly when taking into account the variability of the experiment.

These results can be explained by the fact that even though, as stated earlier, the transport in the microchannel occurs mainly through diffusion, due to the pumping system that is used in these experiments, convective transport in the direction of the fluid flow also has to be considered, particularly when different flow rates are being compared. As the DNA diffusion coefficient is very small, when

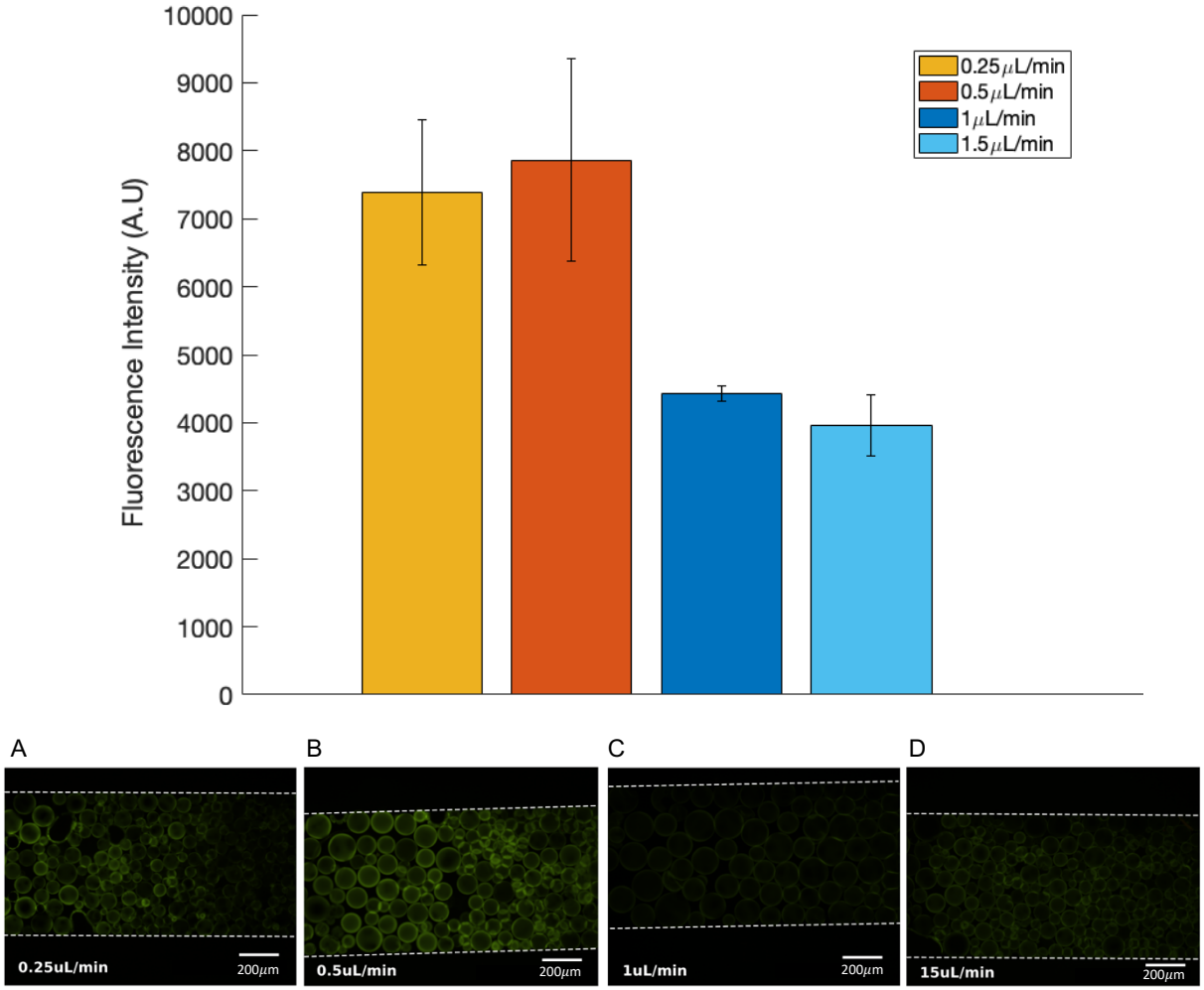

Figure 3.4: *Flow rate optimization for the capture of the target DNA. The error bars in the graphic are the standard deviation of the measured signal of two experiments. A) B) C) and D) Experimental images for the target DNA capture using flow rates of 0.25μL/min, 0.5μL/min, 1μL/min and 1.5μL/min, respectively. (Leica DMLM microscope, Exposure time: 1s, Gain: 1X, Magnification: 10X)*

flowing DNA through a microchannel, the Peclet number is often greater than 1, and particularly with higher flow rates, the convective transport becomes more relevant than diffusion. Therefore, with higher flow rates a large number of the target DNA molecules will pass over the immobilized padlock probe and padlock instead of diffusing into them and hybridizing, leading to a reduced capture of the target DNA. [45] The similarity between both higher flow rates can be explained by the fact that in both cases the rate between convective and diffusive transport, although higher for a 1.5μL/min flow rate, may be very similar. The same principle applies for the similarity between both lower flow rates, as diffusive transport becomes more relevant for the 0.25μL/min than the 0.5μL/min flow rate. Therefore, the

hybridization becomes again limited due to the fact that the padlock probe and padlock have to slowly diffuse through the channel, to hybridize and bind to the beads, as well as target DNA to the immobilized padlocks, even though the rate between convective and diffusive transport is very similar for both flow rates. Hence, the flow rate of 0.5μL/min provided the highest target DNA capture, due to the optimal compromise between convective and diffusive transport it allows and was the chosen flow rate to perform the following experiments.

3.2.1.2 Saline Conditions

In order to understand the DNA hybridization kinetics in different saline conditions, the target DNA capture assay was performed, flowing the target DNA labeled with Atto-430LS in 4 different solutions, presented in Table 3.1. All experiments were performed using the same volumes and concentrations of DNA as the previous ones and the established flow rate of 0.5μL/min, only changing the buffer to which the target DNA was added.

The choice of these solutions comes again from the fact that the end-goal of this project is to have an integrated device to insert a sample collected at the time of the assay, extract the DNA and amplify it. To extract the bacterial DNA, a microfluidic chemical cell lysis module was developed in previous work [58] in which the Genolyse ® DNA extraction kit is used together with B-PER™. To understand if the extracted DNA could be directly captured in the device after cell lysis, target DNA in solutions of lysis buffer and B-PER™, as well as lysis buffer, B-PER™ and neutralization buffer were flown through the microfluidic channel with the padlock probe and padlock previously immobilized on the beads. To amplify the extracted DNA, using the previously developed RCA protocol, the T4 DNA ligase enzyme requires a reaction buffer in order to optimize its activity. Another alternative to capture the DNA in an integrated device would be to clean the solution after cell lysis and flow the target DNA in the ligation solution, which contains the T4 DNA ligase mixed in its reaction buffer and MiliQ water. Hence, the target DNA was also flown through the channel in this ligation solution with the padlock probe and padlock previously immobilized on the beads.

***Table 3.1**- Composition of the solutions used in the saline condition optimization experiments.*

Target DNA Atto-430LS label (5uL) **PBS – 15uL**	Target DNA Atto-430LS label (5uL) **1x T4 DNA Ligase Reaction buffer (2uL) MiliQ water (13uL)**	Target DNA Atto-430LS label (5uL) **Genolyse Lysis Buffer and B-PER (1:1) – to make 20uL**	Target DNA Atto-430LS label (5uL) **Genolyse Lysis Buffer and B-PER (1:1) Neutralization Buffer (2:1) – to make 20uL**

The results for these experiments are presented in Figure 3.5, and it is noticeable, that as expected, using PBS as the buffer for the target DNA hybridization with the padlock provided the best results. This is due to the fact that DNA hybridization is affected by multiple factors, which include pH and salt concentrations.

Regarding the ligation solution, containing $2\mu L$ of reaction buffer and $13\mu L$ of MiliQ water, it is safe to assume that the salt concentrations will be lower given that MiliQ water has very few ions, and the T4 DNA Ligase reaction buffer is very diluted. Given that DNA possesses negative charges along the phosphate backbone, which pose an electrostatic barrier for hybridization to occur, the presence of salts in the solution helps to mask those charges, reducing the electrostatic repulsions, and allowing DNA strands to approach with lower energies. Since the ligation solution has lower salt concentrations, it becomes harder for DNA to hybridize, giving rise to higher stringency conditions, decreasing the capture of the target DNA.

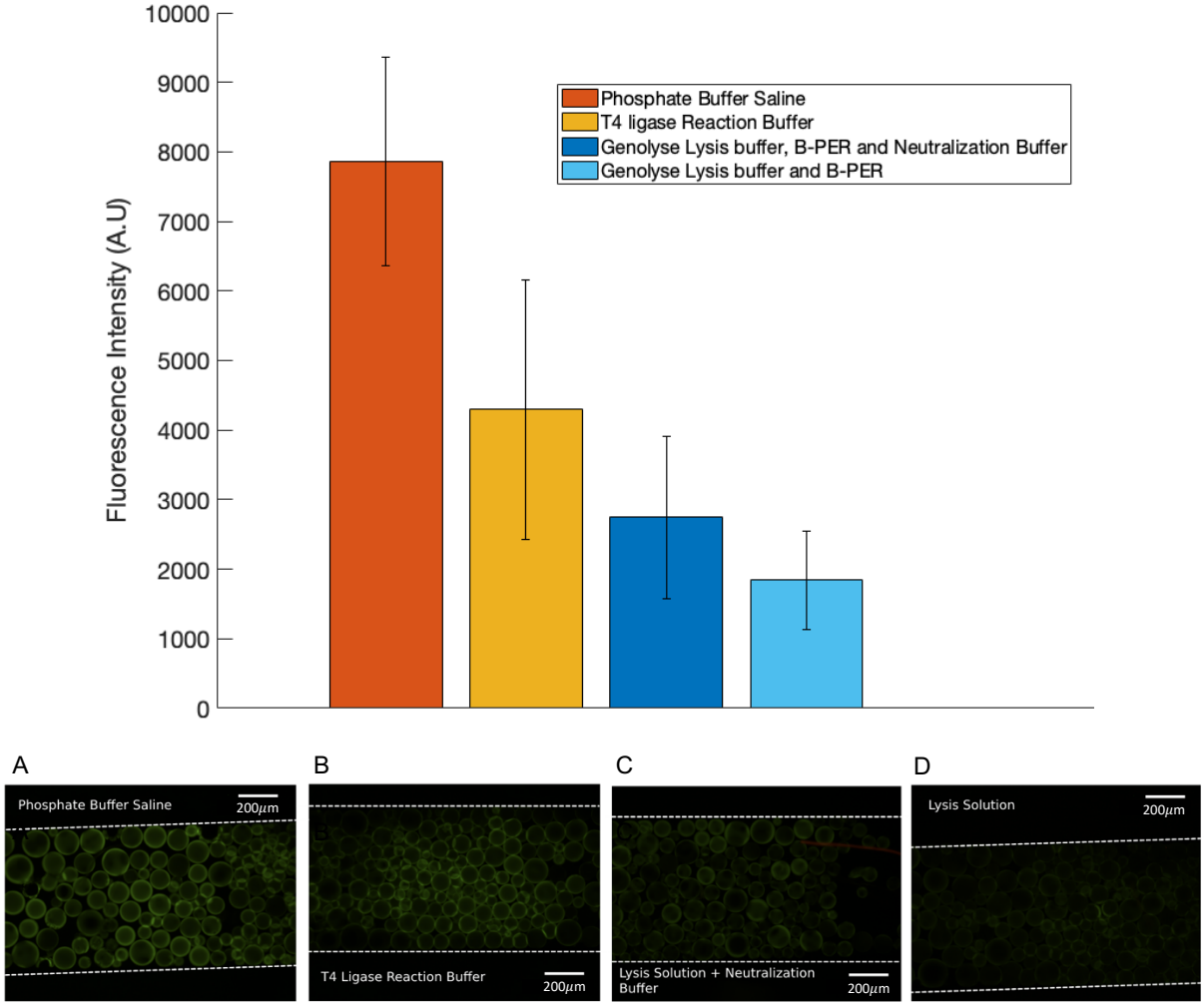

Figure 3.5: *Effects of saline conditions on the Target DNA capture. The error bars in the graphic are the standard deviation of the measured signal of two experiments. A) B) C) and D) Experimental images for the target DNA capture in PBS, T4 DNA Ligase reaction buffer solution, Lysis buffer, neutralization buffer and B-PER solution and Lysis buffer and B-PER solution, respectively. (Leica DMLM microscope, Exposure time: 1s, Gain: 1X, Magnification: 10X)*

Regarding both lysis solutions, the dominant effect responsible for the lower signal is the pH. The optimal pH for DNA hybridization and duplex stability is physiological pH, and lysis buffers act by increasing the pH (usually between 11.5 and 12.5 [59]) to break the cell membrane. The increase in pH makes the DNA bases become more hydrophilic and soluble, making it more difficult for them to interact with complementary bases, destabilizing the duplex. This is coherent with the results, especially given

that when the neutralization buffer, which is supposed to decrease the pH, is added to the solution the signal increases slightly, compared with the lysis solution with no neutralization buffer.

Lastly, although the target DNA capture is less efficient in both the lysis and ligation solutions than in PBS, it is still possible to capture it in all of them, indicating that in an integrated device it might not even be necessary to clean the solution after cell lysis, which would complicate the process and make it more time-consuming.

3.2.1.2 Specificity

Following the saline condition experiments, another two target DNA capture assays were performed, using the same volumes, concentrations, and flow rates as before, but this time with DNA strands non-complementary (ncDNA) to the padlock. The experiment was performed for 2 different

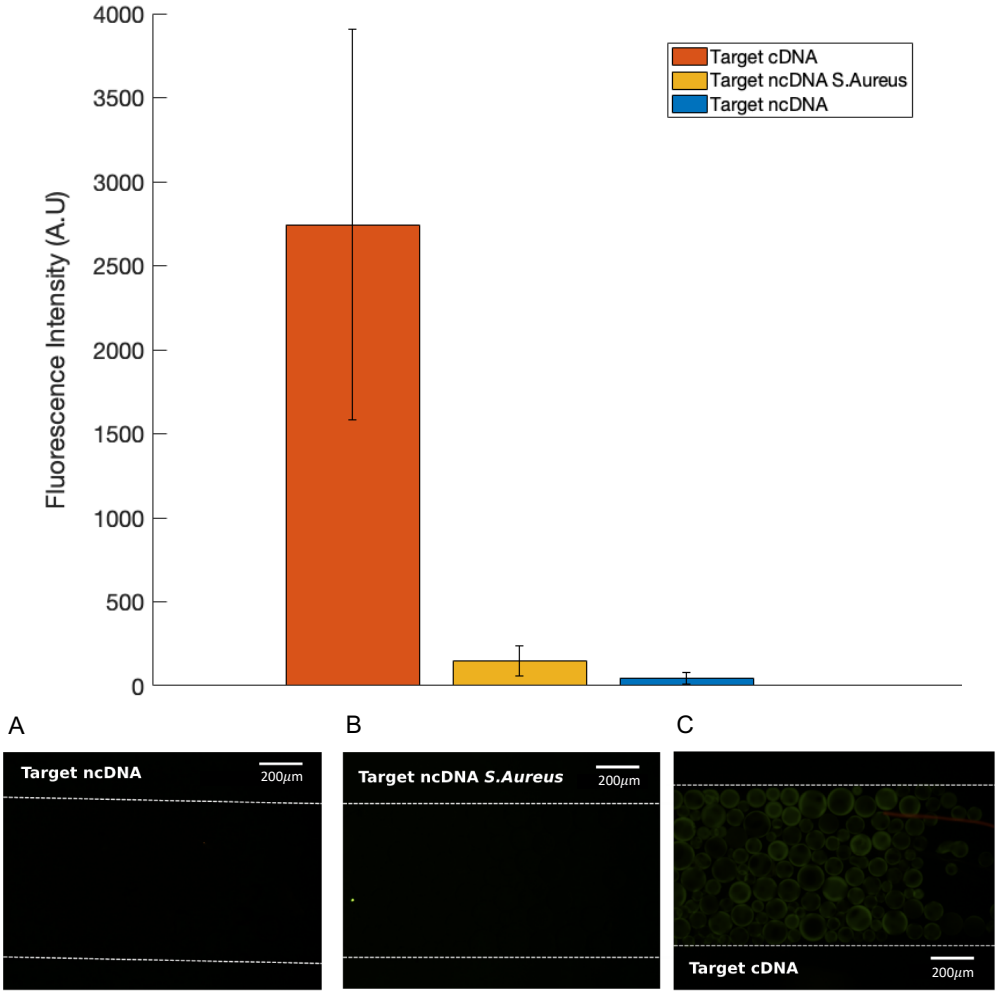

Figure 3.6: *Specificity of the target DNA capture assay. The error bars in the graphic are the standard deviation of the measured signal of two experiments. A) B) and C) Experimental images for the target DNA capture with non-complementary DNA, S.aureus ncDNA and cDNA in lysis solution, respectively. (Leica DMLM microscope, Exposure time: 1s, Gain: 1X, Magnification: 10X)*

ncDNA strands, one of which is from *S. aureus* and has a slightly higher similarity with the padlock than the second ncDNA strand (23.7% and 19.8%, respectively). This would allow to evaluate the specificity

of the target DNA capture assay under the conditions to which it may be exposed to upon integration with the cell lysis module. For that reason, these experiments were again performed in lysis solution, with lysis buffer, B-PER and neutralization buffer, which is the solution used to lyse the cells in the chemical lysis module.

The results are presented in Figure 3.6, and it is clear that the hybridization is significantly inhibited for both non-complementary target DNAs, although the *S. aureus* ncDNA presents a slightly higher fluorescence signal, this increase is very small when taking into account the variability of the experiment, and the massive difference between both the ncDNAs and the cDNA fluorescence signals.

3.2.2 Target DNA capture quantification

After optimizing the target DNA capture protocol, it was necessary to determine how much DNA was actually being captured using this assay. The process consisted of two distinct steps: first to quantify how much fluorescence signal a given concentration of target DNA emitted simply immobilized on the beads, creating a calibration curve. Secondly, compare the fluorescence signal measured at the end of the target DNA capture assay to the ones in the calibration curve and calculate the amount of the DNA that was efficiently captured.

3.2.2.1 Calibration curve

The experiments performed to obtain the calibration curve consisted of packing the channel with Q-Sepharose beads, performing a wash with PBS at 5μL/min, followed by flowing the target DNA labelled with Atto-430LS at 0.5μL/min for 40min, as this was the flow used in the capture assay with which these results will then be compared to. Lastly, another wash with PBS is performed at 5μL/min for 1min to remove any unbound DNA. Five different DNA concentrations were used: 250nM, 100nM, 50nM, 10nM and 1nM.

The Q-Sepharose beads were used to perform these experiments, as they allow to immobilize the DNA onto their surface electrostatically. Therefore, as this capture is very efficient, it is possible to

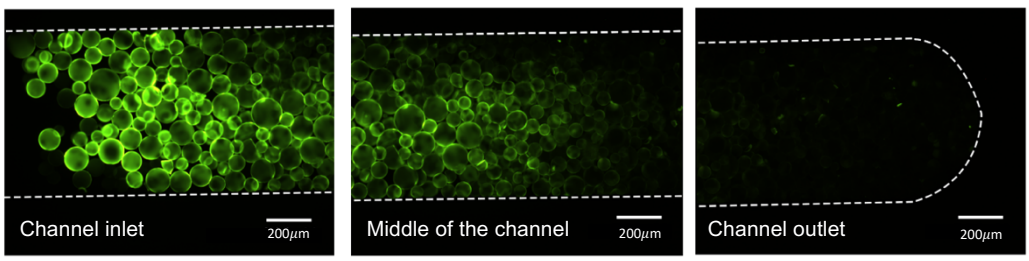

Figure 3.7: *Experimental images of the target DNA capture in Q-Sepharose beads, highlighting the decrease in fluorescence signal throughout the channel as a result of the electrostatic DNA capture on the beads. (Leica DMLM microscope, Exposure time: 1s, Gain: 1X, Magnification: 10X)*

assume that all the DNA is captured. This aspect of DNA immobilization onto Q-Sepharose beads is made very evident in Figure 3.7, as a concentration gradient is visible throughout the different zones of

the channel, with most of the DNA being captured near the inlet where the solutions are introduced into the channel. However, to confirm this assumption, the target DNA solution of the highest concentration used in these experiments (250nM) was collected at the outlet of the channel and flown through a second channel (already packed with Q-Sepharose beads and washed with PBS) at 0.5μL/min, followed by a wash with PBS at 5 μL/min for 1min. The results are presented in Figure 3.8 and show that almost 100% of the DNA was captured by the Q-Sepharose beads in the first channel (presenting a ratio of 82 between the signal obtained in the first and second channel).

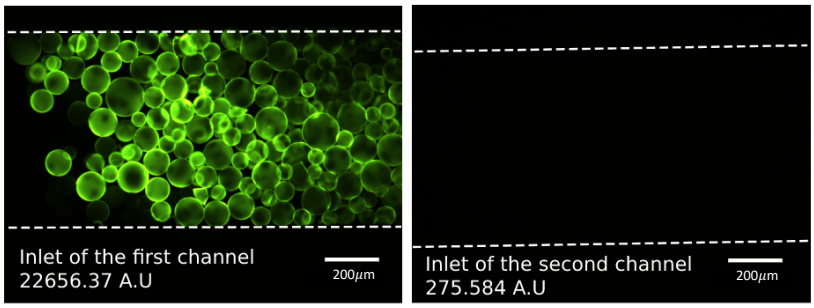

Figure 3.8: *Target DNA capture in Q-Sepharose beads. The target DNA is captured on the first channel, and the solution is collected at the outlet and flown through a second channel with Q-Sepharose beads, where almost no target DNA is captured.*

Following these conclusions, the experiments for all target DNA concentrations were performed and the calibration curve, represented in Figure 3.9, was created using a linear fit for the data, as for the range of concentrations used the fluorescence signal decreases linearly with the concentration.

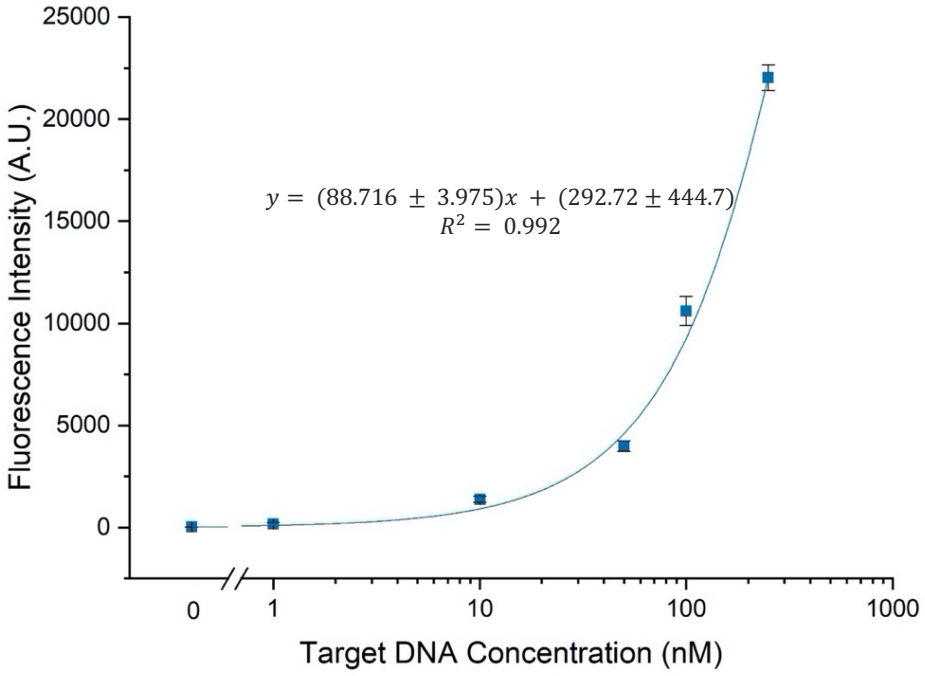

Figure 3.9: *Calibration curve for the capture of the Atto430-LS labelled target DNA on Q-Sepharose beads. The equation represents the linear regression that fits the data. The error bars in the graphic are the standard deviation of the measured signal of two experiments.*

3.2.2.2 Mass balance calculation

In order to accurately quantify how much of the target DNA was being captured using the developed assay, the experiment represented in Figure 3.10 was performed. These experiments consisted of:

- Firstly, to perform the target DNA capture assay following the previously optimized protocol, introducing first the padlock probe (100nM) and padlock (250nM) into the channel at 0.5μL/min, followed by the target DNA at 0.5μL/min. Several concentrations of the Atto-430LS labeled target DNA (250nM, 100nM, 50nM and 10nM) were used in these experiments in order to access the capture efficiency at different concentrations.
- Secondly, after performing the target DNA capture assay, the remaining target DNA solution was collected at the outlet and flown through a second channel packed with Q-Sepharose beads at 0.5μL/min in order to capture the remaining target DNA.

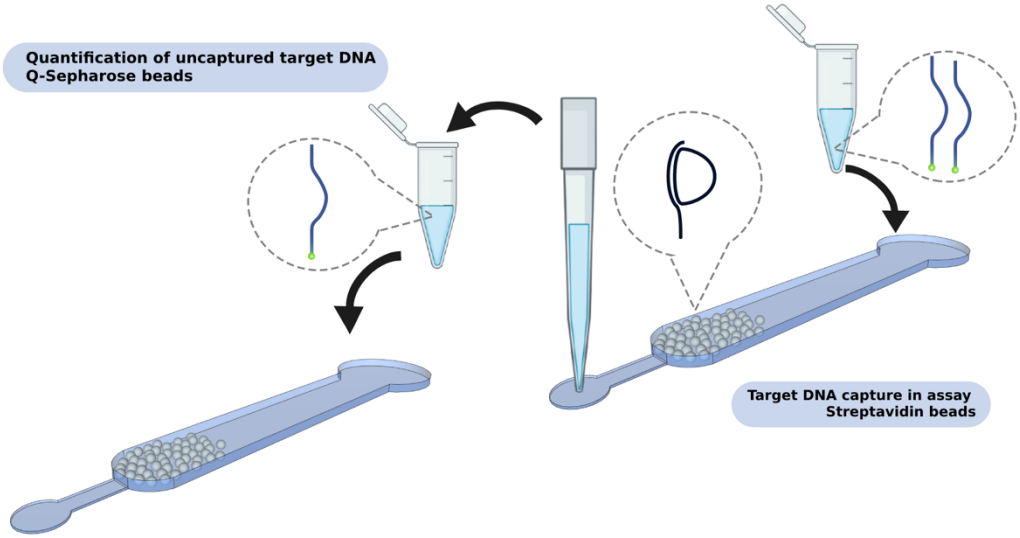

Figure 3.10: *Schematic representation of the mass balance calculation experiments. The target DNA capture assay is first performed on streptavidin beads. After flowing the Atto-430LS labelled target DNA solution through the channel it is collected at the outlet and flown through a second channel packed with Q-Sepharose beads.*

Next, the fluorescence signals in both channels were measured, and are presented in Figure 3.11. It is possible to see that the signals for the 250nM and 100nM target DNA capture assay are very similar, and particularly that the fluorescence signal for the capture of the remaining 250nM target DNA captured on the Q-Sepharose beads is quite high. This indicates that for the highest target DNA concentration, the capture isn't very efficient. However, given that the concentrations of padlock probe and padlock introduced into the channel are quite similar to that of the target DNA and that not all molecules might have been immobilized on the beads, the padlocks might be becoming saturated with target DNA at lower concentrations than the 250nM. This becomes more evident as the concentrations are lowered, and the ratio between the signals (Figure 3.11) of the first and second channel increase. This is made evident in Figure 3.12 as the fluorescence emitted in the target DNA capture assays is somewhat similar for the 3 concentrations (250nM, 100nM and 50nM), but the fluorescence in the channel with the Q-Sepharose beads decreases significantly with the concentration.

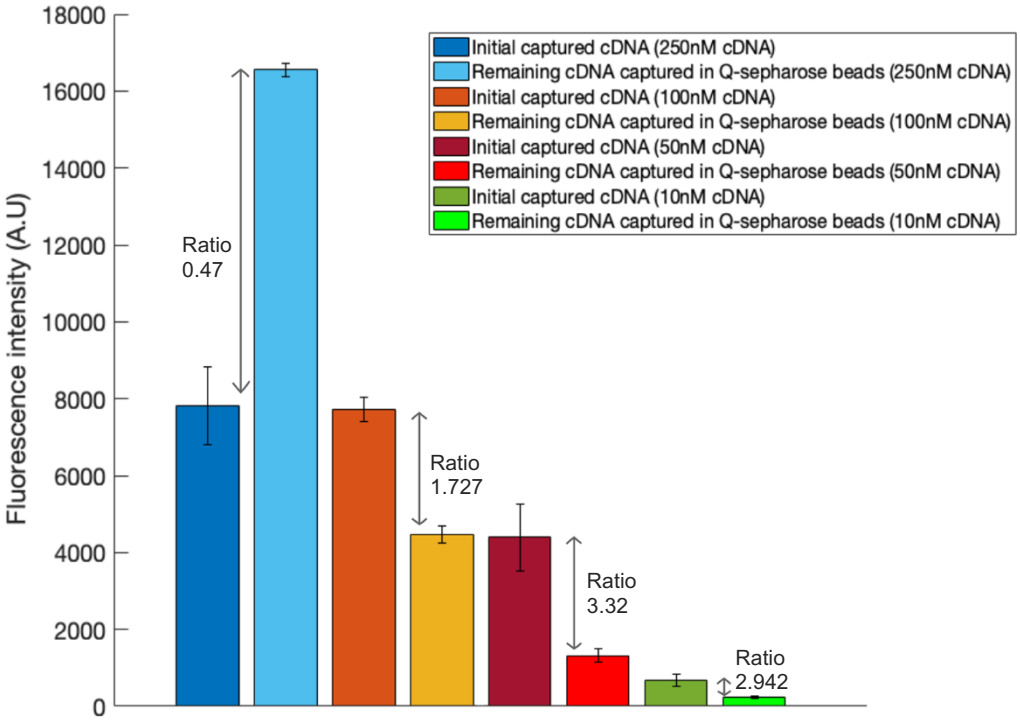

Figure 3.11: *Mass balance calculation experiments. The lighter colored bars represent the uncaptured target DNA and the darker colored bars represent the captured target DNA. The error bars in the graphic are the standard deviation of the measured signal of two experiments. Presented next to the bars are the ratios between the captured and the uncaptured target DNA during the assay.*

Following these experiments, in order to accurately quantify the target DNA capture, a mass balance methodology was used. [60] [61] As previously stated, the signal intensity on the Q-Sepharose beads was proportional to the mass of the target DNA and thus, the mass of DNA hybridized to the padlocks can be obtained by equation 5:

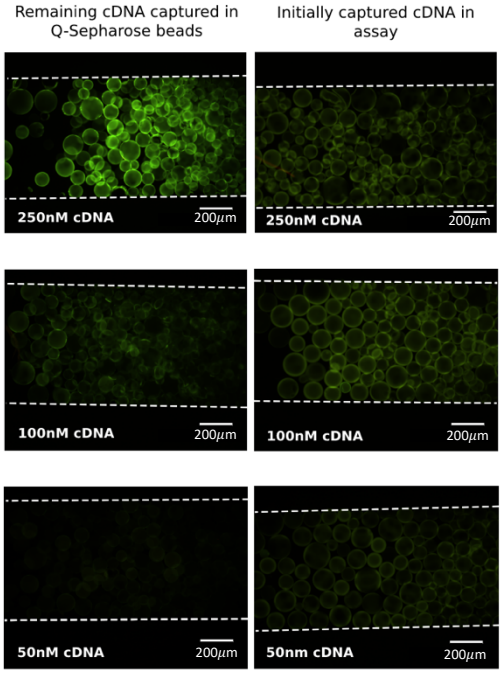

Figure 3.12: *Experimental images of the mass balance calculation experiments. On the left are the images of the Q-Sepharose beads packed channels and on the right are the images of the target DNA capture assay.*

$$m(DNA)_{padlock} = m(DNA)_{in} - m(DNA)_{Q-sepharose\ beads} \quad (5)$$

Where $m(DNA)_{in}$ is the known mass of DNA initially introduced into the first channel, and $m(DNA)_{Q-sepharose\ beads}$ is calculated by measuring the signal intensity of the target DNA present in the channel packed with Q-Sepharose beads after exiting the first channel (where the capture assay was performed) and correlating this signal with the DNA concentration using equation (6) for the calibration curve in Figure 3.9.

$$y = (88.716 \pm 3.975)x + (292.72 \pm 444.7) \quad (6)$$

Table 3.2: *Summarized results from the mass balance calculation.*

Signal (A.U)	$[DNA]_{\text{Q-Sepharose Beads}}$ (nM)	$[DNA]_{\text{IN}}$ (nM)	$[DNA]_{\text{captured}} = [DNA]_{\text{IN}} - [DNA]_{\text{Q-Sepharose Beads}}$	Mass of captured DNA (nmol)	Average mass of captured DNA (mol)
16714.83	185.109	250	64.891	0.001297	$1.335 \times 10^{-12} \pm 5.294 \times 10^{-14}$
16382.714	181.365	250	68.635	0.001373	
4252.094	44.629	100	55.370	0.001107	$1.059 \times 10^{-12} \pm 6.909 \times 10^{-14}$
4685.582	49.515	100	50.485	0.001009	
1510.515	13.727	50	36.273	0.000725	$7.675 \times 10^{-13} \pm 5.951 \times 10^{-14}$
1137.219	9.519	50	40.481	0.000809	
253.351	0	10	10	0.0002	$2 \times 10^{-13} \pm 0$
217.774	0	10	10	0.0002	

The results for the calculations are presented in Table 3.2, and it is possible to access the capture efficiency of the developed assay. For a concentration of 250nM of target DNA only 27% was captured during the assay, increasing for smaller concentrations, with capture efficiencies of 53%, 77% and virtually 100% for 100nM, 50nM and 10nM, respectively. However, in Table 3.2 it is present the fluorescence signal emitted by the remaining 10nM target DNA solution in Q-Sepharose beads ($\sim 236 A.U$) and comparing that fluorescence value to when no target DNA is present on the beads ($\sim 26 A.U$) it is around 12 times higher, indicating that there still is a certain amount of DNA that was not captured during the assay. This highlights that although the calculated efficiency for the capture of the 10nM target DNA concentration was 100%, there is an associated error to the calculations performed from the calibration curve, as well as limitations inherent to the microscope's sensitivity that don't allow to accurately quantify the capture efficiency for lower concentrations.

Although higher target DNA capture efficiencies (95.3% to 97.3% for target DNA concentrations above 3nM) have been reported in the literature, for a similar capture system, using probes immobilized on beads no further optimization was done to the capture assay. [60] This is because although similar, the reported method relied only on an already immobilized probe for the target DNA to hybridize to, while in this assay the padlock immobilization is additionally dependent on the padlock probe binding to the beads through the streptavidin-biotin interaction as well as the padlock hybridizing to the probe.

Therefore, it is reasonable to assume that the capture is inherently somewhat less efficient due to the multitude of factors that influence it.

3.2.3 Rolling circle amplification

Taking into account the optimization performed in the previous sections, as well as the previously developed RCA protocol, a new one represented in Figure 3.13 was tested. The assay began by packing the channel with Streptavidin beads and then washed with PBS at 5μL/min for 1min. The microfluidic structure is then placed onto a hotplate, remaining at 37℃ throughout the remainder of the assay. The channel walls are then blocked by flowing 4% BSA at 2.5μL/min for 10min, followed by the immobilization of the biotinylated padlock probe (100nM) and padlock (250nM) on the beads by flowing the solution at 0.5μL/min for 40min. The target DNA (250nM) is then flown through the channel at 0.5μL/min in lysis solution, in order to evaluate not only if with the new capture assay the amplification was still able to occur but also if the lysis solution affected the enzymes activity. After the target DNA is hybridized with the padlock, the ligation solution is flown trough the channel at 0.5μL/min for 40min, followed by the amplification solution at 0.25μL/min for 60min. The Cy3-labelled detection oligonucleotides (500nM) are then passed through the channel at 2μL/min for 15min followed by a wash with hybridization buffer at 2.5μL/min for 2min. An additional wash with PBS at 5μL/min for 1min was also performed so that the measurement conditions were the same as for the target DNA capture experiments.

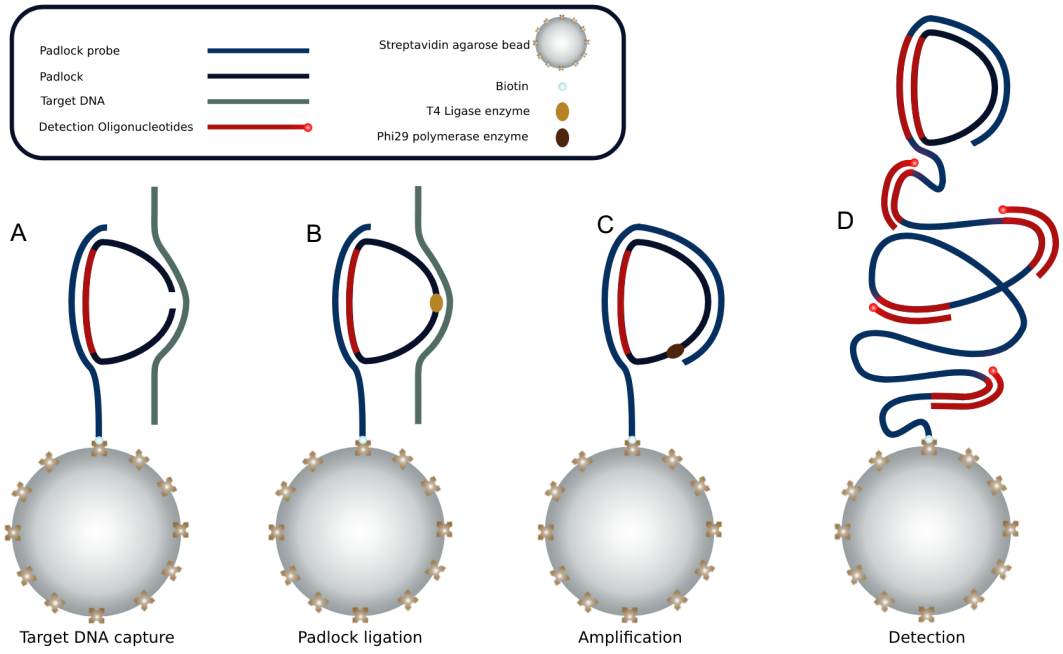

Figure 3.13: *Schematic representation of the RCA assay. A) Capture of the padlock probe on the streptavidin beads, hybridization with the padlock and the target DNA. B) Ligation of the padlock with T4 DNA ligase. C) Amplification of the complementary padlock sequence using the Phi29 DNA polymerase. D) Detection of the amplified product by hybridizing Cy3-labeled detection oligonucleotide sequence with the highlighted section of the amplified sequence.*

The RCA assay was performed with a complementary target DNA and a non-complementary target DNA, and the results are represented in Figure 3.14. The fluorescence signal for the cDNA is

much higher than the ncDNA (with a ratio of 4.9) which shows that the T4 DNA ligase enzyme specificity is not compromised by the saline conditions imposed by the lysis solution. This could happen given that when the ligation solution is flown through the channel remainders of the lysis solution are still found within the channel and the change in pH could affect the enzyme's activity.

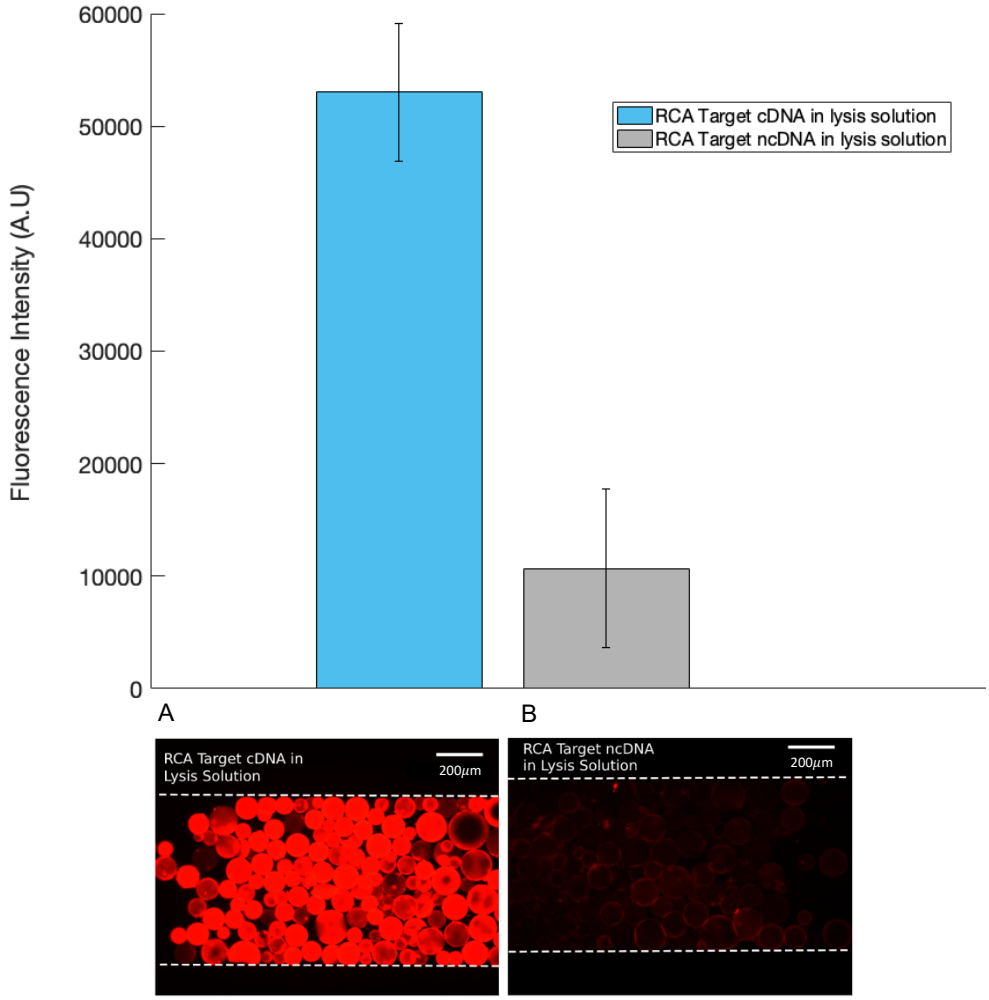

Figure 3.14: *Rolling Circle Amplification assay in Lysis solution with cDNA and ncDNA. The error bars in the graphic are the standard deviation of the measured signal of two experiments. Experimental images of the RCA assay in lysis solution. A) RCA with cDNA. B) RCA with ncDNA.(Leica DMLM microscope, Exposure time: 1s, Gain: 1X, Magnification: 10X)*

3.2.3.1 Attempt at integration

Following the RCA protocol stated above, an attempt at integration of the lysis and amplification modules was performed. This involved using a real *Staphylococcus aureus* sample, performing cell lysis in the previously developed microfluidic chemical lysis module, followed by bacterial DNA amplification in the same microfluidic structure. This structure's fabrication and design are not mentioned in this work since it was only used to perform these experiments and it is not considered relevant to the results.

In order to perform the RCA, the *S. aureus* DNA had to be denatured after lysis, which was performed off-chip by heating the sample at 60℃ and then flowing it through the channel without cooling.

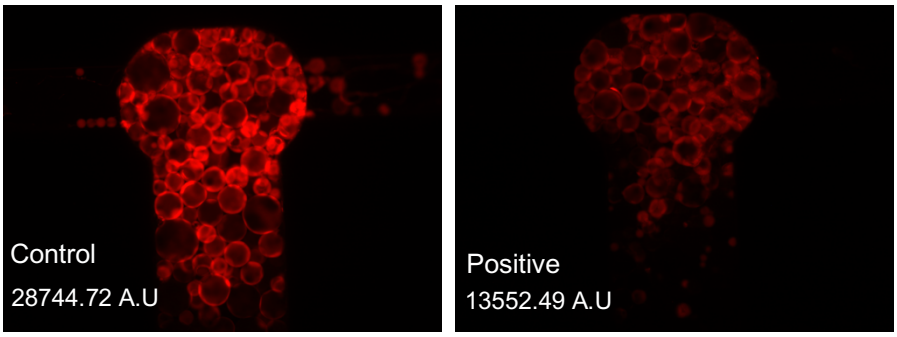

Figure 3.15: *Experimental images for the lysis and RCA module integration experiments. (Leica DMLM microscope, Exposure time: 1s, Gain: 1X, Magnification: 10X)*

This temperature was chosen as it is a compromise between the 95℃ usually used to denature DNA and the maximum temperature to which the PDMS structure can be heated without the creation of air bubbles. The results are presented in Figure 3.15, and it is possible to see that the control experiment, which had no *S. aureus* DNA presented a higher fluorescence signal than the one with *S. aureus* DNA. These experiments revealed that the *S. aureus* DNA might not have been denatured at 60℃ and therefore no amplification occurred, since dsDNA cannot hybridize with the padlock and therefore the T4 DNA ligase can't close the gap between the padlock ends. Another deduction that can be made from these experiments is that the detection oligonucleotides were hybridizing to something other than the RCA products as the fluorescence signal is higher for the control.

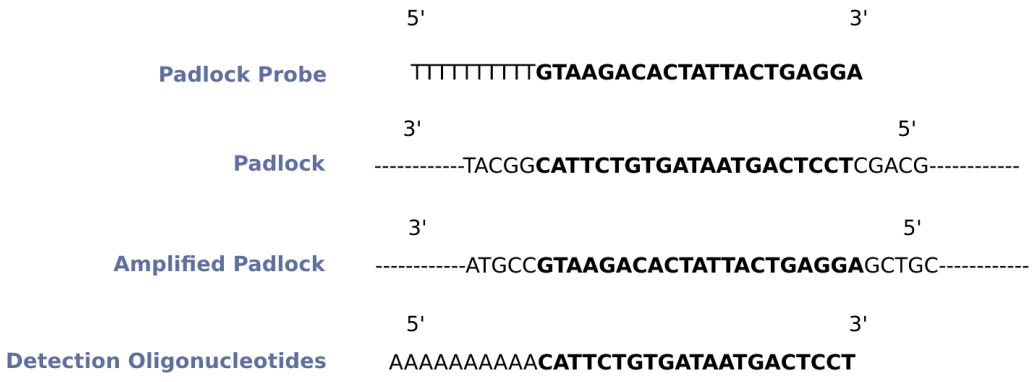

Figure 3.16*: Representation of the padlock probe, padlock, amplified padlock and detection oligonucleotides sequences, highlighting the complementary sections.*

Given that without amplification the only DNA strands present in the device are the padlock probe and padlock, it was hypothesized that the detection oligonucleotides might be hybridizing to them or becoming trapped on the porous beads. Given that the detection oligonucleotides are complementary to the padlock probe, since they were designed to be complementary to the amplified complementary strand of that section of the padlock (sequences illustrated in Figure 3.16) it is most likely that the detection oligonucleotides were hybridizing to the padlock probes. In order to determine that this was the reason for the results obtained in the integration of the lysis and amplification modules several experiments were preformed, represented in Figure 3.17.

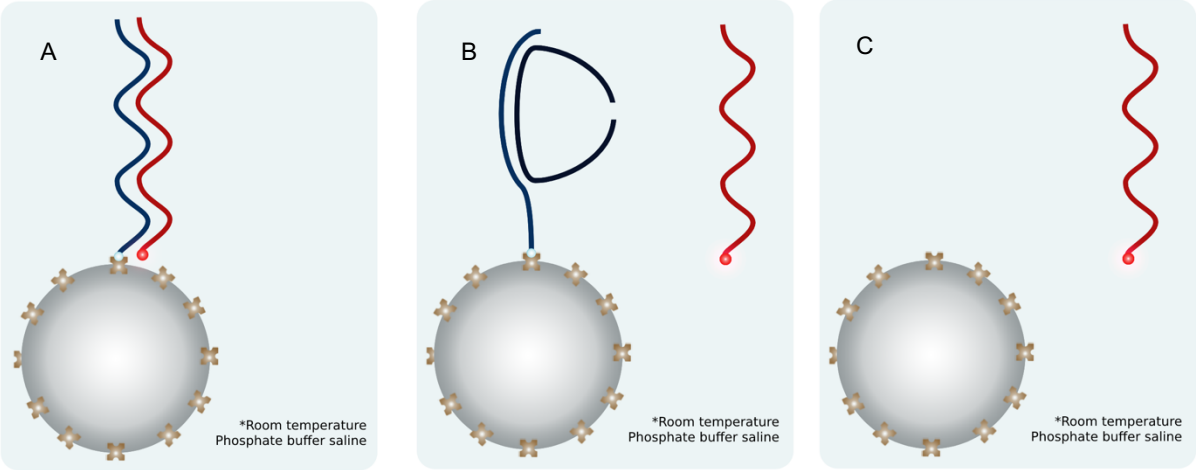

Figure 3.17: *Schematic representation of the experiments performed to understand the interferences in the integration experiments. A) Padlock probe and detection oligonucleotides. B) Padlock probe, padlock and detection oligonucleotides. C) Detection oligonucleotides.*

The first experiment to be performed, represented in Figure 3.17A was done by packing the channel with streptavidin beads, followed by a wash with PBS at 5μL/min for 1min, and then flowing the padlock probe (100nM) at 0.5μL/min for 40min. Next, the same concentration of detection oligonucleotides used in the RCA assay (500nM) was flown into the channel at 2μL/min for 15min, followed by a wash to remove any unbound molecules with PBS. The second experiment (Figure 3.17 B) was very similar to the first one, but instead of flowing just the padlock probe in the first solution, the padlock was also present, in order to hybridize with the padlock probe. Lastly, in order to determine if the detection oligonucleotides were becoming trapped in the porous beads, a third experiment (Figure 3.17C) was performed, consisting of packing the channel with streptavidin beads, washing with PBS at 5μL/min for 1min and then flowing the detection oligonucleotides solution at 2μL/min for 15min.

The results for these experiments are presented in Figure 3.18. Comparing the fluorescence signal from the first experiment (Figure 3.17A) with the one obtained from the control integration experiment it is possible to conclude that the reason for the high fluorescence signal in the control is the hybridization of the detection oligonucleotides with the padlock probe. This is further highlighted by the fact that the fluorescence signal in the second experiment (Figure 3.17B), where the padlock is hybridized to the padlock probe is much lower. However, in this second experiment it was expected that very little fluorescence was emitted given that the detection oligonucleotides are not complementary with the padlock. This leads to the hypothesis that when only the padlock probe and padlock are present in the channel with no amplification products, the detection oligonucleotides that are in a much higher concentration than the padlocks compete to hybridize with the padlock probe, and due to the concentration gradient generated are able to do so. Lastly, the third experiment (Figure 3.17C) revealed that the detection oligonucleotides becoming trapped on the beads was not what was interfering with the detection of the amplified products in the integration experiment, and that the amount of detection oligonucleotides that become trapped on the beads is negligible.

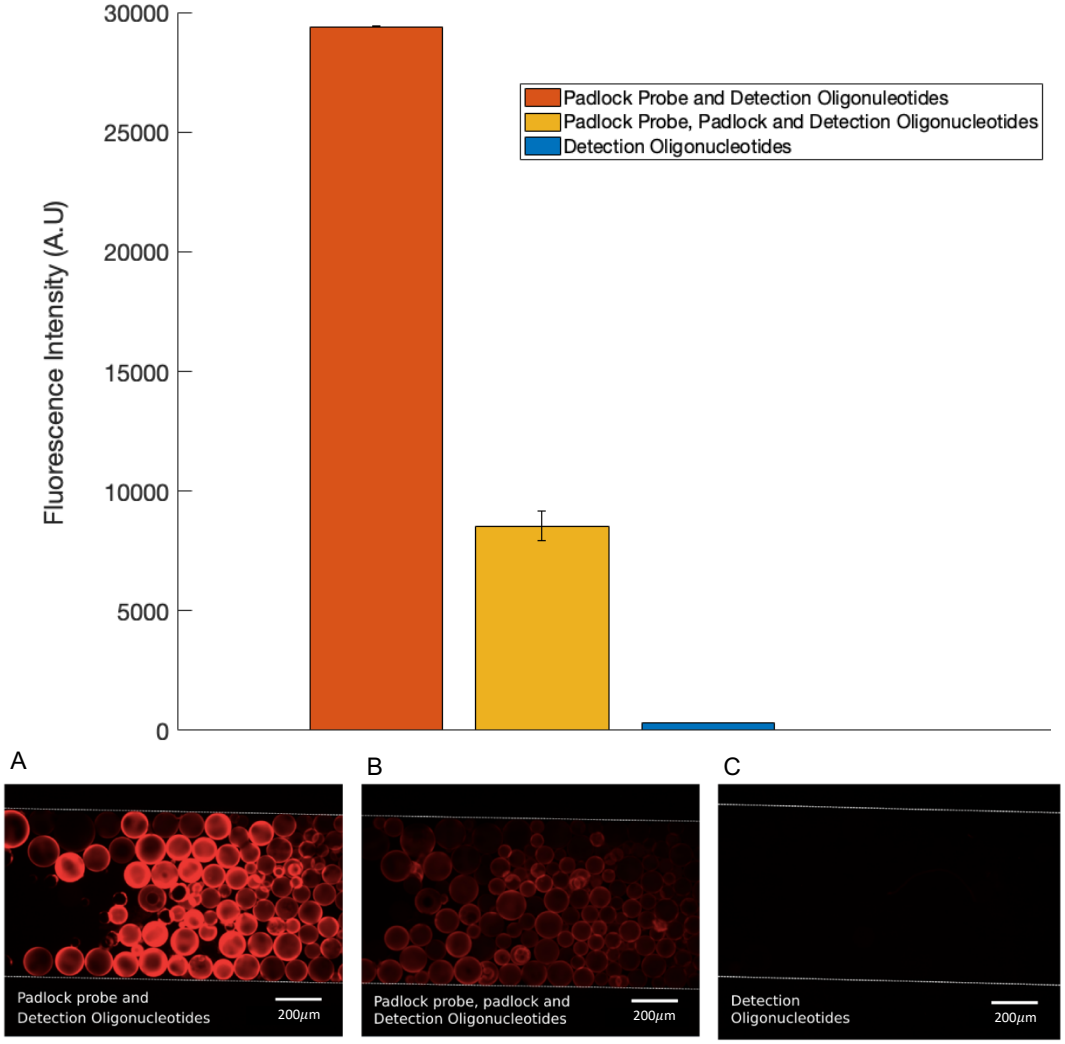

Figure 3.18: *Experiments regarding the interferences observed in the integration attempts. The error bars in the graphic are the standard deviation of the measured signal for two experiments. Experimental images for the experiments performed to understand the interferences observed in the integration experiments. A) Padlock probe and detection oligonucleotides. B) Padlock probe, padlock and detection oligonucleotides. C) Detection oligonucleotides. (Leica DMLM microscope, Exposure time: 1s, Gain: 1X, Magnification: 10X)*

One final conclusion is that the RCA protocol would have to be further adjusted to take into account these interferences caused by the new target DNA capture assay, which have been previously reported in the literature [33]. These interferences were not considered in the previous assay, given that in the simplified RCA presented earlier, when there was no target DNA present there was no DNA strand that the detection oligonucleotides could hybridize to.

3.2.3.2 Blocking optimization

To address the issues that arose from the detection oligonucleotides hybridizing with the padlock probe when no amplification occurs or the padlock is not hybridized to the padlock probe, several blocking strategies were tested. The first strategy (Figure 3.19A) consisted of using polyacrylate (PA) 8000 as a blocking agent, which resembles the padlock probe in length and charge, and has been previously used as blocking agent. [60] In this experiment the channel was packed with streptavidin beads, followed by a wash with PBS at 5μL/min for 1min, the biotinylated padlock probe (100nM) and padlock (250nM) are then flown through the channel at 0.5μL/min for 40min as in the target DNA capture and RCA assays, binding to the streptavidin beads. A solution of 5% PA 8000 is flown at 0.5μL/min for 40min as to resemble the target DNA capture assay conditions. The detection oligonucleotides are then flown at the same flow rate and concentration as in the RCA assay, followed by a wash with PBS at 5μL/min for 1min. The second strategy (Figure 3.19B) consisted of using a biotinylated detection oligonucleotide sequence with no label fluorophore in order to hybridize with the free padlock probes so the labeled detection oligonucleotides would no longer be able to hybridize to them. In this experiment, the channel is again packed with streptavidin beads and washed, followed by flowing the padlock probe (100nM) and padlock (250nM), using the same flow rates, volumes, and concentrations as the previous experiment. Next, the biotinylated detection oligonucleotides are flown at 0.5μL/min for 40min followed by the Cy3-labelled detection oligonucleotides (500nM) at 2μL/min for 15min. The last blocking strategy (Figure 3.19C) that was tested, was to incubate the padlock probe (100nM) and padlock (250nM) off-

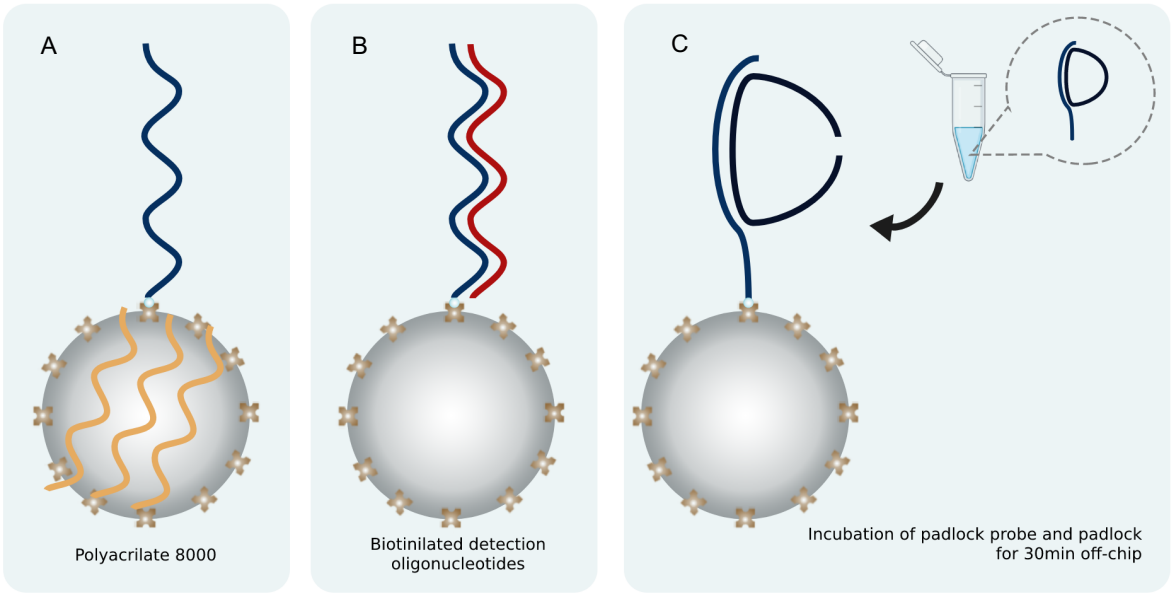

***Figure 3.19**: Schematic representation of the blocking optimization experiments, representing only the beads with free padlock probes. A) Using polyacrylate as a blocking agent. B) Using biotinylated detection oligonucleotides as blocking. C) Blocking by incubating the padlock probe and padlock off-chip for 30min with agitation.*

chip for 30min with agitation with the intention that when the molecules were introduced into the channel, all the padlock probes would be hybridized with the padlocks and therefore it would be harder for the detection oligonucleotides to hybridize with the padlock probe. After the incubation, the padlock probe and padlock solution was flown through the already packed and washed channel at 0.5μL/min for 40min, followed by flowing the detection oligonucleotide solution at 2μL/min for 15min.

The results for these experiments are presented in Figure 3.20, and it is clear that the best blocking agent is the biotinylated detection oligonucleotides. This is due to the fact that the interference signal that was obtained in the previous experiments was not a non-specific signal, but instead it was 2 complementary oligonucleotide sequences hybridizing with each other. PA 8000 didn't work as a blocking agent as it is usually used to block non-specific signal due to its similarity with the DNA strands. However, since the signal is not non-specific the Cy3-labelled oligonucleotides are still able to hybridize with the padlock probe with the polyacrylate having little interference. The biotinylated detection oligonucleotides on the other hand presented a higher blocking efficiency, since they are also complementary to the padlock probe and are in the same concentration as the Cy3-labelled detection

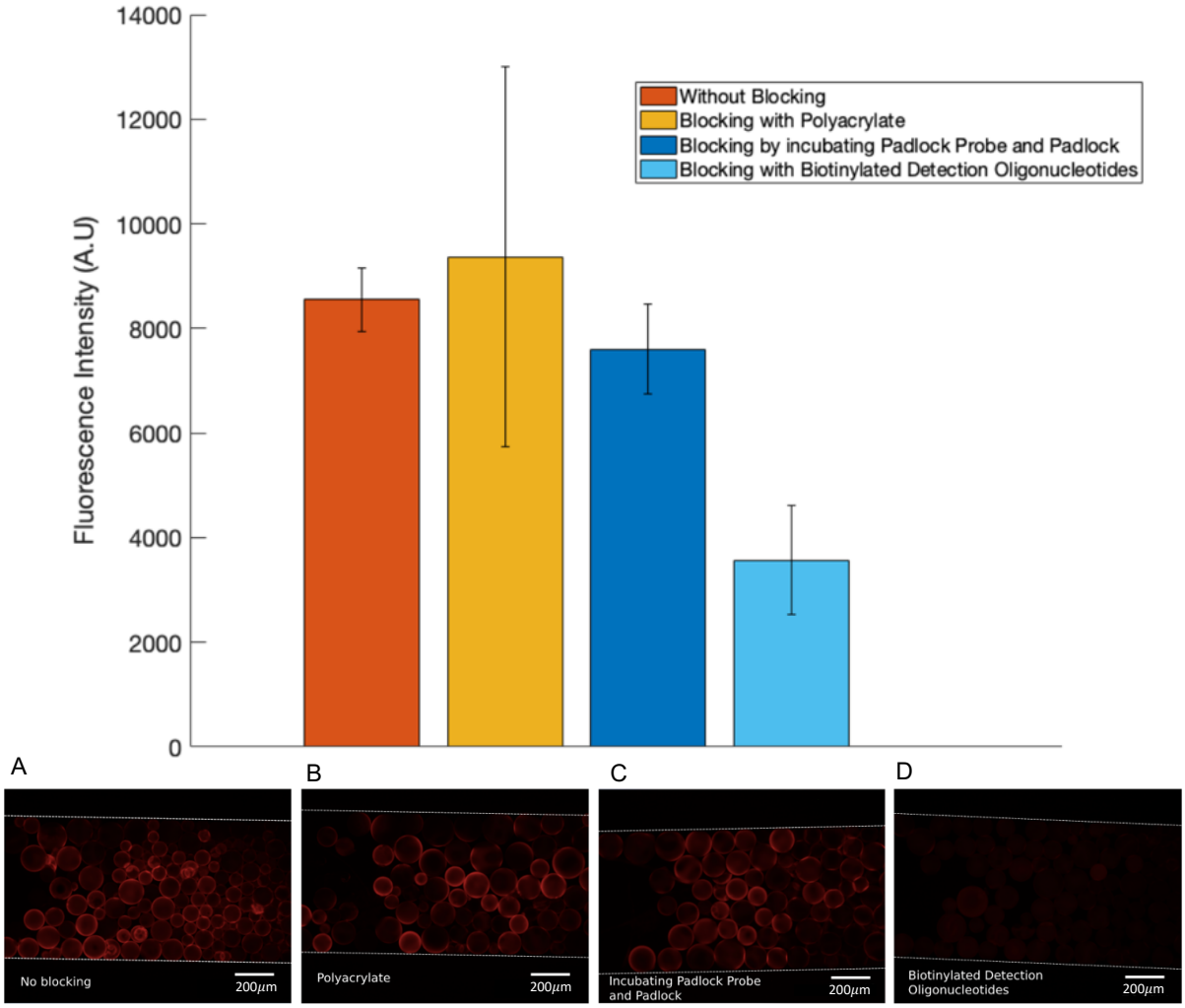

Figure 3.20: *Blocking optimization experiments. The error bars in the graphic are the standard deviation of the measured signal for two experiments. Experimental images for the blocking optimization experiments. A) No blocking. B) Blocking with polyacrylate. C) Blocking by incubating the padlock probe and padlock. D) Blocking with biotinylated detection oligonucleotides. (Leica DMLM microscope, Exposure time: 1s, Gain: 1X, Magnification: 10X)*

hybridize with the padlock probe. Lastly, the incubation of the padlock probe and padlock was also not very efficient. Although the signal decreased slightly which might be due to the fact that hybridization in solution generally presents higher hybridization efficiencies than on a surface, as diffusion and mass transport are more efficient, the optimization regarding the flow rate and the way the molecules are introduced into the channel may have made it so that the hybridization efficiency in the channel is similar to that in solution.

From these results, the biotinylated detection oligonucleotides were chosen as a blocking agent to perform the following experiments. It also became evident that the major issue was the Cy3-labelled detection oligonucleotides hybridizing to the padlock probes, which in addition to the reasons reviewed above may also be related with the increase in temperature for the DNA denaturation process. The oligonucleotide sequences for the padlock probe and padlock have melting temperatures of 54℃ and 70℃, respectively, and so when passing the target DNA solution at 60℃ without cooling, it may be reaching the melting temperature of the duplex. This would lead to the denaturation of the padlock probe and padlock, leaving only the probe bound to the beads through the streptavidin-biotin bond, which the

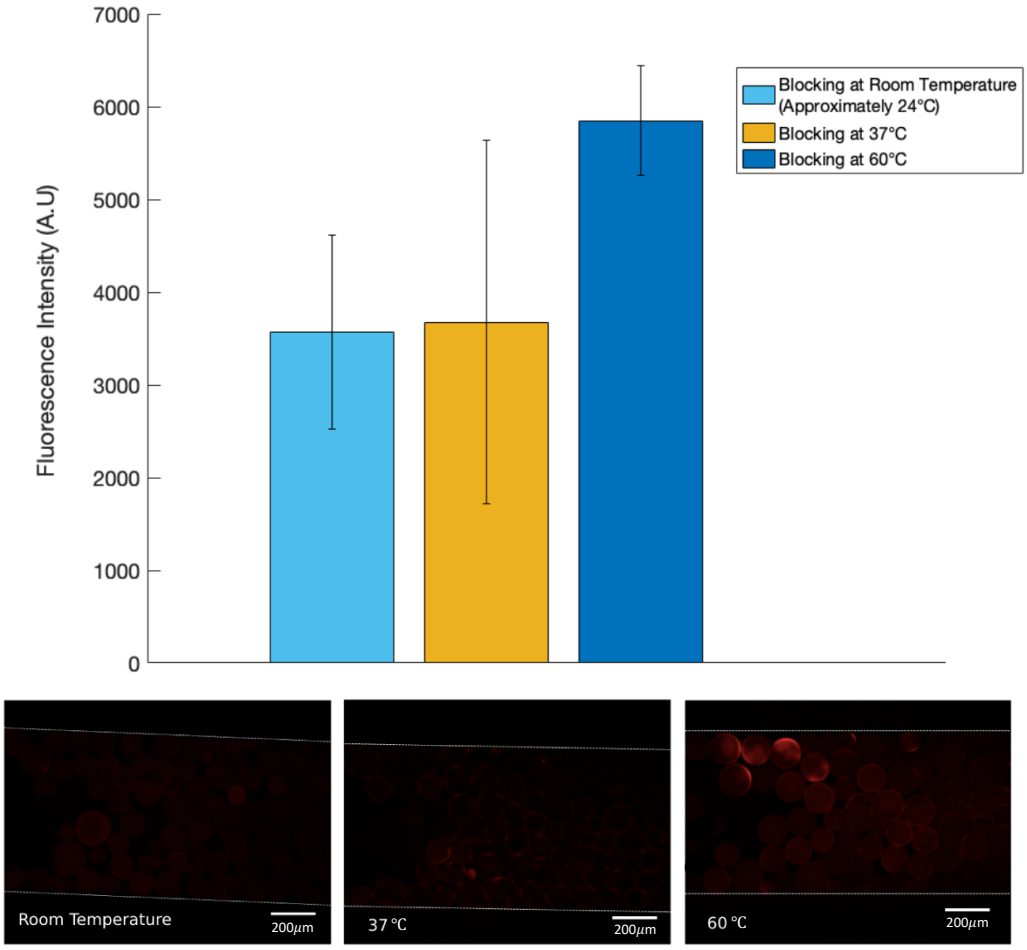

Figure 3.21: *Blocking with biotinylated detection oligonucleotides at different temperatures. The error bars in the graphic are the standard deviation of the measured signal for two experiments. Experimental images for the blocking experiments at different temperatures. A) Blocking with biotinylated detection oligonucleotides at room temperature. B) Blocking with biotinylated detection oligonucleotides at 37℃. C)Blocking with biotinylated detection oligonucleotides at 60℃. (Leica DMLM microscope, Exposure time: 1s, Gain: 1X, Magnification: 10X).*

Cy3-labelled detection oligonucleotides could then hybridize to. In order to determine if this would be a relevant factor when performing the RCA assay and denaturing the DNA, the blocking experiments with the biotinylated detection oligonucleotides were performed again, but this time at 37℃ and 60℃, as these are the relevant temperatures for the RCA assay.

These experiments followed the protocol described above for the blocking assay with the biotinylated detection oligonucleotides, flowing the padlock probe (100nM) and padlock (250nM) at 0.5μL/min for 40min, but this time with the added step of flowing the target cDNA (250nM) at either 37℃ or 60℃, followed then by the biotinylated detection oligonucleotides (500nM) with a flow rate of 0.5μL/min for 40min. Lastly, the Cy3-labelled detection oligonucleotides are flown through the channel followed by a wash with PBS at 5μL/min for 1min. The results are presented in Figure 3.21, and it is noticeable that at 60℃ the blocking becomes much less efficient, even though the fluorescence signal is still lower than without any blocking (in Figure 3.20). This reveals that at 60℃ we may be reaching the melting temperature of the padlock probe-padlock duplex and therefore some may denature, and more padlock probes become available for the Cy3-labelled detection oligonucleotides to hybridize to, even in the presence of biotinylated detection oligonucleotides to hybridize with some of the free probes.

To circumvent this issue altogether, a new sequence of Cy3-labelled detection oligonucleotides was acquired. This new sequence is no longer complementary to the padlock probe, and therefore the background signal should decrease, particularly at higher temperatures, where denaturation of the padlock probe and padlock might occur. In order to assess if the background signal was still significant

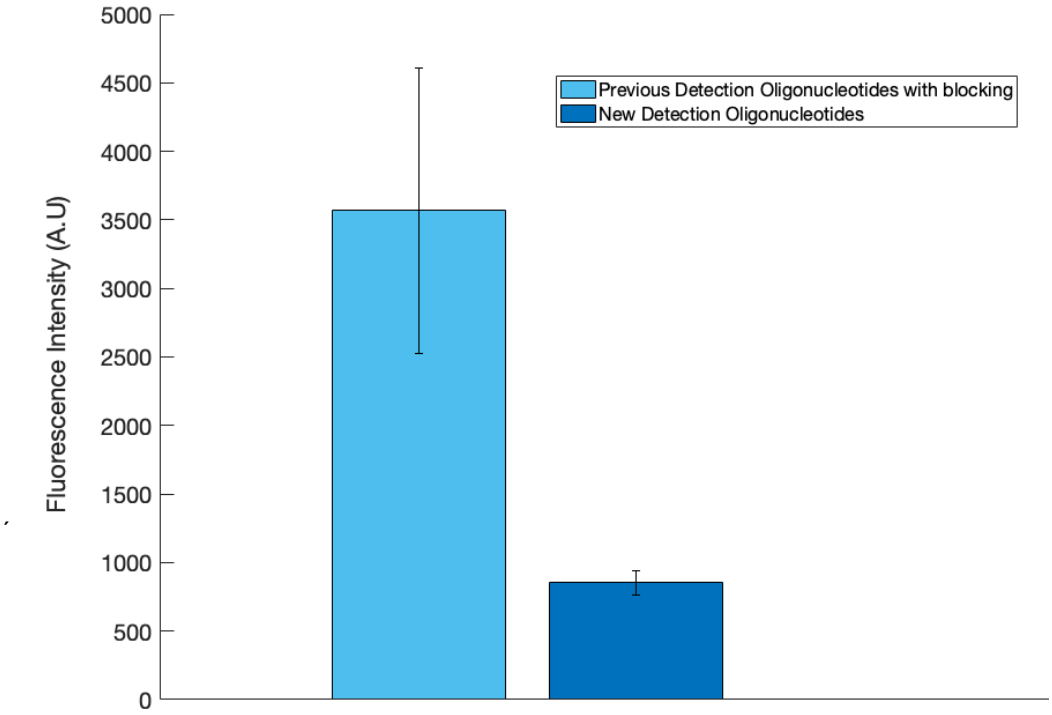

Figure 3.22: *Background signal comparison between the previous detection oligonucleotide sequence (complementary to padlock probe) and the new detection oligonucleotide sequence (only complementary to the amplified padlock). The error bars in the graphic are the standard deviation of the measured signal for two experiments.*

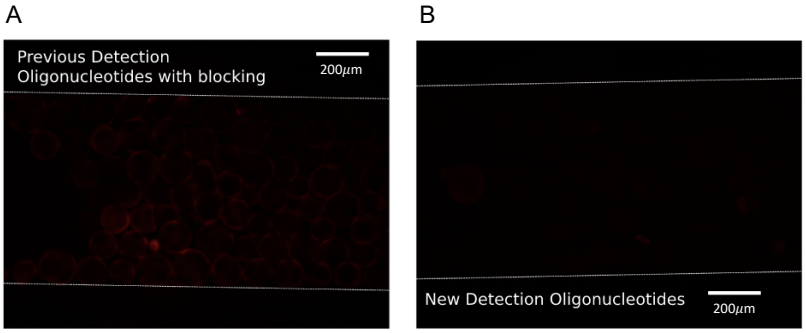

Figure 3.23: *Experimental images for the background signal comparison experiments A) Previous detection oligonucleotides. B) New detection oligonucleotides. (Leica DMLM microscope, Exposure time: 1s, Gain: 1X, Magnification: 10X)*

with the new sequence of Cy3-labelled detection oligonucleotides, the previous experiment (Figure 3.17B) was performed again with the new detection oligonucleotides, at room temperature, without any blocking. The results are presented in Figure 3.22 and 3.23, and as expected, the fluorescence signal is much lower with the new sequence of detection oligonucleotides then with the previous ones, even with blocking. Therefore, this new sequence of detection oligonucleotides was used from this point forward as it provided the least background signal.

Lastly, to evaluate the background signal in the actual RCA, the assay was performed again, following the protocol described in the beginning of this section and represented in Figure 3.13. However, instead of flowing the target cDNA in lysis solution, it was flown in PBS. The results are presented in Figure 3.24 and it is possible to see that the background signal in the RCA assay with the new detection oligonucleotides is higher than in the previous experiment (with only the padlock probe, padlock and detection oligonucleotides), but it is possible to distinguish between the positive and control, with a ratio of 2.43. This increase in background signal in the RCA assay compared to the results presented in Figure 3.23 with the new detection oligonucleotides can be due to the fact that the RCA assay involves flowing more solutions for a prolonged period of time, which can lead to the development of agglomerates in the channel, as can be seen in Figure 2.24B. The detection oligonucleotides can then become trapped in these agglomerates leading to non-specific signal.

Although a similar difference between positive and control for the RCA using the target cDNA at 37℃ had already been accomplished with the previous detection oligonucleotides, with this new sequence it is more likely that this low background signal will be maintained when using *S. aureus* genomic DNA, and higher temperatures have to be used to denature it.

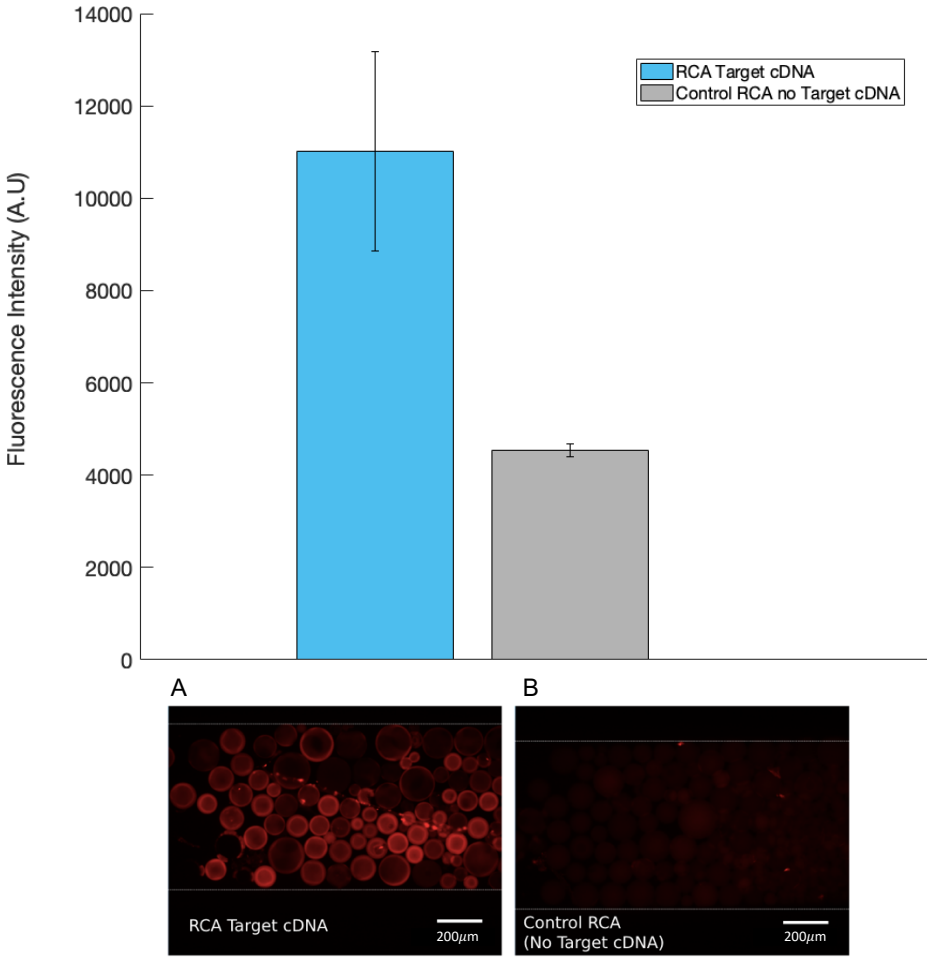

Figure 3.24: *Rolling Circle Amplification assay in PBS with cDNA and no target cDNA. The error bars in the graphic are the standard deviation of the measured signal of two experiments. A) and B) Experimental images for the RCA assay with cDNA and no cDNA, respectively. (Leica DMLM microscope, Exposure time: 510ms, Gain: 1X, Magnification: 10X)*

3.2.3.2 Rolling Circle Amplification Quantification

Following the blocking optimization, the RCA assay was again performed (Figure 3.25), following the protocol described in the beginning of this section, but flowing the target DNA in PBS instead of lysis solution. The new detection oligonucleotides labeled with Atto-430LS were used instead of the detection oligonucleotides labeled with Cy3. The assay was performed for a 10nM and 1nM concentration of target DNA, as well as a control with no target DNA.

The results are presented in Figure 3.26, and comparing the signal in this control, using the Atto-430LS labelled detection oligonucleotides with the control performed with the Cy3-labelled oligonucleotides it is clear that there is much less background signal. Given that the only variable that has changed between both assays is the fluorophore used as a label, the difference in the results can be attributed to that change. From the experiments performed in section 3.2.3.1 it was concluded that

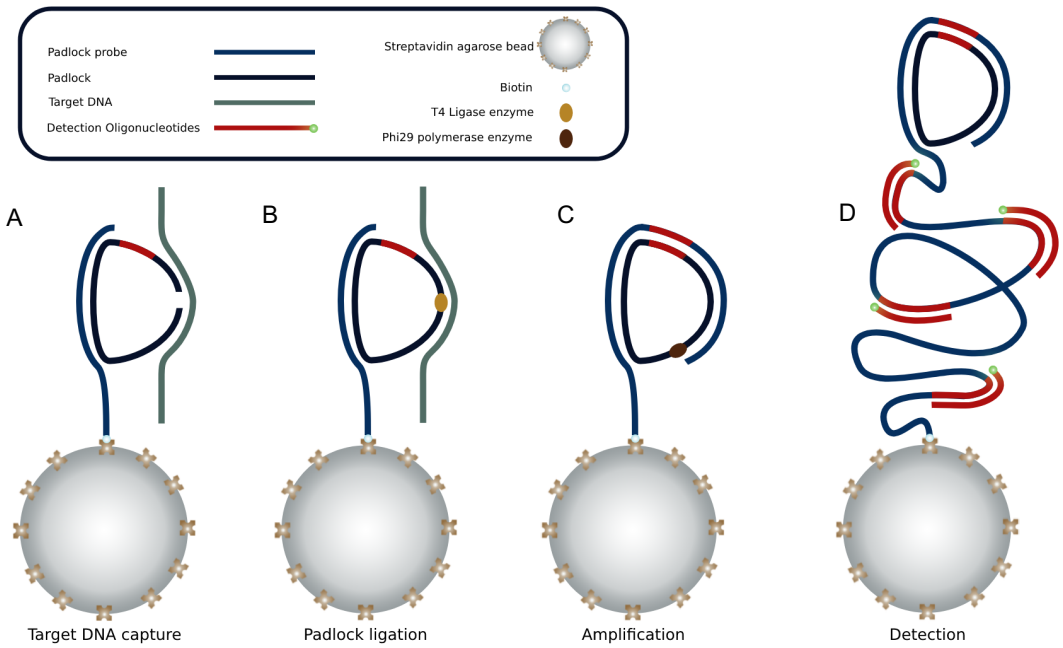

Figure 3.25: *Schematic representation of the RCA assay. A) Capture of the padlock probe on the streptavidin beads, hybridization with the padlock and the target DNA. B) Ligation of the padlock with T4 DNA ligase. C) Amplification of the complementary padlock sequence using the Phi29 DNA polymerase. D) Detection of the amplified product by hybridizing a Atto-430LS labeled detection oligonucleotide sequence with the highlighted section of the amplified padlock.*

the fluorescence signal emitted by having just the detection oligonucleotides present in the channel with the beads is negligible. However, these experiments were performed at room temperature and consisted of flowing only one solution, and from the experiments performed in section 3.2.3.2 it was possible to see that at higher temperatures the blocking became less efficient and the background signal was higher. As mentioned in section 3.2.3.2, at higher temperatures, this effect may be due to the temperature reaching the melting temperature of the padlock probe-padlock duplex. However, it may also be due to the fact that at higher temperatures more detection oligonucleotides become trapped on the beads. Additionally, as mentioned earlier, by flowing multiple solutions through the channel when performing the RCA assay, molecule agglomerates are created, in which the detection oligonucleotides can become trapped in, increasing the non-specific signal. Given that the fluorophores are structurally different, these effects may be more prominent when using the Cy3-labelled detection oligonucleotides, but further experiments would have to be performed in order to accurately evaluate this effect.

Regarding the amplification of the 10nM target DNA, in Figure 3.26 it is possible to see that the fluorescence signal emitted by just the captured 10nM target DNA is around 15 times lower than the signal after amplification. This highlights the fact that the amplification is indeed occurring in the microfluidic channel.

It has been reported in literature that the Phi29 enzyme can amplify a 100bp padlock into a complementary concatemer with approximately 1000 copies in 1h. [39] Therefore, to understand if the proposed assay's yield is similar to that reported in literature, several calculations were performed in order quantify the fluorescence signal. Firstly, from the calibration curve in Figure 3.9 it is possible to

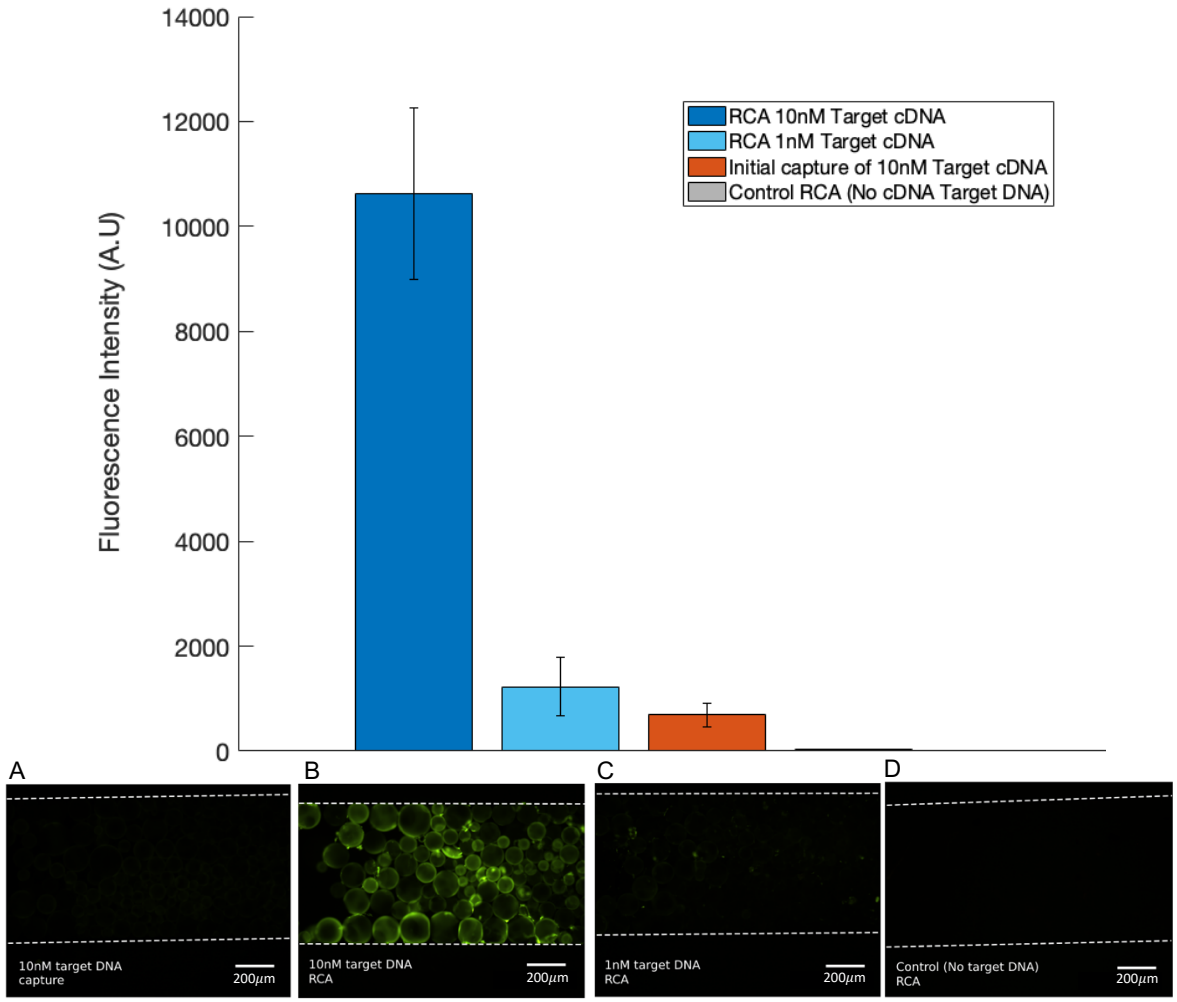

Figure 3.26: *Capture and rolling circle amplification of 10nM of target DNA, rolling circle amplification of 1nM of target DNA and control for the RCA assay. The error bars in the graphic are the standard deviation of the measured signal for two experiments. Experimental images for the target DNA capture and RCA assays. A)10nM Target DNA capture assay. B) 10nM target DNA RCA assay. C)1nM target DNA RCA assay. D) Control for the RCA assay with no target DNA. (Leica DMLM microscope, Exposure time: 510ms, Gain: 1X, Magnification: 10X*

estimate how much signal a single Atto-430LS labelled molecule would emit, which is around 7.85×10^{-9}A.U. From there, assuming 100% capture of the 10nM target DNA, and given that only padlocks that are hybridized to the target are circularized and can be amplified, there would be 1.204×10^{11} padlocks available for amplification. Assuming the 1000-fold amplification reported in literature, and that each padlock only has one repetition of the sequence complementary to the detection oligonucleotides there would be 1.204×10^{14} padlock copies to which the detection oligonucleotides can hybridize to. This should result in a fluorescence signal around 945704A.U, which is lower than the signal that was obtained. Applying the same reasoning for the RCA initiating from 1nM of target DNA, after amplification, the fluorescence signal should be around 94570.4A.U, which is again lower than the signal obtained in the experiment. From the signals obtained in both experiments and using the estimated value for the fluorescence signal of a single fluorophore, the number of detected products is 1.35×10^{12} and 1.56×10^{11} for the 10nM and 1nM target DNA concentration, respectively. This accounts for approximately 1% detection of the amplified products. It has been reported that the amplification performing the RCA assay using beads in a microfluidic channel results in a detection rate

of around 8% [52] which is quite higher than the one obtained for the developed assay. However, it is still superior to a previously reported detection rate of 0.02%, performing the RCA in solution and detecting the amplification products in a microchip. [52]

From these results it would be reasonable to conclude that the RCA assay could be further optimized. However, it must be taken in consideration that this assay was performed under continuous flow, while the RCA assay where the detection rate of 8% was achieved the ligation and amplification steps were performed in a stationary fashion. Additionally, the detection oligonucleotide solution was flown in the microfluidic channel followed by a 20min incubation. This in conjunction with the different detection methodology used can be the reason for the higher detection rate. To overcome this detection limitation one approach that was attempted was to excite the Atto-430LS labelled detection oligonucleotides with a UV-filter instead of the blue-filter used in the previous experiments. The results are presented in Figure 3.27 and is visible that just by changing the excitation wavelength the fluorescence signal is around 3 times higher. This could result in a higher rate of detection, in addition to allowing the detection of smaller concentrations of RCA products.

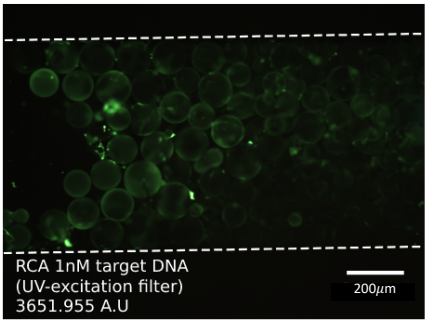

Figure 3.27: *Experimental image of the RCA assay with 1nM target DNA exciting the Atto-430LS labeled detection oligonucleotides with a UV-Filter. (Leica DMLM microscope, Exposure time: 1s, Gain: 1X, Magnification: 10X*

3.3 Rolling circle amplification using *Staphylococcus Aureus* genomic DNA as a target sample

After optimizing both the capture and RCA assays regarding several aspects, using a synthetic oligonucleotide sequence for the target DNA, the RCA assay was performed again, using *Staphylococcus Aureus* genomic DNA (4375copies/mL). The assay followed again the protocol mentioned in section 3.2.3 but, flowing the genomic DNA in PBS at 60 ℃ for denaturation to occur. The detection of the amplified products was done using the new sequence of detection oligonucleotides labeled with Cy3.

The results are presented in Figure 3.28, and although the signal for the experiment with *S. Aureus* genomic DNA is slightly higher than the control, the difference between them is quite small and therefore it is possible to conclude that the genomic DNA may not have been efficiently captured and amplified. Given that until now the target DNA sequence to be captured was quite small compared to the size of the *S. aureus* genomic DNA (2.8Mbp) it is possible that due to its large size it may get trapped

on the porous beads or just flow through the channel without hybridizing to the padlock. Another possibility was that the 60℃ may not be sufficient to denature the genomic DNA, and therefore the RCA assay was also performed denaturing the *S. Aureus* genomic DNA off-chip at 95℃ for 5min, followed by cooling in room-temperature water. However, as shown by the results in Figure 3.28 the signal is even lower than that for the RCA with on-chip denaturation at 60℃, indicating that the most likely cause for no amplification occurring is that the *S. Aureus* genomic DNA is not being efficiently captured.

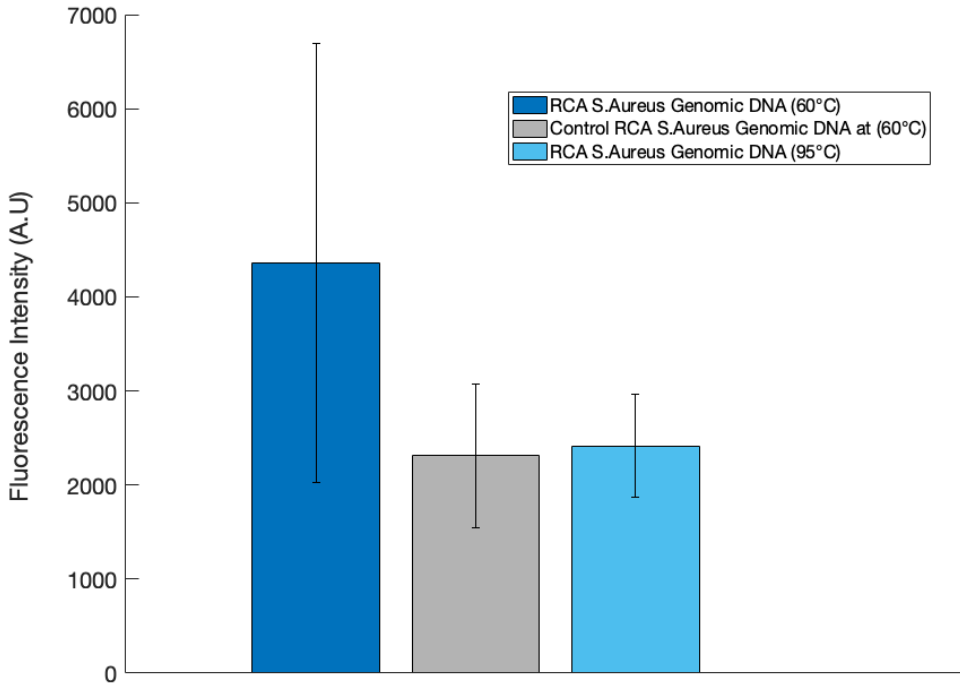

Figure 3.28: *Rolling circle amplification with Staphylococcus Aureus genomic DNA denaturing at 60℃ and 95℃, along with the control for the RCA assay denaturing at 60℃. The error bars in the graphic are the standard deviation of the measured signal for two experiments.*

From these results it is possible to conclude that in order for complete integration with the microfluidic cell lysis chip, further optimization is necessary. This optimization will most likely include digesting the *S. Aureus* DNA with restriction enzymes so the sequence in the *S. Aureus* complementary to the padlock can more easily hybridize, followed by amplification. Additionally, since it is not clear whether steric hindrance caused by the large size of the genomic DNA is the single cause for the lack of target DNA capture and amplification, several denaturation temperatures will also have to be tested. This is because, when using PDMS heating the device at 95℃ would cause the formation of air bubbles. The temperature would also be higher than the melting temperature of the padlock probe-padlock duplex, so a compromise would have to be made regarding the denaturation temperature used in the device.

4. Conclusions and future outlooks

The field of microfluidics provides an excellent platform for developing nucleic acid detection and amplification assays due to the small sizes that allow for portability, reduction in reagent and sample consumption, cost-effective fabrication, faster reaction times, and high sensitivity. This becomes particularly important for POC platforms that require fast and accurate results. Therefore, throughout this work a microfluidic rolling circle amplification system was developed and optimized.

The proposed assay requires a padlock probe hybridized to a padlock immobilized on streptavidin beads, for capturing the target DNA prior to amplification through RCA. This capture was optimized regarding several aspects, such as the flow rates and saline conditions. Several flow rates were studied in order to understand which provided the highest capture efficiency, leading to the conclusion that smaller flow rates ($0.5\mu L$/min and $0.25\mu L$/min) resulted in a higher capture of the target DNA, due to the optimal compromise between convective and diffusive transport. Given that the end-goal of the project would be to have a device with integrated cell lysis, DNA capture, amplification and detection the target DNA capture was also performed under different saline conditions. The capture was evaluated in 2 different lysis solutions, a ligation solution and PBS in order to understand if the RCA assay could be performed directly with the target DNA in the lysis solution or if purification would be required. Although the capture decreased in both lysis and ligation solutions when compared with the capture in PBS, it was still possible to capture the target DNA in all tested solutions. This indicates that purification of the sample after lysis may not be necessary, making the final device integration much easier, as well as more cost-effective.

Following the optimization, the target DNA capture was quantified using a mass-balance methodology. First, a calibration curve of the capture of several target DNA concentrations on Q-Sepharose beads was created. These beads allow the DNA to be immobilized through electrostatic interactions, leading to a very efficient capture, that was further evaluated by collecting the target DNA solution at the outlet after flowing it through a channel packed with Q-Sepharose beads, and flowing it through a second channel also packed with Q-Sepharose beads. When comparing the fluorescence signals, it became very clear that almost a 100% capture efficiency is achieved with this method with the signal of the first channel being 82 times higher than the second. To quantify the target DNA capture assay, this was performed for several concentrations (250nM, 100nM, 50nM and 10nM), the target DNA solution was collected at the outlet of the channels and flown through a second channel packed with Q-Sepharose beads. By analyzing the fluorescence signal in the second channel it is possible to correlate that signal with the calibration curve and extract how much target DNA was captured in the target DNA assay. From these calculations, capture efficiencies ranging from 27% to 77% (250nM to 50nM of target DNA, respectively) were obtained, leading to the conclusion that the capture was more efficient for lower concentrations. Given that for pathogen detection the limit of detection for benchtop methods is around 10-1000 CFU/mL the goal for this module is to effectively capture low DNA concentrations, and therefore no further optimization was made to the target DNA capture module. [62]

Using the optimized target DNA capture and RCA module, an attempt at using a real *Staphylococcus aureus* sample and integrating it with a previously developed cell lysis module was performed. These experiments revealed that the background signal was very high making it so the control with no target DNA present for capture and amplification had a signal very similar to the experiment with target DNA. Following this, several experiments were performed revealing that the source of the high background signal was the detection oligonucleotides hybridizing with the free padlock probes, which has been previously reported in the literature as a problem inherent to the RCA assay structure. [33] Several blocking strategies were attempted in order to reduce this background signal, such as sodium polyacrylate, incubating the padlock probe and padlock prior to introducing the solution into the channel, and using biotinylated detection oligonucleotides (with no label) to hybridize with the free padlock probes. This culminated in changing the detection oligonucleotide sequence, so it was no longer complementary to the padlock probe. However, from these experiments it was also noticeable that the increase in temperature used to denature the *Staphylococcus aureus* DNA may be approaching the padlock probe-padlock melting temperature, making it so that more padlock probes were available to hybridize with the complementary detection oligonucleotides.

Using the new detection oligonucleotide sequence for the detection of the RCA products, the RCA assay was again performed for concentrations of 10nM and 1nM of target DNA. As expected, the signal decreased around 10-fold with the decrease in the concentration of target DNA. Although the assay has been optimized regarding several aspects, the RCA assay could still be further optimized in order to obtain a higher yield, given that the percentage of detectable products is lower than previously reported in literature for a similar method. [52] However, further investigation is required in order to understand if the lower percentage of detectable products is related with the assay itself or with the detection methodology, given that it was already noted that by exciting the Atto-430LS labelled detection oligonucleotides with a UV-filter instead of the blue-filter results in a higher fluorescence signal. Furthermore, with the current assay architecture it is still not possible to capture and amplify *Staphylococcus aureus* genomic DNA. This can be due to lack of efficient capture of the target, either due to inefficient denaturation or difficulty in hybridizing with the immobilized padlocks due to steric hindrance caused by the large size of the genomic DNA. To access this prior to capturing, the *Staphylococcus aureus* genomic DNA could be subjected to digestion by restriction enzymes so that it would be easier for the target sequence to hybridize with the immobilized padlock with little interference. Simultaneously, several denaturation temperatures and times should also be evaluated to understand if the lack of ssDNA available to hybridize with the padlocks is due to inefficient denaturation. Ultimately, the chosen denaturation temperature and time will be a compromise between the 95℃, most commonly used for denaturation, and the melting temperature of the padlock probe-padlock duplex, as well as the temperature the PMDS device can withstand without the creation of air bubbles. Following the resolution of these current issues, the integration of this module with the cell lysis module should be possible, resulting in a true POC sample-in-answer-out type of device for *Staphylococcus aureus* detection, that could then be adapted in order to detect other pathogens.

5. References

[1] U.S Centers for Disease Control and prevention. (2019). *Antibiotic Resistance Threats in the United States*.

[2] Prestinaci, F., Pezzotti, P., & Pantosti, A. (2015). Antimicrobial resistance: a global multifaceted phenomenon. *Pathogens and Global Health*, *109*(7), 309–318.

[3] C Reygaert, W. (2018). An overview of the antimicrobial resistance mechanisms of bacteria. *AIMS Microbiology*, *4*(3), 482–501.

[4] Boolchandani, M., D'Souza, A. W., & Dantas, G. (2019). Sequencing-based methods and resources to study antimicrobial resistance. *Nature Reviews Genetics*.

[5] Monroe, S., & Polk, R. (2000). Antimicrobial use and bacterial resistance. *Current Opinion in Microbiology*, *3*(5), 496–501

[6] *Antimicrobial resistance*. (2020, October 13). World Health Organization. https://www.who.int/news-room/fact-sheets/detail/antimicrobial-resistance

[7] European Center for Disease Prevention and Control. (2009). *The bacterial challenge: time to react*

[8] Sun, J., Huang, J., Li, Y., Lv, J., & Ding, X. (2019). A simple and rapid colorimetric bacteria detection method based on bacterial inhibition of glucose oxidase-catalyzed reaction. *Talanta*, *197*, 304–309

[9] Zheng, W., Sun, W., & Simeonov, A. (2017). Drug repurposing screens and synergistic drug-combinations for infectious diseases. *British Journal of Pharmacology*, *175*(2), 181–191.

[10] Shi, X., Kadiyala, U., VanEpps, J. S., & Yau, S. T. (2018). Culture-free bacterial detection and identification from blood with rapid, phenotypic, antibiotic susceptibility testing. *Scientific Reports*, *8*(1).

[11] Sista, R., Hua, Z., Thwar, P., Sudarsan, A., Srinivasan, V., Eckhardt, A., Pollack, M., & Pamula, V. (2008). Development of a digital microfluidic platform for point of care testing. *Lab on a Chip*, *8*(12), 2091

[12] Foudeh, A. M., Fatanat Didar, T., Veres, T., & Tabrizian, M. (2012). Microfluidic designs and techniques using lab-on-a-chip devices for pathogen detection for point-of-care diagnostics. *Lab on a Chip*, *12*(18), 3249

[13] Sharma, S., Zapatero-Rodríguez, J., Estrela, P., & O'Kennedy, R. (2015). Point-of-Care Diagnostics in Low Resource Settings: Present Status and Future Role of Microfluidics. *Biosensors*, *5*(3), 577–601

[14] Kapoor, G., Saigal, S., & Elongavan, A. (2017). Action and resistance mechanisms of antibiotics: A guide for clinicians. *Journal of Anaesthesiology Clinical Pharmacology*, *33*(3), 300.

[15] McGowan, J. E., & Tenover, F. C. (1997). CONTROL OF ANTIMICROBIAL RESISTANCE IN THE HEALTH CARE SYSTEM. *Infectious Disease Clinics of North America*, *11*(2), 297–311.

[16] Griffith, M., Postelnick, M., & Scheetz, M. (2012). Antimicrobial stewardship programs: methods of operation and suggested outcomes. *Expert Review of Anti-Infective Therapy*, *10*(1), 63–73

[17] Cox, G., & Wright, G. D. (2013). Intrinsic antibiotic resistance: Mechanisms, origins, challenges and solutions. *International Journal of Medical Microbiology*, *303*(6–7), 287–292

[18] Munita, J. M., & Arias, C. A. (2016). Mechanisms of Antibiotic Resistance. *Microbiology Spectrum*, *4*(2)

[19] Frost, L. S., Leplae, R., Summers, A. O., & Toussaint, A. (2005). Mobile genetic elements: the agents of open source evolution. *Nature Reviews Microbiology*, *3*(9), 722–732.

[20] Thomas, C. M., & Nielsen, K. M. (2005). Mechanisms of, and Barriers to, Horizontal Gene Transfer between Bacteria. *Nature Reviews Microbiology*, *3*(9), 711–721.

[21] Vernikos, G., & Medini, D. (2014). Horizontal Gene Transfer and the Role of Restriction-Modification Systems in Bacterial Population Dynamics. *Evolutionary Biology: Genome Evolution, Speciation, Coevolution and Origin of Life*, 169–190.

[22] Blair, J. M. A., Webber, M. A., Baylay, A. J., Ogbolu, D. O., & Piddock, L. J. V. (2014). Molecular mechanisms of antibiotic resistance. *Nature Reviews Microbiology*, *13*(1), 42–51.

[23] Turner, N. A., Sharma-Kuinkel, B. K., Maskarinec, S. A., Eichenberger, E. M., Shah, P. P., Carugati, M., Holland, T. L., & Fowler, V. G. (2019). Methicillin-resistant Staphylococcus aureus: an overview of basic and clinical research. *Nature Reviews Microbiology*, *17*(4), 203–218.

[24] Lee, A. S., de Lencastre, H., Garau, J., Kluytmans, J., Malhotra-Kumar, S., Peschel, A., & Harbarth, S. (2018). Methicillin-resistant Staphylococcus aureus. *Nature Reviews Disease Primers*, *4*(1)

[25] Gordon, R., & Lowy, F. (2008). Pathogenesis of Methicillin-Resistant Staphylococcus aureus Infection. *Clinical Infectious Diseases*, *46*(S5), S350–S359.

[26] Oliveira, D. C., & de Lencastre, H. (2011). Methicillin-Resistance in Staphylococcus aureus Is Not Affected by the Overexpression in Trans of the mecA Gene Repressor: A Surprising Observation. *PLoS ONE*, *6*(8), e23287.

[27] Fridkin, S. K., Hageman, J. C., Morrison, M., Sanza, L. T., Como-Sabetti, K., Jernigan, J. A., Harriman, K., Harrison, L. H., Lynfield, R., & Farley, M. M. (2005). Methicillin-Resistant Staphylococcus aureus Disease in Three Communities. *New England Journal of Medicine*, *352*(14)

[28] Rajapaksha, P., Elbourne, A., Gangadoo, S., Brown, R., Cozzolino, D., & Chapman, J. (2019). A review of methods for the detection of pathogenic microorganisms. *The Analyst*, *144*(2), 396–411.

[29] Lazcka, O., Campo, F. J. D., & Muñoz, F. X. (2007). Pathogen detection: A perspective of traditional methods and biosensors. *Biosensors and Bioelectronics*, *22*(7), 1205–1217.

[30] Váradi, L., Luo, J. L., Hibbs, D. E., Perry, J. D., Anderson, R. J., Orenga, S., & Groundwater, P. W. (2017). Methods for the detection and identification of pathogenic bacteria: past, present, and future. Chemical Society Reviews, 46(16), 4818–4832.

[31] Saravanan, A., Kumar, P. S., Hemavathy, R. V., Jeevanantham, S., Kamalesh, R., Sneha, S., & Yaashikaa, P. R. (2020). Methods of detection of food-borne pathogens: a review. *Environmental Chemistry Letters*, *19*(1), 189–207.

[32] Byrne, B., Stack, E., Gilmartin, N., & O'Kennedy, R. (2009). Antibody-Based Sensors: Principles, Problems and Potential for Detection of Pathogens and Associated Toxins. *Sensors*, *9*(6), 4407–4445.

[33] Chang, C. M., Chang, W. H., Wang, C. H., Wang, J. H., Mai, J. D., & Lee, G. B. (2013). Nucleic acid amplification using microfluidic systems. *Lab on a Chip*, *13*(7), 1225.

[34] Ahrberg, C. D., Manz, A., & Chung, B. G. (2016). Polymerase chain reaction in microfluidic devices. *Lab on a Chip*, *16*(20), 3866–3884.

[35] Craw, P., & Balachandran, W. (2012). Isothermal nucleic acid amplification technologies for point-of-care diagnostics: a critical review. *Lab on a Chip*, *12*(14), 2469.

[36] Notomi, T., Okayama, H., Masubuchi H.,Yonekawa, T. , Watanabe, K., Amino,N. , Hase, T (2000), Loop-mediated isothermal amplification of DNA, *Nucleic Acids Research*, 28(12), 63e-663

[37] Bruce, K. L., Leterme, S. C., Ellis, A. V., & Lenehan, C. E. (2014). Approaches for the detection of harmful algal blooms using oligonucleotide interactions. *Analytical and Bioanalytical Chemistry*, *407*(1), 95–116.

[38] Ali, M. M., Li, F., Zhang, Z., Zhang, K., Kang, D. K., Ankrum, J. A., Le, X. C., & Zhao, W. (2014). Rolling circle amplification: a versatile tool for chemical biology, materials science and medicine. *Chemical Society Reviews*, *43*(10), 3324.

[39] Soares, R. R. G., Madaboosi, N., & Nilsson, M. (2021). Rolling Circle Amplification in Integrated Microsystems: An Uncut Gem toward Massively Multiplexed Pathogen Diagnostics and Genotyping. *Accounts of Chemical Research*.

[40] Soares, R., Santos, D., Chu, V., Azevedo, A., Aires-Barros, M., & Conde, J. (2017). A point-of-use microfluidic device with integrated photodetector array for immunoassay multiplexing: Detection of a panel of mycotoxins in multiple samples. *Biosensors and Bioelectronics*, *87*, 823–831.

[41] Gardeniers, H., & den Berg, A. V. (2004). Micro- and nanofluidic devices for environmental and biomedical applications. *International Journal of Environmental Analytical Chemistry*, *84*(11), 809–819.

[42] Sia, S. K., & Whitesides, G. M. (2003). Microfluidic devices fabricated in Poly(dimethylsiloxane) for biological studies. *ELECTROPHORESIS*, *24*(21), 3563–3576.

[43] Soares, R. R. G., Akhtar, A. S., Pinto, I. F., Lapins, N., Barrett, D., Sandh, G., Yin, X., Pelechano, V., & Russom, A. (2021). Sample-to-answer COVID-19 nucleic acid testing using a low-cost centrifugal microfluidic platform with bead-based signal enhancement and smartphone read-out. *Lab on a Chip*, *21*(15), 2932–2944.

[44] Convery, N., & Gadegaard, N. (2019). 30 years of microfluidics. *Micro and Nano Engineering*, *2*, 76–91.

[45] Kim, J. H. S., Marafie, A., Jia, X. Y., Zoval, J. V., & Madou, M. J. (2006). Characterization of DNA hybridization kinetics in a microfluidic flow channel. *Sensors and Actuators B: Chemical*, *113*(1), 281–289.

[46] Tabeling, P. (2021). *Introduction to Microfluidics*. Oxford University Press.

[47] Li, X. J., & Zhou, Y. (2021). *Microfluidic Devices for Biomedical Applications* (2nd ed.). Woodhead Publishing.

[48] Xiang, Q., Xu, B., Fu, R., & Li, D. (2005). Real Time PCR on Disposable PDMS Chip with a Miniaturized Thermal Cycler. *Biomedical Microdevices*, *7*(4), 273–279.

[49] Hataoka, Y., Zhang, L., Mori, Y., Tomita, N., Notomi, T., & Baba, Y. (2004). Analysis of Specific Gene by Integration of Isothermal Amplification and Electrophoresis on Poly(methyl methacrylate) Microchips. *Analytical Chemistry*, *76*(13), 3689–3693.

[50] Wang, C. H., Lien, K. Y., Wu, J. J., & Lee, G. B. (2011). A magnetic bead-based assay for the rapid detection of methicillin-resistant Staphylococcus aureus by using a microfluidic system with integrated loop-mediated isothermal amplification. *Lab on a Chip*, *11*(8), 1521.

[51] Mahmoudian, L., Kaji, N., Tokeshi, M., Nilsson, M., & Baba, Y. (2008). Rolling Circle Amplification and Circle-to-circle Amplification of a Specific Gene Integrated with Electrophoretic Analysis on a Single Chip. *Analytical Chemistry*, *80*(7), 2483–2490.

[52] Sato, K., Tachihara, A., Renberg, B., Mawatari, K., Sato, K., Tanaka, Y., Jarvius, J., Nilsson, M., & Kitamori, T. (2010). Microbead-based rolling circle amplification in a microchip for sensitive DNA detection. *Lab on a Chip*, *10*(10), 1262.

[53] Soares, R. R., Pettke, A., Robles-Remacho, A., Zeebaree, S., Ciftci, S., Tampere, M., Russom, A., Puumalainen, M. R., Nilsson, M., & Madaboosi, N. (2021). Circle-to-circle amplification coupled with microfluidic affinity chromatography enrichment for in vitro molecular diagnostics of Zika fever and analysis of anti-flaviviral drug efficacy. *Sensors and Actuators B: Chemical*, *336*, 129723.

[54] Kühnemund, M., Witters, D., Nilsson, M., & Lammertyn, J. (2014). Circle-to-circle amplification on a digital microfluidic chip for amplified single molecule detection. *Lab Chip*, *14*(16), 2983–2992.

[55] Conze, T., Shetye, A., Tanaka, Y., Gu, J., Larsson, C., Göransson, J., Tavoosidana, G., Söderberg, O., Nilsson, M., & Landegren, U. (2009). Analysis of Genes, Transcripts, and Proteins via DNA Ligation. *Annual Review of Analytical Chemistry*, *2*(1), 215–239.

[56] ÖZay, B., & McCalla, S. E. (2021). A review of reaction enhancement strategies for isothermal nucleic acid amplification reactions. *Sensors and Actuators Reports*, *3*, 100033.

[57] Henry, O. Y., & O'Sullivan, C. K. (2012). Rapid DNA hybridization in microfluidics. *TrAC Trends in Analytical Chemistry*, *33*, 9–22.

[58] Caneira, C. R. F., Monteiro, S., Santos, R., Chu, V., & Conde, J. P. (2019, October). *A microfluidic module for integrated lysis and genetic material detection of gram-positive and gram-negative bacteria [Poster session]. MicroTAS, Basel, Switzerland.*

[59] Shehadul Islam, M., Aryasomayajula, A., & Selvaganapathy, P. (2017). A Review on Macroscale and Microscale Cell Lysis Methods. *Micromachines*, *8*(3), 83.

[60] Caneira, C. R., Soares, R. R., Pinto, I. F., Mueller-Landau, H. S., Azevedo, A. M., Chu, V., & Conde, J. P. (2019). Development of a rapid bead-based microfluidic platform for DNA hybridization using single- and multi-mode interactions for probe immobilization. *Sensors and Actuators B: Chemical*, *286*, 328–336.

[61] Pinto, I. F., Santos, D. R., Caneira, C. R. F., Soares, R. R. G., Azevedo, A. M., Chu, V., & Conde, J. P. (2018). Optical biosensing in microfluidics using nanoporous microbeads and amorphous silicon thin-film photodiodes: quantitative analysis of molecular recognition and signal transduction. *Journal of Micromechanics and Microengineering*, *28*(9), 094004.

[62] Foudeh, A. M., Fatanat Didar, T., Veres, T., & Tabrizian, M. (2012). Microfluidic designs and techniques using lab-on-a-chip devices for pathogen detection for point-of-care diagnostics. *Lab on a Chip*, *12*(18), 3249.